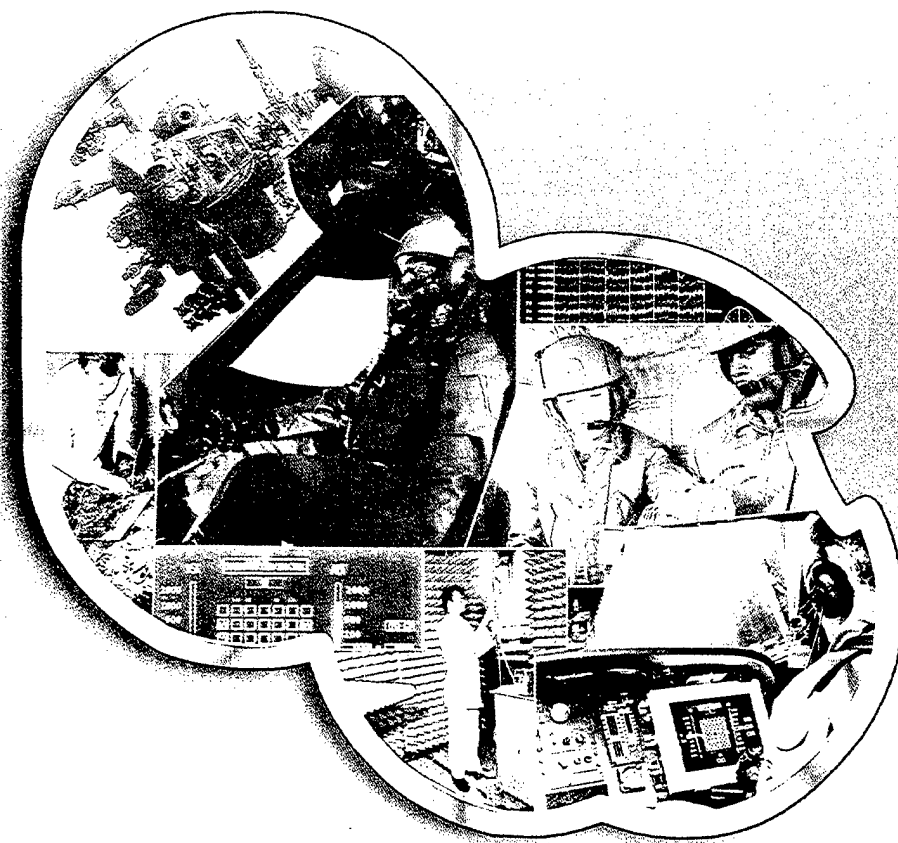USAARL Report No. 2003-13

Analysis of Head Motion in Rotary-Wing Flight Using Various Helmet-Mounted Display Configurations (Part III. Roll)

By Jessica A. Stelle, Ryan J. Rostad, Clarence E. Rash, and John S. Crowley

Aircrew Health and Performance Division
and
Aircrew Protection Division

August 2003

2003 1001 091

U.S. Army
Aeromedical Research
Laboratory

USAARL

Notice

REPORT DOCUMENTATION PAGE

Form Approved
OMB No. 0704-0188

1. AGENCY USE ONLY *(Leave blank)*	2. REPORT DATE August 2003	3. REPORT TYPE AND DATES COVERED Final

4. TITLE AND SUBTITLE
Analysis of Head Motion in Rotary-wing Flight Using Various Helmet-Mounted Display Configurations (Part III. Roll)

5. FUNDING NUMBERS
PE 622787A
PR 879
TA P
WU DA361539

6. AUTHOR(S)
Stelle, Jessica, A., Rostad, Ryan, J., Rash, Clarence, E., Crowley, John, S.

7. PERFORMING ORGANIZATION NAME(S) AND ADDRESS(ES)
U.S. Army Aeromedical Research Laboratory
ATTN: MCMR-UAD
P.O. Box 620577
Fort Rucker, AL 36362-0577

8. PERFORMING ORGANIZATION REPORT NUMBER
2003-13

9. SPONSORING / MONITORING AGENCY NAME(S) AND ADDRESS(ES)
U.S. Army Medical Research and Materiel Command
504 Scott Street
Fort Detrick, MD 21702-5012

10. SPONSORING / MONITORING AGENCY REPORT NUMBER

11. SUPPLEMENTARY NOTES

12a. DISTRIBUTION / AVAILABILITY STATEMENT
Approved for public release, distribution unlimited

12b. DISTRIBUTION CODE

13. ABSTRACT *(Maximum 200 words)*
In spite of an immense increase in interest in helmet-mounted displays (HMDs) over the past two decades, there have been few studies on head motion while using HMDs in operational flight. Rotary-wing flight conducted using a number of HMD configurations has resulted in a head position database that will be useful in filling this void. Various analysis techniques have been applied to investigate characteristics of roll (tilt) head position distributions for a slalom flight maneuver for four visual environments: good visual environment (daytime, unaided), night vision goggles, HMD with thermal imagery, and HMD with thermal imagery and symbology.

14. SUBJECT TERMS
helmet-mounted displays (HMDs), head motion, head position, head tracking, roll (tilt)

15. NUMBER OF PAGES
133

16. PRICE CODE

17. SECURITY CLASSIFICATION OF REPORT Unclassified	18. SECURITY CLASSIFICATION OF THIS PAGE Unclassified	19. SECURITY CLASSIFICATION OF ABSTRACT Unclassified	20. LIMITATION OF ABSTRACT SAR

Table of contents

Table of contents (continued)

List of figures

Table of contents (continued)
List of figures (continued)

List of tables

Introduction

From the mid to late 1990s, the Defense Evaluation and Research Agency (DERA), Farnborough, United Kingdom, conducted a rotary-wing (helicopter) research effort known as the Day/Night All Weather (D/NAW) program. The principal aim of this program was to enable safe tactical helicopter flight in severely limited visibility. The major focus of the program was advanced helmet- or head-mounted display (HMD) technologies and the associated symbology design issues (Crowley, 1998).

HMDs are devices or systems that present the pilot(s) with pilotage imagery, flight information, and/or fire control (weaponry) imagery and symbology (Rash, 1999). They are, by definition, head- or helmet-mounted systems. Melzer and Moffitt (1997) describe an HMD as minimally consisting of "an image source and collimating optics in a head mount." Rash (1999) expands this description to include a visual coupling system which performs the function of slaving head and/or eye positions and motions to one or more aircraft systems. Examples of rotary-wing HMDs include the U. S. Army's fielded Integrated Helmet and Display Sighting System (IHADSS) used on the AH-64 Apache attack helicopter and the under-development Helmet Integrated Display and Sight System (HIDSS) to be used on the RAH-66 Comanche helicopter.

From March to September 1997, under the auspices of the D/NAW program, a series of flights was flown to establish baseline flight performance for future HMD performance comparisons. These flights consisted of several flight path maneuvers (e.g., slalom, rapid egress, side-step, etc.) and visual environments, defined by the mode of visual information presentation (i.e., unaided day, using night vision goggles (NVGs), and using two HMD configurations). For safety considerations, all flights, except those with NVGs, were conducted during the day.

As an aside to the normal flight performance parameters measured during the flights, head azimuth, elevation, and roll position data also were collected, not as part of the experimental design but as standard practice. Analysis of azimuth and elevation head motion were previously presented in Rostad et al. (2001) and Rostad and Rash (2002), respectively. This paper reports the analysis of the roll data for the slalom maneuver.

It has been argued that the availability of this head position data is advantageous for two reasons. First, extremely limited operational head position data have been presented in the literature. Very little data have been collected in the operational flight environment using HMDs. Second, for the same flights for which head position data are presented here, measures of motion sickness symptoms, pre- and postflight, were made. In order to test the hypothesis that motion sickness symptoms may be correlated with differences in head motion attributed to the different visual environments (or conversely, head motion is affected by the onset of motion sickness symptoms due to different visual environments), it is necessary to be able to describe the different visual environment head position distributions using a set of parameters (e.g., central moments).

Background

A major operational characteristic of HMDs is their capability to allow the pilot to control external imaging sensors and weapons via head movement. This head slaving capability is achieved through the use of head trackers of various technologies, e.g., mechanical, electro-optical, magnetic, ultrasonic, etc. Most recently, magnetic systems have been the most widely used head tracking technology and are considered to be relatively mature for use in the aviation environment (Borah, 1998). The performance of a head tracking system (sometimes referred to as a visually coupled system [VCS]) is determined by a number of parameters, which include motion box size, pointing angle accuracy, pointing angle resolution, update rate, and jitter. Specifications for these parameters usually are affected by the aircraft platform (fixed wing and rotary-wing). A more detailed discussion of tracking performance parameters can be found in Kocian and Task (1995).

Despite the growing popularity of HMDs, there has been only a relatively small increase in studies investigating visually coupled systems. Most of these studies have looked at the performance of head (or eye) tracking technologies (Borah, 1989; Robinson and Wetzel, 1989; and Cameron, Trythall and Barton, 1995) or head motion prediction (Azuma and Bishop, 1995; Curtis and Sowizral, 1994). However, there have been very limited data collected and made available on head position and velocity within the operational flight environment, especially for flights using HMDs. This is particularly true for roll head motion.

Virtually all head tracking systems provide only head azimuth and elevation information. However, there has been a growing interest in providing 3-axis information, with head roll added. The addition of roll information provides the capability of keeping the imagery aligned with the aircraft structure (Task and Kocian, 1995). The availability of roll compensation is considered to be an advantage and should reduce workload. Haworth (1997) has argued that as wider field-of-view (FOV) HMDs are developed, the displayed imagery becomes more compelling and may require roll compensation. While U.S. Army AH-64 Apache aviators have informally stated that they would not like the addition of roll compensation (Rash, 1999), Craig, Jennings, and Swail (2000) found that roll compensation in HMD systems reduces pilot workload and motion sickness during critical flight periods where pilot workload may already be high. In a much earlier study, Michael, Jardine and Goom (1978) concluded that any rotary-wing aircraft maneuver that caused the weapon-aiming HMD sighting image to roll resulted in considerable tracking/aiming performance degradation.

Several anatomical and biomechanical studies have reported values for range of head motion for roll (tilt or lateral bending). The reported ranges of these values are presented in Table 1. Caution must be taken when reviewing the values for head motion in Table 1. These values, based on laboratory anatomical and biomechanical measures, would most likely be reduced in an operational cockpit where seat, restraint system and cockpit design present physical obstructions and other limits to allowable ranges of motion. In addition, it has been shown that head motion is reduced by inertial loading such as that induced by the increased head supported weight of HMDs (Gauthier, Martin and Stark, 1986), and the increased neck muscle loading associated

with the use of HMDs increases fatigue which may indirectly reduce the frequency and range of head motion (Phillips and Petrofsky, 1983).

The data summarized in Table 1 do not represent a description of head motion values as would be encountered in actual flight scenarios.

Table 1.
Reported anatomical and biomechanical roll head motion ranges.

	Sherk (1989)	Glanville and Kreezer (1937); Hertzberg (1972)
Roll (tilt)	Avg of 59° from right to left	-40° to +40°

The findings presented herein attempt to expand the almost nonexistent database of roll head position and velocity values for actual flight scenarios while wearing HMDs.

Experimental design

The original overall study design for the flights consisted of six flight maneuvers, two levels of aggressiveness (LOAs) and four visual conditions. Each of these factors is described in the sections below. A full flight trial was limited to approximately 90 minutes in duration. A flight was defined as consisting of a varying numbers of "runs" where a "run" was the completion of the full set of all six maneuvers at a given LOA by a single pilot for one of the four visual conditions. While the elements of the experimental design are briefly described in the following sections, detailed discussions can be found in Rostad et al., 2001.

Instrumentation

Aircraft

All flights were in a Lynx ZD285 helicopter (Figure 1), which is a standard Lynx AH Mk 7 airframe with Gem Mk 205 engines but modified to exclude infrared suppressors, missile mounts, or other role equipment. The aircraft was configured for two experimenters seated in the rear cabin; an evaluated pilot, who served as a subject, in the front left seat; and a safety pilot in the front right seat. The instrument panel was modified to provide the safety pilot with ready access to all normal cockpit instruments. The subject pilot was provided with a cut-down panel providing primary flight instruments only.

An additional aircraft modification was the outfitting of all forward cockpit windows (but not overhead windows) with custom amber-tinted panels. The purpose of this modification was to allow the day-use, simulated HMD visual environment.

VCS

The VCS was comprised of a direct current (DC) electromagnetic head positioning system (HPS) with a transmitter affixed to the airframe close to the subject pilot's head with a sensor attached to his helmet. The HPS provided six degrees of freedom (DOF) output over a large range of head movements. The platform could be directed to the HPS line of sight over a range

Figure 1. The DERA Lynx research helicopter outfitted with custom amber-tinted panels.

of ± 120° azimuth and +30° to -90° elevation at a maximum rate of 110°/sec. The platform also carried a thermal imager derived from the Class II Thermal Imaging Common Module (TICM II) with an FOV of 55° horizontal by 37° vertical, producing a raster output in a 625 line/50 Hz format. A Radstone symbol generator was used to produce symbology.

The HPS sampled head position approximately every 5 ms. However, to reduce the volume of the data for storage and analysis, the available head position data files were transformed to 100 ms (0.1 sec)-samples.

HMD

The aircraft was equipped with an HMD, manufactured by GEC, which used 625 line/50 Hz miniature (1-inch diameter) monochrome cathode ray tubes (CRTs) as image sources (Figure 2). The optical train provided a fully overlapped 53° horizontal by 37° vertical FOV. Although capable of binocular operation, the HMD was driven by a single video channel in a biocular mode (same image in both eyes). The HMD could display symbology only (not used in this study), thermal imaging only (TIO), or combined thermal imaging and symbology. The HMD imagery was relatively dim and could not be seen easily under daylight conditions. For safety reasons flights in this study were conducted only under daylight conditions. For this combination of reasons, a modification to the HMD was necessary.

4

Simulated degraded visual environment (SDVE)

The daytime study flight requirement created several problems:
- The HMD imagery was difficult to see against the bright daytime sky.
- The flat surfaces of the HMD combiner optics resulted in numerous reflections that distracted and disoriented the pilot.
- The daytime visual environment was full of visual cues that were absent during night flight.

Figure 2. Flight helmet with 53-degree FOV HMD.

Therefore, to be able to use the HMD during the required daytime flights, a novel hood assembly referred to as a SDVE was developed (Crowley, 1998). The SDVE consisted of a full HMD hood assembly and a blue filter that was complementary to the amber screens already in place over all cockpit transparencies except the overhead panels. The combination of the amber and blue filters prevented exterior viewing by the subject pilot. The hood assembly consisted of a tailored fire-retardant black cloth hood worn over the pilot's helmeted head (Figure 3).

The subject pilot could not see anything directly outside the aircraft but was able to view his arms, the controls, most of the instrument panel, and the left side cockpit structure when looking ahead. The instrument panel was heavily tinted and darkened due to the dark blue filter. This made it so that pilots could not read any numbers on the gauges, but could make out the main

needle on the bigger gauges. This was thought to be a reasonable trade-off, considering that in a nighttime environment cockpit instruments would probably be turned down to minimize troublesome reflections.

NVGs

A single pair of Fenn NG600 (Gen III) NVGs was used for all flights. The Fenn NG600 was 3rd GEN and had a 47° circular FOV.

Figure 3. The SDVE system.

Subjects

There were four subject pilots, all male. Ages were 31, 33, 34 and 37 with 1500, 1830, 2000 and 2700 flight hours, respectively.

Visual environments

The study employed four types of visual environments. These environments were:
- Good visual environment (GVE)
- NVG

- TIO
- Rotary-wing symbology (RWS)

GVE flight was conducted in a normal daytime environment only when "good visibility" was available. These flights served as a baseline to document a reference level of functional quality performance.

NVG flights were flown in a nighttime environment using the Fenn NG600 night vision goggle system. A mean ambient light level of 10 milliLux was the target illumination level. However, any illumination within the range 5-50 milliLux was deemed acceptable. Along with the GVE flights, these flights also were used to develop a baseline for evaluating the VCS.

TIO flights were flown in a daytime environment using the SDVE hood and amber filter windscreen systems. Under the SDVE, the subject pilots were presented with thermal imagery only on the 53° HMD. No symbology was presented.

RWS flights were flown in a daytime environment using the SDVE hood and amber filter windscreen systems. Under the SDVE, the subject pilots were presented with thermal imagery and symbology on the 53° HMD.

Flight maneuvers

Flights were flown during the period mid-March to late-September 1997. The subjects flew a total of six maneuvers: Slalom, curved approach, hovering (spot) turns, rapid egress, bob-up/down, and sidestep. The focus for this analysis is on the slalom maneuver due to its more consistent flight pattern and easily defined flight cycle.

All six maneuvers were performed successively in each run starting with the slalom and ending with the sidestep maneuver. Under ideal conditions, the maneuvers would be randomly presented. However, this counterbalancing design was not possible because the VCS was not available during the first two months of planned flights.

All flights were conducted during daytime hours with the exception of the NVG flights. Flights occurred in the region of southern England known as the Salisbury Plain training area at a location known as Haxton Down, approximately 6.6 miles (11 kilometers) north of the Boscombe Down airfield. All flights approached the test area by originating from the Boscombe Down airfield via a set route flown by the safety pilot at 90 knots indicated air speed (KIAS) at 200 feet above ground level (AGL), descending to 50 feet AGL on approach to the course. The safety pilot aligned the aircraft over the track and handed the controls over to the subject pilot at an appropriate ground speed, at 50 feet AGL, and at a point at least 200 m (650 feet) prior to the first slalom turn. Ground speed at release was to be approximately 30 knots for low LOA and 40 knots for moderate LOA.

There were two LOAs: Low and moderate. Low LOA consisted of the use of up to a 30° angle of bank (AOB), as required, and a moderate speed (> 0 knots, but 30 knots desired) to

achieve an unhurried progression through the course. Pedal-assisted skidding turns were acceptable. There were no time constraints. The moderate LOA intended to exploit the full VCS flight envelope as far as possible and to target 30-degree AOB in all turns with up to 45-degree transients (at safety pilot discretion). Speed was adjusted to achieve rapid progression through the course with an appropriate turn radius (>0 knots, 40 knots desired). Pedal-assisted skidding turns were again acceptable. The required slalom course maneuver completion time was less than 90 seconds.

The slalom segment of the test course consisted of a south to north transit through the Haxton Down area at nap of the earth (NOE) heights and speeds. At Haxton Down, a convenient group of south-north oriented woods labeled Woods One through Four (with "gates" between woods), with intervening east-west avenues, provided a serpentine (slalom) course. The directions of the progressive course turns were: Right, followed by two left turns, two more right turns, and ending with two left turns (Figure 4). Ground track was maintained as close as possible (but not less than 5 meters) from N-S edges of woods, and as close as possible to centerlines of east-west avenues.
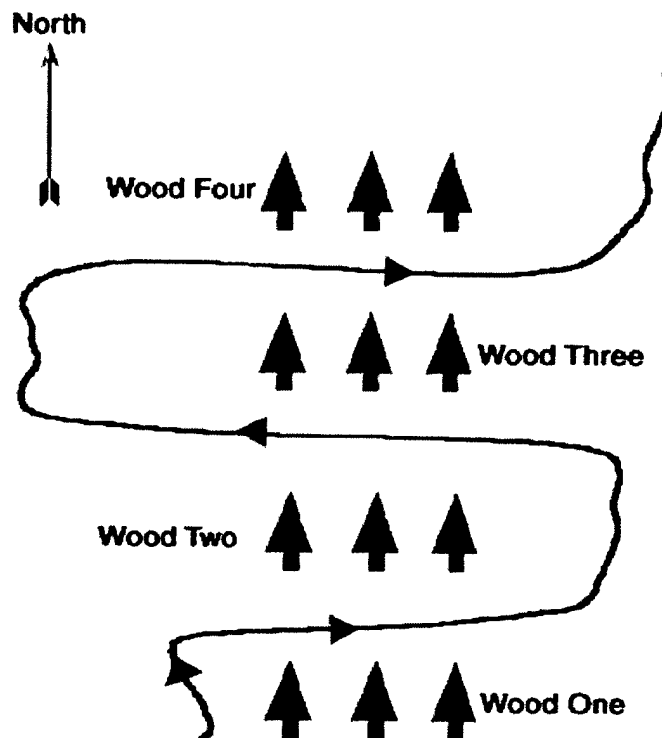
Figure 4. Representative flight path for slalom flight maneuver.

Six performance objectives were defined for the study: 1) ability to maneuver with respect to ground features in NOE flight in the degraded visual environments (NVGs and HMDs), 2) ability to maintain spatial awareness and obstacle clearance during a complex multi-axis maneuver, 3) check for undesirable display dynamics when performing maneuvers representative of moderate aggressiveness NOE flight, 4) ability to control height during turning flight, 5) ability to adjust airspeed to maintain a ground track defined by obstacles, and 6) ability to control sideslip in turns at moderate airspeed.

Database

The provided head motion database consisted of 628 files. The files were divided into 33 subdirectories, where each subdirectory contained the files for a given flight. A flight was defined as consisting of varying numbers of "runs" where a "run" was the completion of the full set of all six maneuvers at a given LOA by a single pilot for one of the four visual conditions. A given file in the database contained data pertaining to a single subject for one combination of LOA, flight maneuver, visual environment, and type of run (practice, intermediate or full). There were 107 files for the slalom maneuver.

This analysis focused on head motion for the slalom maneuver. Of the 107 files provided in the database, four were eliminated from the analysis due to missing or corrupted data. This left 103 files for analysis.

Data analysis

As with the azimuth and elevation analyses, the question to be answered by this analysis is: Are the distributions for roll head motion position (and velocity) different for the four visual environments? The head motion data files under analysis herein for the slalom maneuver are time series of head roll position values for four different visual environments, confounded by two levels of aggressiveness and three run types. In addition to analyses of position data, transformations on these data included construction of velocity, reversal, and excursion distributions. Briefly, a reversal was defined as a change in head motion direction (e.g., turning from looking right to looking left), and an excursion was defined as the change in angular position between two reversal points.

Data preparation

The slalom files consisted of data collected for a flight pattern flown over a set course running north and south with the turns going east and west (Figure 4). In order to be able to compare across subjects and visual conditions, it was decided to equalize across files by using data over a defined section within the slalom maneuver. This section, referred to as a cycle, was defined as shown in Figure 5. A cycle consisted of two right hand turns and two left hand turns. We also wanted to include a small portion before and after the turns in order to capture pilot head movements during preparation for and recovery from turns. In order to do this consistently, the means of the minimum and the maximum values of the longitude both prior and following the four turns were calculated. The point where the longitude exceeded the mean before the first right hand turn was used as the start point of the cycle. The point where the longitude fell below the mean after the last left hand turn was used as the end point of the cycle.

Once a cycle was defined for each file, the data were smoothed using a three-point moving average routine in preparation for analysis.
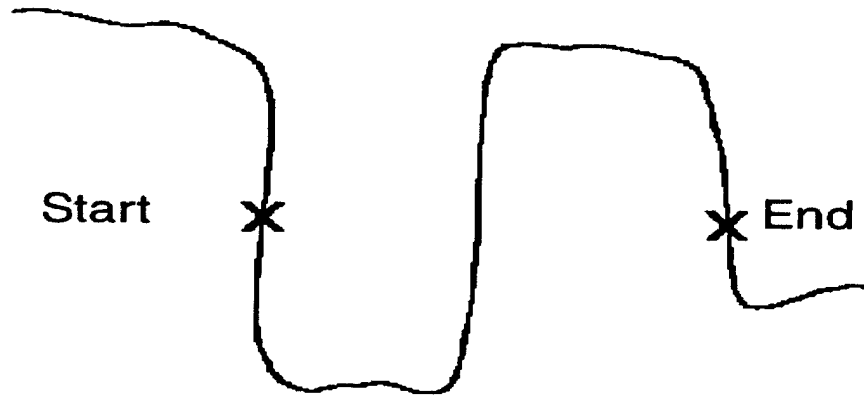
Figure 5. Definition of cycle used in analysis to equalize the slalom maneuver.

Data analysis methods

Multiple approaches were used to answer the research question. The first approach was to transform all of the position time series data into histograms that represented position distributions. Then, the distribution moments (and additional distribution statistics) were calculated for each distribution. The second approach was to construct graphical representations of the distributions in the form of box plots.

A distribution can be fully defined by four moments: Mean, variance (or standard deviation), skewness, and kurtosis. However, it is useful to calculate additional distribution statistics (e.g., minimum, maximum, median, interquartile range (IQR), etc.).

Position analyses

Position distribution histograms

The use of histograms to represent the position distributions is a fundamental technique to allow an overall appreciation of head motion. The histograms presented herein use 1-degree intervals. There were 103 elevation position distributions available for analysis. The resulting position histograms are presented in Appendix A. Subject #1 has a total of 25 histograms that represent the various combinations of LOA, run type, and visual environment; subject #2 has 24 histograms; subject #3 has 34 histograms; and subject #4 has 20 histograms.

Individual position distributions

These individual distributions are worth examining for general characteristics and trends for each subject and visual condition. Such an examination yields the following:

Subject #1. The individual head position distributions for subject #1 (Figures A-1 to A-4, Appendix A) present the following characteristics: a) The distributions were generally unimodal for all visual conditions, b) GVE and NVG distributions were similar with

10

means around 0°, and c) TIO and RWS distributions were similar with means at approximately -2° (a minor roll/tilt to the left), and d) the overall range appears to be smaller for TIO and RWS than for the GVE and NVG visual conditions.

<u>Subject #2</u>. The head position distributions for subject #2 (Figures A-5 to A-8, Appendix A) present the following characteristics: a) There appeared to be greater variability in overall range than for subject #1, b) for GVE and NVG, the distributions presented medians clustered between 0° and +5° (slight roll/tilt to the right), c) the distributions were generally unimodal, and d) the overall range appears to be smaller for TIO and RWS than for the GVE and NVG visual conditions, and have a typical median very close to 0.

<u>Subject #3</u>. The head position distributions for subject #3 (Figures A-9 to A-12, Appendix A) present the following characteristics: a) The GVE visual condition exhibited less of a central tendency with some individual distributions appearing almost uniform with less variability in distribution shape within a given flight, b) NVG distributions were unimodal and showed greater central tendency with a median value just slightly positive of 0°, and c) TIO and RWS showed a lesser range with a more pronounced central mode located typically at 0°.

<u>Subject #4</u>. The head position distributions for subject #4 (Figure A-13 to A-14), Appendix A) present the following characteristics: a) For GVE, distributions were highly variable in shape, ranging from almost uniform to a relatively well-defined central mode, based upon flight number, b) for NVG, all distributions presented a well-defined central mode but with variability in range, and c) for GVE and NVG all distribution means and medians were located between 0° and +5°.

Note: Head position data for subject #4 were not available for TIO and RWS visual environments.

Combined distributions

This rather large aggregate of histograms makes it difficult to compare head motion across visual environments. To overcome this problem, the authors have argued that distribution comparisons can be based on combined distributions that are total data sets formed by combining data from all runs for a given visual environment (Rostad et al., 2001). These combined distributions are not based on the average of individual runs but rather the summation of individual runs.

The general tenet of the argument for basing analyses on combined distributions is that the influence of the LOA and run type confounds, contributes to, but does not define, the general shape and characteristics of the head motion distribution for a given visual environment.

Based on this argument, Figures 6-9 present the combined roll position distributions by subject and visual environment. Note that head position data for subject #4 were available for only two visual environments, GVE and NVG. As with the individual distributions, these combined

11

distributions also can be examined visually for general characteristics and trends, which should generally be similar to those found for the individual distributions. The following observations are made:

<u>Subject #1</u>. The combined GVE head position distribution for subject #1 (Figure 6) presented the following characteristics: a) It is unimodal at approximately +1°, and b) the approximate range was -31° to +23°.

The combined NVG head position distribution for subject #1 (Figure 6) presented the following characteristics: a) It was unimodal with modes at +1°, and b) the approximate range was -23° to +17°.

The combined TIO head position distribution for subject #1 (Figure 6) presented the following characteristics: a) There was a strong central mode at approximately -2°, and b) the approximate range was -11° to +8°.

The combined RWS head position distribution for subject #1 (Figure 6) presented the following characteristics: a) There was a strong central mode at approximately -2°, and b) the approximate range was -10° to +5°.

<u>Subject #2</u>. The combined GVE head position distribution for subject #2 (Figure 7) presented the following characteristics: a) There was a strong but suppressed central mode at approximately +2°, and b) the approximate range was -21° to +28°.

The combined NVG head position distribution for subject #2 (Figure 7) presented the following characteristics: a) It was unimodal with mode at +7°, and b) the approximate range was -11° to +30°.

The combined TIO head position distribution for subject #2 (Figure 7) presented the following characteristics: a) There was a strong central mode at approximately +1°, and b) the approximate range was -9° to +12°.

The combined RWS head position distribution for subject #2 (Figure 7) presented the following characteristics: a) There was a strong central mode at approximately +1°, and b) the approximate range was -10° to +14°.

<u>Subject #3</u>. The combined GVE head position distribution for subject #3 (Figure 8) presented the following characteristics: a) There was a strong central mode at +6°, and b) the approximate range was -17° to +28°.

The combined NVG head position distribution for subject #3 (Figure 8) presented the following characteristics: a) It was unimodal with mode at +2°, and b) the approximate range was -18° to +25°.

The combined TIO head position distribution for subject #3 (Figure 8) presented the following characteristics: a) There was a less defined central mode at approximately 0°, and b) the approximate range was -19° to +13°.

The combined RWS head position distribution for subject #3 (Figure 8) presented the following characteristics: a) There was a strong central mode at approximately -1°, and b) the approximate range was -18° to +18°.
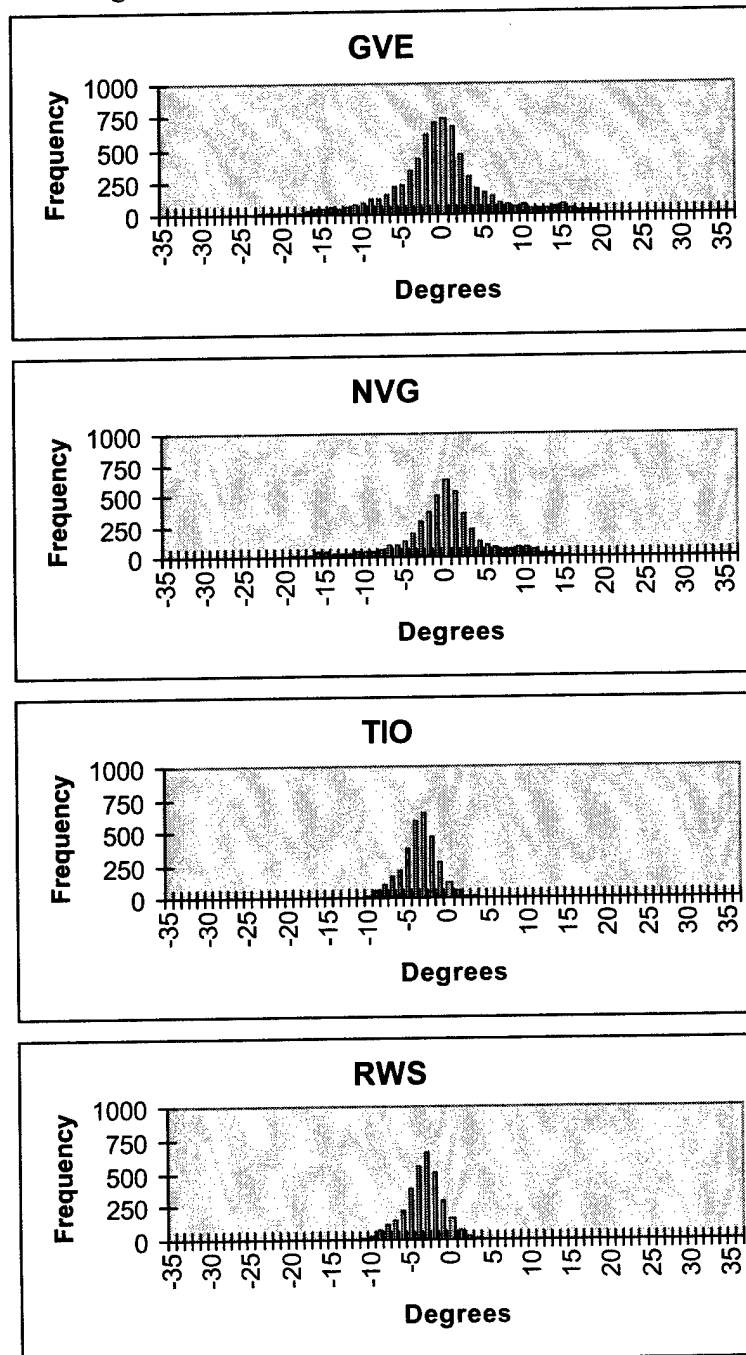
Figure 6. Combined position histograms for subject #1.
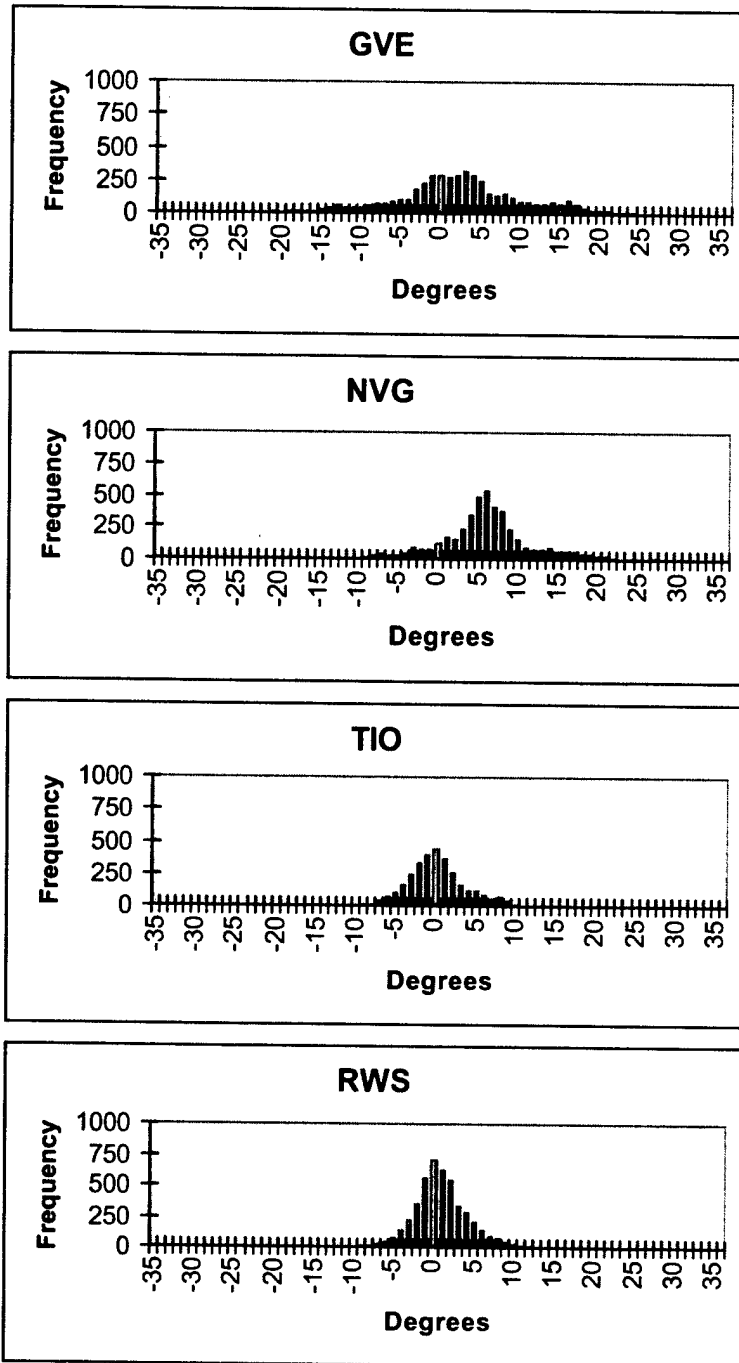
Figure 7. Combined position histograms for subject #2.
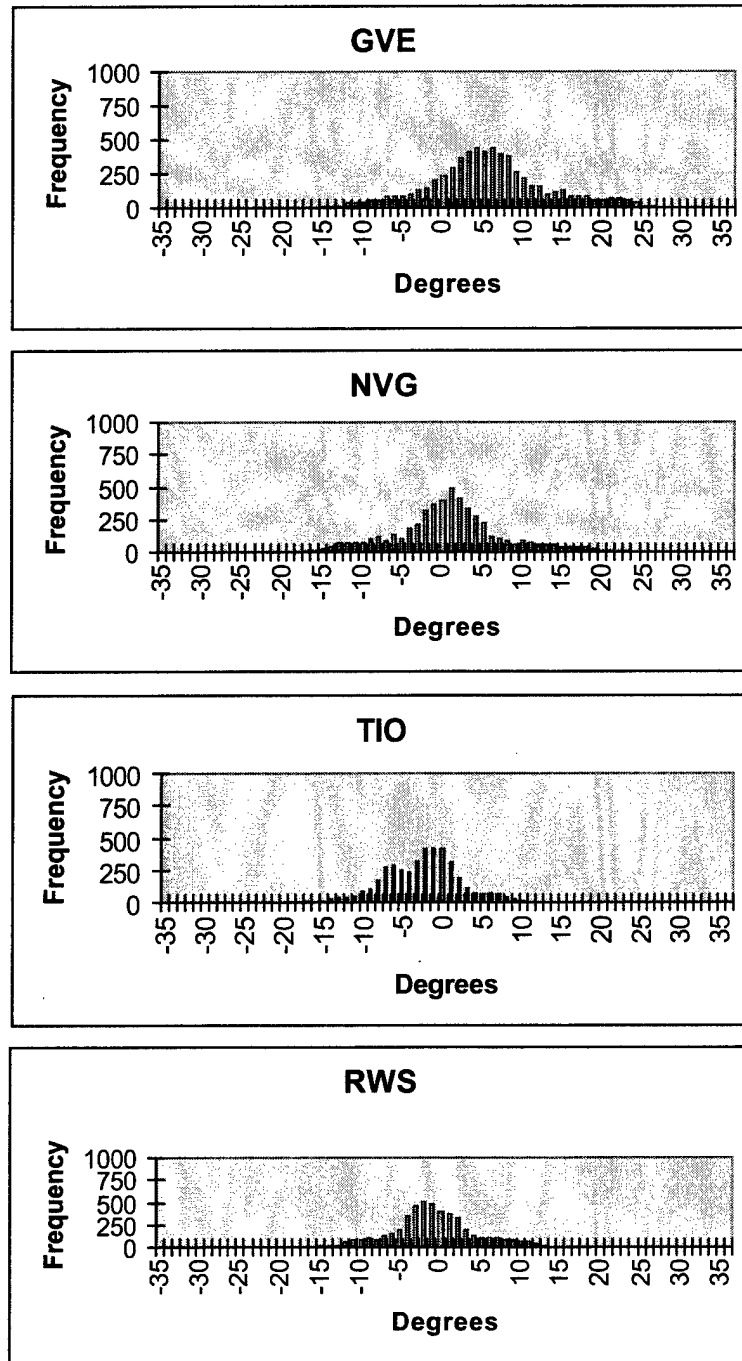
Figure 8. Combined position histograms for subject #3.
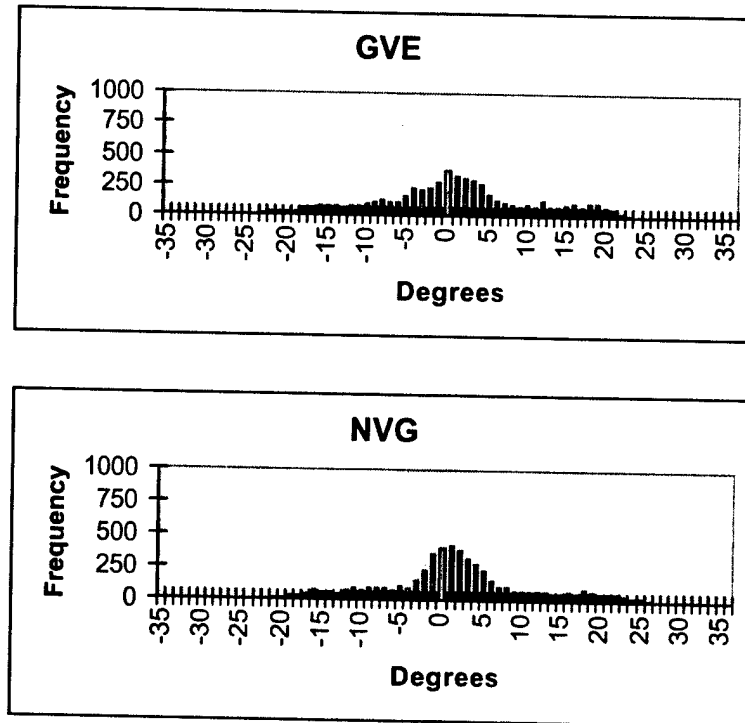
Figure 9. Combined position histograms for subject #4.

Subject #4. The combined GVE head position distribution for subject #4 (Figure 9) presented the following characteristics: a) It was unimodal with poorly defined mode at +1°, and b) the approximate range was -24° to +25°.

The combined NVG head position distribution for subject #4 (Figure 9) presented the following characteristics: a) It was unimodal mode at +2°, and b) the approximate range was -21° to +28°.

Note: Head position data for subject #4 were not available for TIO and RWS visual environments.

Moments and additional distribution statistics

While distribution shape provides a basic understanding of the ongoing head motion, the semi-quantitative nature of distribution histograms does not allow for analytical comparison. For this reason, distributions often are described or defined by the distribution's moments. There are four such moments: mean, variance or standard deviation, skewness, and kurtosis. It is also useful to calculate additional distribution statistics, e.g., minimum, maximum, median, etc.

Summary individual and combined distribution moments and statistics tables for all subjects, grouped by visual environment, are provided in Appendix B. However, accepting the argument that comparisons can be based on the combined distributions, a summary of distribution moments and statistics by subject and visual environment for the combined distributions only is

16

presented in Table 2. Examination of Appendix B and Table 2 led to the identification of a number of characteristics and trends:

Subject #1. The summary GVE head position distribution statistics for subject #1 present the following characteristics: a) The individual distributions all had negative medians (left head tilt) ranging from –0.2° to –3.0°, b) the combined median was -1.1°, c) for the combined distribution, roll head position standard deviation was larger than for the other visual environments, d) the IQR was –4.1° to +1.4° (5.5°), and e) based on virtually all of the statistics, there was a demonstrated preference for a negative (left) head tilt.

Table 2.
Combined roll head position summary by subject and visual environment.
(Time expressed in seconds; Other dimensional statistics expressed in degrees)

Subject	Visual Environment	Min	Max	Mean	Median	S.D.	IQR	Skew	Kurt
1	GVE	-35.4	21.3	-1.3	-1.1	6.8	- 4.1 to 1.4	-0.2	2.1
1	NVG	-24.9	15.3	-1.1	-0.7	6	- 3.4 to 1.5	-0.5	1.5
1	TIO	-15.3	6.3	-4.1	-3.9	2.3	- 5.3 to -2.7	-0.1	1.1
1	RWS	-13.4	18.2	-4.1	-3.8	2.4	- 5.4 to -2.5	-0.1	2.5
2	GVE	-25.6	26.3	1.9	1.7	8.2	- 2.5 to 6.6	0.0	0.2
2	NVG	-12.4	28.5	5.7	5.4	5.9	2.8 to 8.1	0.4	1.2
2	TIO	-10.8	10.7	-0.3	-0.6	3.6	-2.6 to 1.6	0.4	0.1
2	RWS	-11.7	12.1	0.5	0.3	3.3	-1.5 to 2.3	0.3	0.7
3	GVE	-22.5	26.2	4.9	4.5	7.7	0.5 to 8.8	0.1	0.3
3	NVG	-19.4	23.9	0.6	0.4	7.2	-3.2 to 3.8	0.3	0.5
3	TIO	-20.6	11.5	-3.1	-2.6	4.7	-6.3 to -0.2	-0.2	0.4
3	RWS	-19.3	15.6	-1.4	-1.7	5.4	-4.2 to 1.4	0.2	0.5
4	GVE	-32.1	24.0	0.6	0.3	10.1	-5.2 to 6.4	-0.0	-0.3
4	NVG	-22.5	26.9	1.6	1.0	9.4	-2.9 to 5.8	0.2	0.1
4	TIO								
4	RWS					None			

The combined NVG head position distribution statistics for subject #1 present the following characteristics: a) The individual distributions demonstrated consistent negative median and mean values, b) the combined median was –0.7°, c) head position standard deviation was the second largest of the four visual environments, and d) the IQR was –3.4° to +1.4° (4.8°).

The combined TIO head position distribution statistics for subject #1 present the following characteristics: a) The individual distributions demonstrated consistent negative median and mean values, b) the combined median was –3.9°, c) standard

17

deviation was similar for the RWS visual environment and was the smallest of the four visual environments, and d) the IQR was −5.3° to +2.7° (5.0°).

The combined RWS head position distribution statistics for subject #1 present the following characteristics: a) The individual distributions demonstrated consistent negative median and mean values b) the combined median was −3.8°, and very similar to that for TIO and c) the IQR was −5.4° to −2.5° (7.9°).

When these four visual environment characteristics were studied in comparison for subject #1, the following observations were made: a) The medians were all negative, with a distinctive similarity for the two HMD conditions, TIO and RWS, b) GVE had the largest IQR, c) TIO and RWS were very similar in characteristics and had the smallest standard deviations and the smallest IQRs, and d) for all visual environments, statistics showed a preference for negative (left) head roll.

Subject #2. The summary GVE head position distribution statistics for subject #2 present the following characteristics: a) The individual distributions had predominantly positive medians (right head tilt) ranging from −2.0 ° to +3.5°, b) the combined median was +1.7°, c) for the combined distribution, roll head position standard deviation was larger than for the other visual environments, d) the IQR was −2.5° to +6.6° (9.1°), and e) based on virtually all of the statistics, there was a demonstrated preference for a positive (right) head tilt.

The combined NVG head position distribution statistics for subject #2 present the following characteristics: a) The individual distributions demonstrated consistent positive median and mean values, b) the combined median was +5.4°, c) head position standard deviation was the second largest of the four visual environments, and d) the IQR was +2.8° to +8.1° (10.9°).

The combined TIO head position distribution statistics for subject #2 present the following characteristics: a) The individual distributions demonstrated consistent negative median values, b) the combined median was −0.6°, c) standard deviation was similar in size to that of the RWS visual environment, and d) the IQR was -2.6° to +1.6° (4.2°).

The combined RWS head position distribution statistics for subject #2 present the following characteristics: a) The individual distributions did not demonstrate any consistency of the head tilt directions for the median and mean values b) the combined median was +0.3°, c) the IQR was −1.5° to +2.3° (3.8°), and d) the standard deviation was similar to that of the TIO visual environment but was the smallest of the four visual environments.

When these four visual environment characteristics were studied in comparison for subject #2, the following observations were made: a) The medians were primarily positive with the exception of TIO, b) GVE had the largest IQR, c) TIO and RWS were

18

very similar in characteristics and had the smallest standard deviations and the smallest IQRs, and d) for all visual environments, statistics showed a preference for positive (right) head roll.

Subject #3. The summary GVE head position distribution statistics for subject #3 present the following characteristics: a) The individual distributions all had positive medians (right head tilt) ranging from +2.2° to +6.3°, b) the combined median was +4.5°, c) for the combined distribution, head roll position standard deviation was larger than for the other visual environments, d) the IQR was +0.7° to +8.8° (9.5°), and e) based on virtually all of the statistics, there was a demonstrated preference for a positive (right) head tilt.

The combined NVG head position distribution statistics for subject #3 present the following characteristics: a) The individual distributions demonstrated consistent positive median and mean values, b) the combined median was +0.4°, c) head position standard deviation was the second largest of the four visual environments, and d) the IQR was −3.2° to +3.8° (7.0°).

The combined TIO head position distribution statistics for subject #3 present the following characteristics: a) The individual distributions demonstrated consistent negative median and mean values, b) the combined median was −2.6°, c) standard deviation was similar for the RWS visual environment and was the smallest of the four visual environments, and d) the IQR was −6.3° to −0.2° (6.1°).

The combined RWS head position distribution statistics for subject #3 present the following characteristics: a) The individual distributions demonstrated consistently negative median and mean values b) the combined median was −1.7°, and similar to that for TIO and c) the IQR was −4.2° to +1.4° (5.6°).

When these four visual environment characteristics were studied in comparison for subject #3, the following observations were made: a) The medians and means had distinctive similarity for the two HMD conditions and the two non-HMD conditions, b) GVE had the largest IQR, c) TIO and RWS were very similar in characteristics and had the smallest standard deviations and the smallest IQRs, and d) for all visual environments, statistics did not show a preference for either negative (left) or positive (right) head roll.

Subject #4. The summary GVE head position distribution statistics for subject #4 present the following characteristics: a) The individual distributions have a mix of positive and negative medians (left and right head tilt) ranging from −1.9° to +2.0°, b) the combined median was +0.3°, c) for the combined distribution, roll head position standard deviation was larger than for NVG, d) the IQR was −5.2° to +6.4° (11.6°), and e) based on virtually all of the statistics, there was a slight preference for a positive (right) head tilt.

The combined NVG head position distribution statistics for subject #4 present the following characteristics: a) The individual distributions demonstrated consistent positive

median and mean values, b) the combined median was +1.0°, c) head position standard deviation and IQR were smaller than for GVE, and d) the IQR was –2.9° to +5.8° (8.7°).

When these two visual environment characteristics were studied in comparison for subject #4, the following observations were made: a) The medians and means were both positive, b) GVE had the larger standard deviation and IQR, c) for both visual environments, statistics showed a preference for positive (right) head roll.

Note: Head position data for subject #4 were not available for TIO and RWS visual environments.

Graphical comparisons

While considerable information is available in Table 2, and several pages have been spent enumerating and comparing the distribution characteristics presented in Table 2, distributions are often better understood through graphical techniques. While the shapes of the head position distributions under analysis generally appear to be symmetrical, no conclusion about normality can be made at this point. Graphical techniques such as box plots can provide excellent methods of comparing distributions.

The box plot technique provides a visual summary of a data set by emphasizing a select set of statistic values, e.g., median, quartiles, and IQR. Box plots for combined roll position distributions for all subjects are presented in Figures 10-13. Individual box plots for all subjects by visual environment are presented in Appendix C.
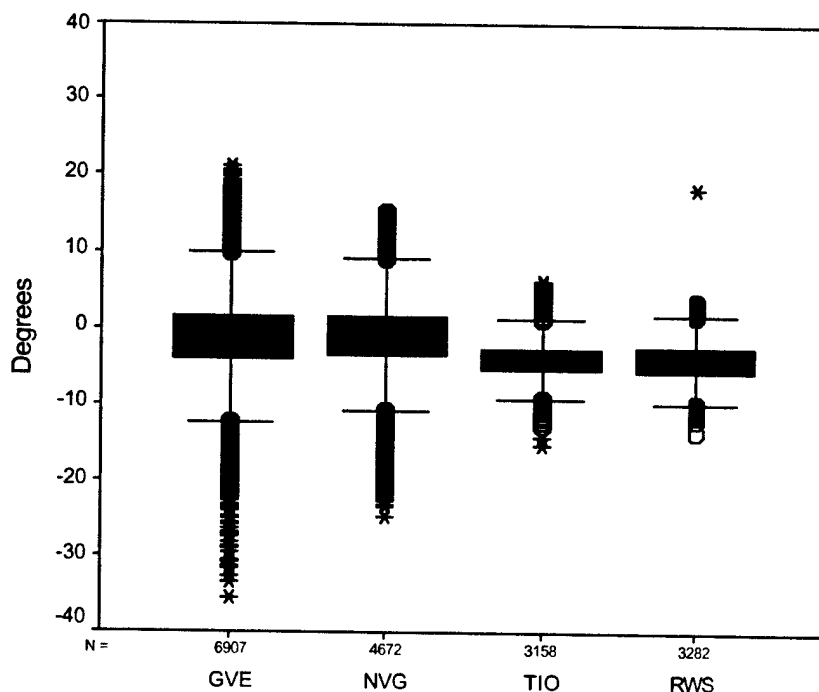
Figure 10. Combined roll position box plots for subject #1.

20
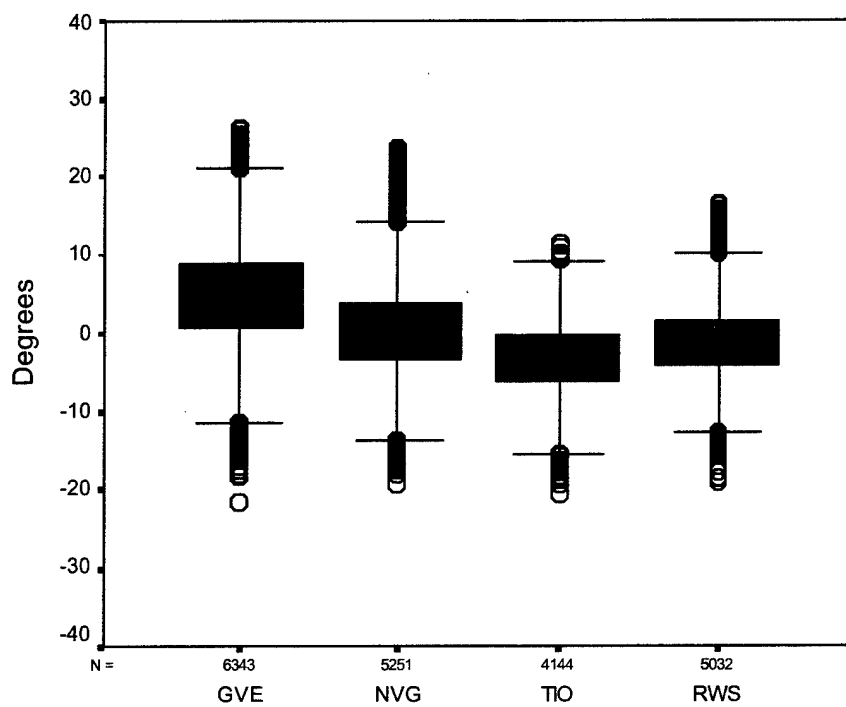
Figure 11. Combined roll position box plots for subject #2.
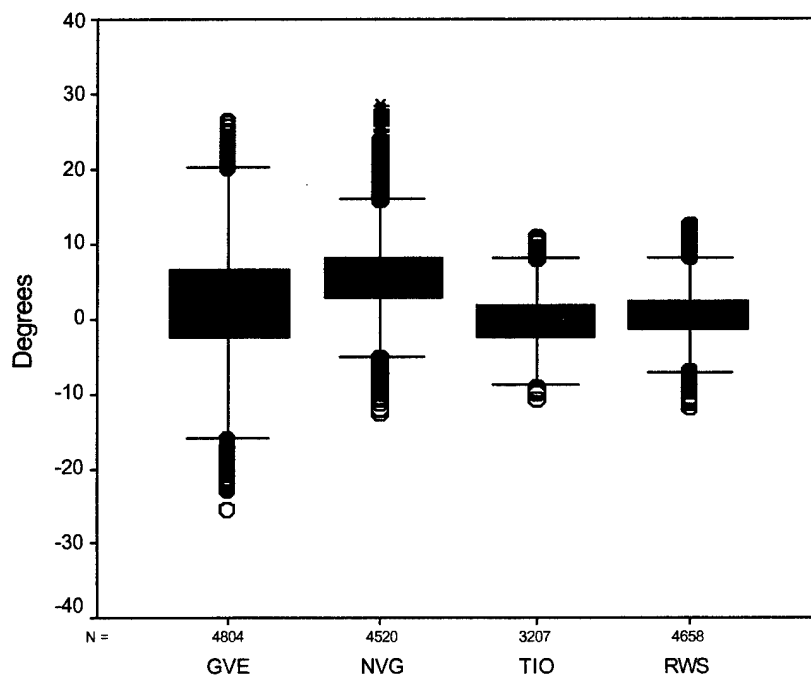
Figure 12. Combined roll position box plots for subject #3.
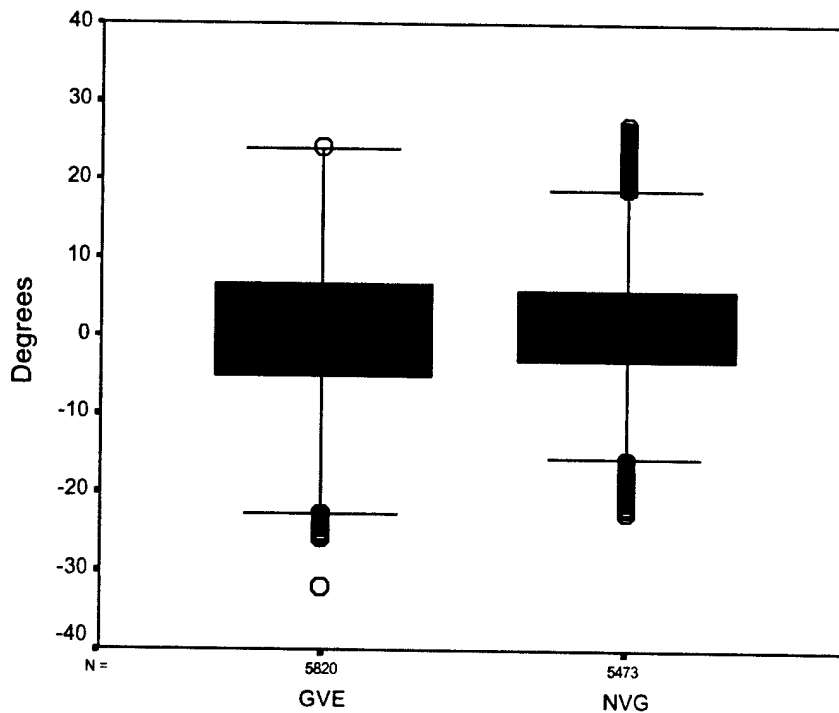
Figure 13. Combined roll position box plots for subject #4.

From the combined box plots for subject #1 in Figure 10, the following characteristics and trends can be construed: a) The GVE and NVG have the largest IQRs and are similar in size, b) the IQRs for the TIO and RWS also are similar, c) the GVE and NVG medians are relatively the same, as are those for TIO and RWS, and d) roll positions for TIO and RWS were distinctly negative (left tilted).

From the combined box plots for subject #2 in Figure 11, the following characteristics and trends can be construed: a) The GVE has the largest IQR, b) the NVG has the most positive (right head roll tilt), and c) the TIO and RWS are most similar in shape.

From the combined box plots for subject #3 in Figure 12, the following characteristics and trends can be construed: a) The GVE has the largest range and IQR, b) GVE and NVG medians are positive (right shifted), and c) the TIO and RWS are most similar in shape.

From the combined box plots for subject #4 in Figure 13, the following characteristics and trends can be construed: a) The GVE has the greater IQR, and b) the medians are both slightly positive (right tilt).

Distribution comparison

The comparison of distributions is generally accomplished using a chi-square goodness of fit test. However, as was shown in the azimuth position study (Rostad et al., 2001), this test was not found to be meaningful. This finding was not surprising since the argument previously presented for comparing combined distributions rather than individual distributions pointed out the often considerable differences between the specific characteristics of individual head position

22

distributions even for the same subject performing the same maneuver with same visual environment. For this reason, the validity of using the chi-square statistic to test for differences in the combined distribution was compromised.

Because the chi-square statistic could not be used to meaningfully test for differences between combined head position distributions, another approach was investigated. In the azimuth analysis of the histograms, the distribution moments, and the graphical plots, a common trend was noticed. In each analysis, there seemed to be a strong indication that the spread of the head positions for the four visual environments exhibited a common rank order. It was concluded that the IQR was the best metric for comparing the position distributions. In the investigation of elevation head position, no distribution spread statistic was found to be significant in discriminating between elevation position distributions for the four visual environments. However, the two measures of central tendency, the mean and median, were found to be consistently greater in the downward direction for the GVE and NVG conditions than for the two HMD conditions, TIO and RWS.

To investigate any trends in the current roll data, Table 3 was constructed to allow comparison of various spread statistics, which included the IQR, the range, and the standard deviation. Ranking within subjects is provided in parentheses.

<div align="center">

Table 3.

Comparison of IQR, range and standard deviation for combined distributions.
(expressed in degrees, ranks within subject given in ( ))

</div>

Subject	Visual environment	IQR	Range	S.D.
1	GVE	5.5 (1)	56.7 (1)	6.8 (1)
1	NVG	4.9 (2)	40.2 (2)	6.0 (2)
1	TIO	2.6 (4)	21.6 (4)	2.3 (4)
1	RWS	2.9 (3)	31.6 (3)	2.4 (3)
2	GVE	9.1 (1)	51.9 (1)	8.2 (1)
2	NVG	5.3 (2)	40.9 (2)	5.9 (2)
2	TIO	4.2 (3)	21.5 (4)	3.6 (3)
2	RWS	3.8 (4)	23.8 (3)	3.3 (4)
3	GVE	9.3 (1)	48.7 (1)	7.7 (1)
3	NVG	7.0 (2)	43.3 (2)	7.2 (2)
3	TIO	6.1 (3)	32.1 (4)	4.7 (4)
3	RWS	5.6 (4)	35.9 (3)	5.4 (3)
4	GVE	11.6 (1)	56.1 (1)	10.1 (1)
4	NVG	8.7 (2)	49.4 (2)	9.4 (2)

Table 3, at first glance, suggests a strong trend in the ranks of the various spread statistics within subjects for the four visual conditions. This observation is borne out in Table 4, where

the Spearman rank-correlation values show extremely strong associations between the spread statistics and visual environments. For the range spread statistic, there was a perfect correlation. GVE had the largest head roll range, followed by NVG, RWS and TIO, for each subject. For the IQR and standard deviation spread statistics, the two nonHMD visual condition values were always larger than for the two HMD visual conditions. For all three spread statistics, GVE was always the largest, followed by NVG.

Table 4.
Spearman rank-correlation coefficients for IQR, range and standard deviation for combined distributions.

IQR						Range						S.D.			
	#1	#2	#3	#4			#1	#2	#3	#4			#1	#2	#3	#4
#1		+0.8	+0.8	+1.0		#1		+1.0	+1.0	+1.0		#1		+0.8	+1.0	+1.0
#2			+1.0	+1.0		#2			+1.0	+1.0		#2			+0.8	+1.0
#3				+1.0		#3				+1.0		#3				+1.0
#4						#4						#4				

In summary, the investigation of roll head position found that all three distribution spread statistics could be used to discriminate between roll position distributions for the four visual environments.

Rate analyses

Up to this point, all of the characteristics of head roll motion that have been investigated have related to position. As was learned in the azimuth and elevation position analysis studies (Rostad et al., 2001; Rostad and Rash, 2002), additional information regarding head motion can be obtained from investigating the frequencies, magnitudes and rates (velocities) of change in head position. Three characteristics for an investigation of change in head position are reversals, excursions, and head velocities. Reversals, which measure frequency of head movement, are defined as the number of times that the pilot changes movement from one direction to the other during the cycle. Excursions (magnitudes) are a measurement of the angular distance that the pilot's head travels in degrees between reversals, and velocities are a measure of the rate of speed in which the pilot moves his head during excursions.

Reversals

This temporal characteristic is based on the number of times the pilot reverses head movement from one direction to the other, e.g., reversing from moving upward to moving downward. To account for the differences in run times, a reversal rate, expressed as the number of reversals per minute, was adopted. Tables D-1 to D-4 in Appendix D present the number of reversals and reversal rates for each run for all subjects by visual environment. Mean reversal rates were calculated and are presented in Table 5, with rank orders within subjects provided in parentheses. These mean reversal rates are plotted with ±1 standard deviation bars in Figure 14.

24

Table 5.
Mean roll reversal rates.

	Subject #1	Subject #2	Subject #3	Subject #4
GVE	37.5 (4)	35.0 (2)	31.0 (3)	28.0 (2)
NVG	40.5 (3)	38.5 (1)	35.0 (2)	31.1 (1)
TIO	40.7 (2)	32.2 (4)	36.2 (1)	
RWS	43.0 (1)	34.5 (3)	30.9 (4)	

Note: Means expressed in reversals per minute.

In Rostad et al. (2003), mean reversal rate was found to be, at best, only a weak indicator of the difference in azimuth and elevation head motion within the four different visual environments. An examination of Figure 14 for head roll shows considerable variability in the mean reversal rates between visual environments for all of the subjects. As with the measures of dispersion, ranking of these rates appears to be the only meaningful analysis. However, an inspection of the ranks presented in Table 5 seems to provide no clear trend. To objectively test this observation, the Spearman rank-correlation was used to test correlation between subjects (Table 6). Due to the variation across subjects and the lack of sample size, mean reversal rate does not appear to be a useful indicator of the difference in head roll motion within the four different visual environments.
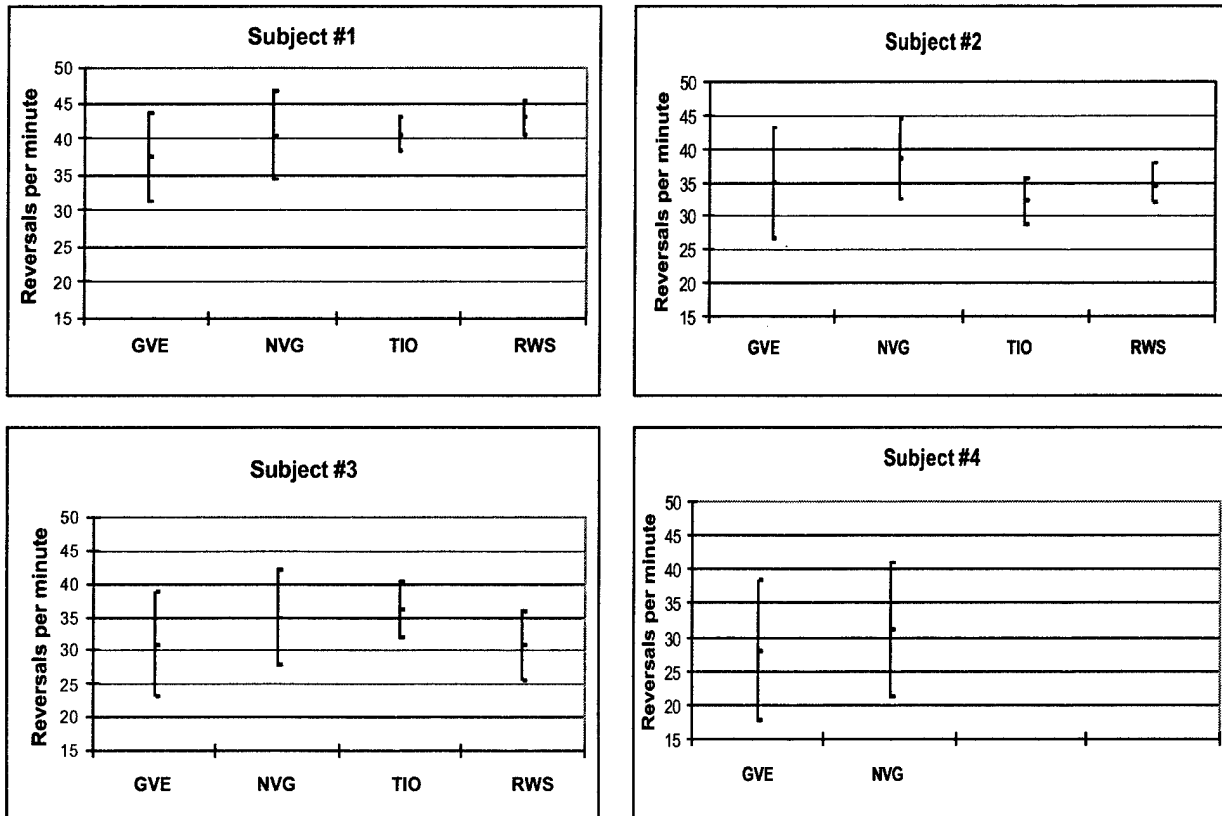
Figure 14. Reversal standard deviation charts showing ±1 standard deviation and means by subject, by visual environment.

Table 6.
Spearman ranking correlation for mean roll reversal rates.

Reversal Rates				
	#1	#2	#3	#4
#1		-0.6	-0.2	+1.0
#2			-0.2	+1.0
#3				+1.0
#4				

Excursions

An additional temporal characteristic investigated was head excursions. An excursion is defined as the distance the pilot moved his head between reversals expressed in degrees. Distribution histograms for excursion values for individual runs for each subject and visual environment are presented in Appendix E. Combined histograms overlaid with cumulative frequency curves are shown in Figures 15-18. Excursion values representing the 25th-, 50th-, 95th-, and 99th-percentile points are presented in Table 7 for the combined excursion distributions. Tables summarizing the roll excursion data by subject and visual environment are presented Appendix F. Excursion box plots are presented in Appendix G.

Examining the histograms, tables and box plots (Appendices E-G, respectively), the following observations or features were noted. First, the distributions of excursion values varied greatly even for individual runs for a given subject and visual condition. Second, across all subjects and visual environments, the largest head roll excursion recorded was 44.0°. For all subjects, across all visual conditions, 95% of the excursions were 16° or less in size. From Table 7, the 25th-percentile values typically were 2° for each subject for nonHMD visual conditions, and 1° for HMD visual conditions; the 50th-percentile values were between 2° and 4°, with a value of 4° for nonHMD visual conditions, and 2°-3° for HMD visual conditions. An inspection of 95th and 99th-percentile values showed no clear trend between visual conditions, with the exception of higher values for GVE. Based on these values, there is a slight suggestion that the added head supported weight of the NVG and two HMD conditions appeared to have had an influence on the distribution of head excursions.

Overall, examination of the distribution of the head excursions provided no definitive differences between the four visual environments.

In an attempt to obtain an overall sense of the range of roll excursions exhibited by all of the pilots for all of the visual environments, a histogram of excursion size combined across all runs was constructed (Figure 19). This overall distribution has the following statistics: mean of 4.8°, median of 3.0°, standard deviation of 5.2°, and IQR of 4.0°. An overlaid cumulative frequency curve indicates 50% of all excursions were 3° or less. The 95% and 99% excursion values were

16° and 24°, respectively. The largest (maximum) excursion exhibited by any pilot during any run was 44.0°.
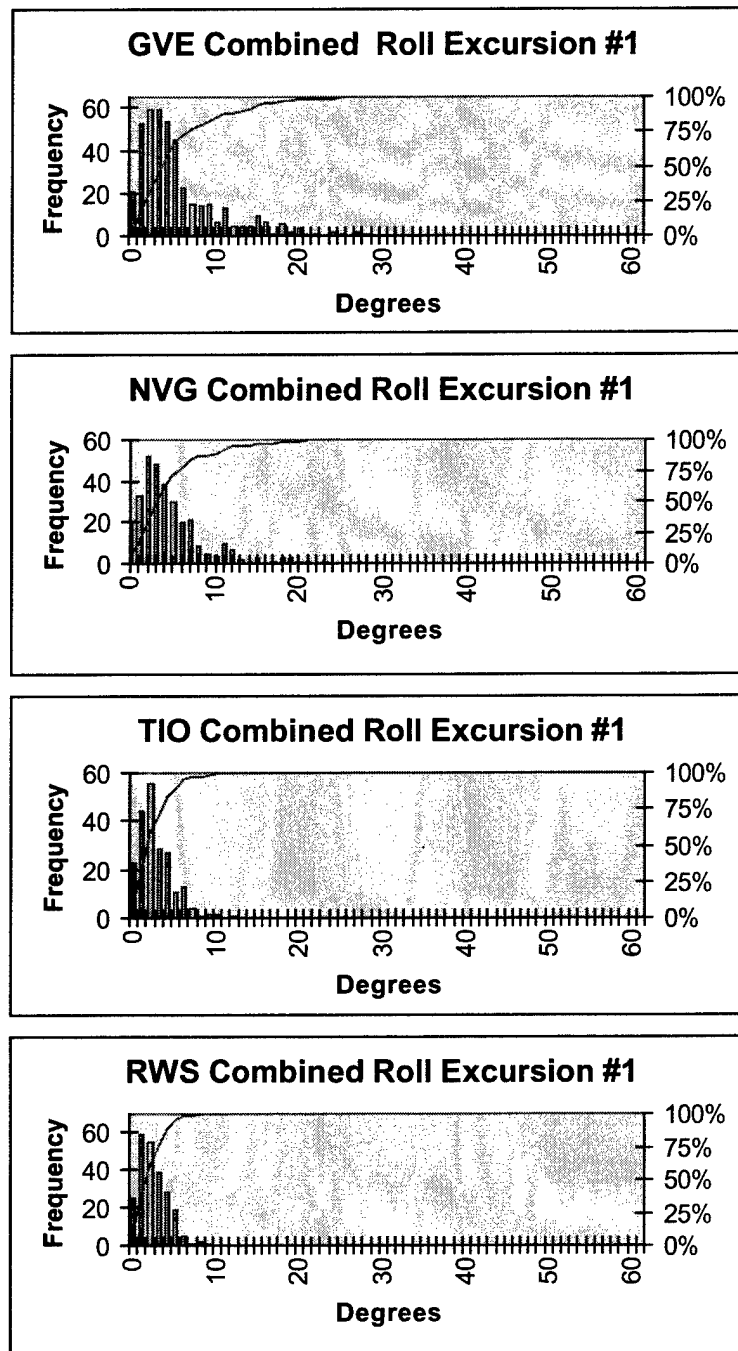
Figure 15. Subject #1 combined excursion histograms by flight type with cumulative frequency curve.
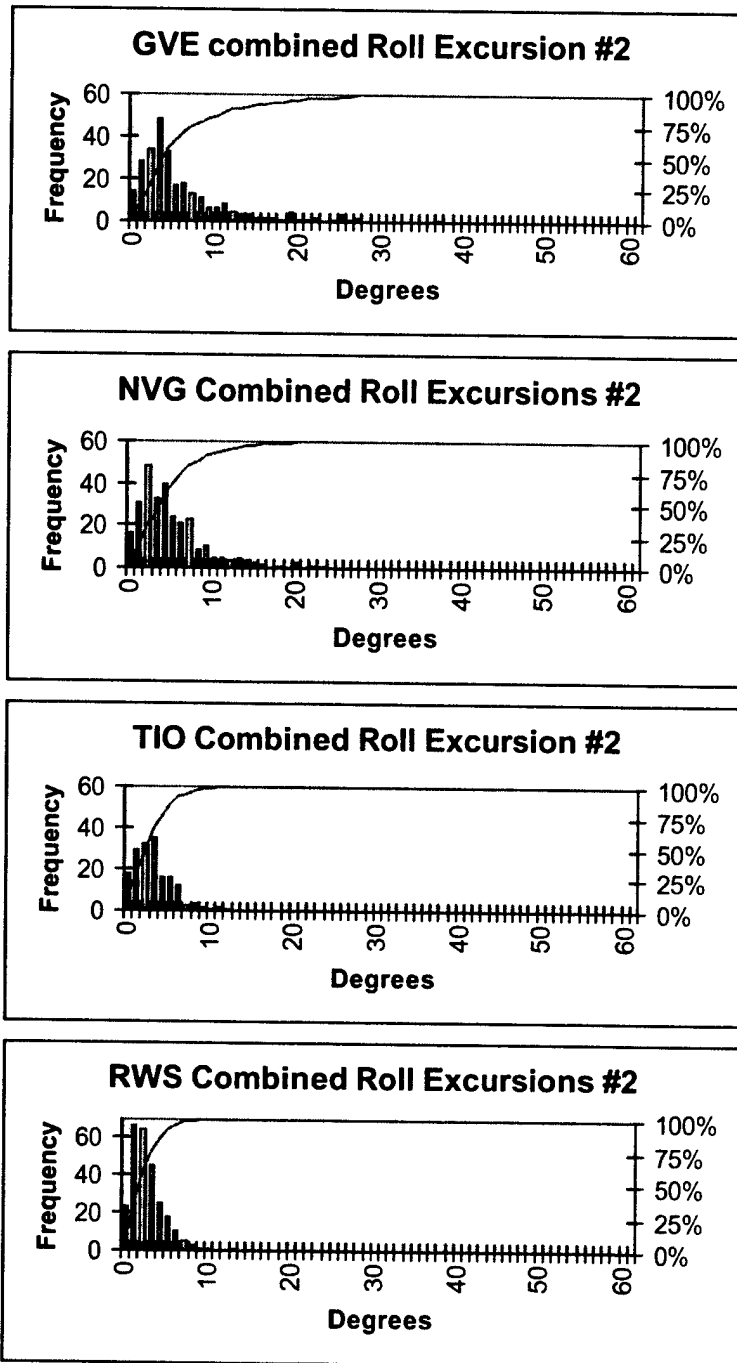
Figure 16. Subject #2 combined excursion histograms by flight type with cumulative frequency curve.

GVE Combined Roll Excursion #3

NVG Combined Roll Excursion #3

TIO Combined Roll Excursion #3

RWS Combined Roll Excursion #3
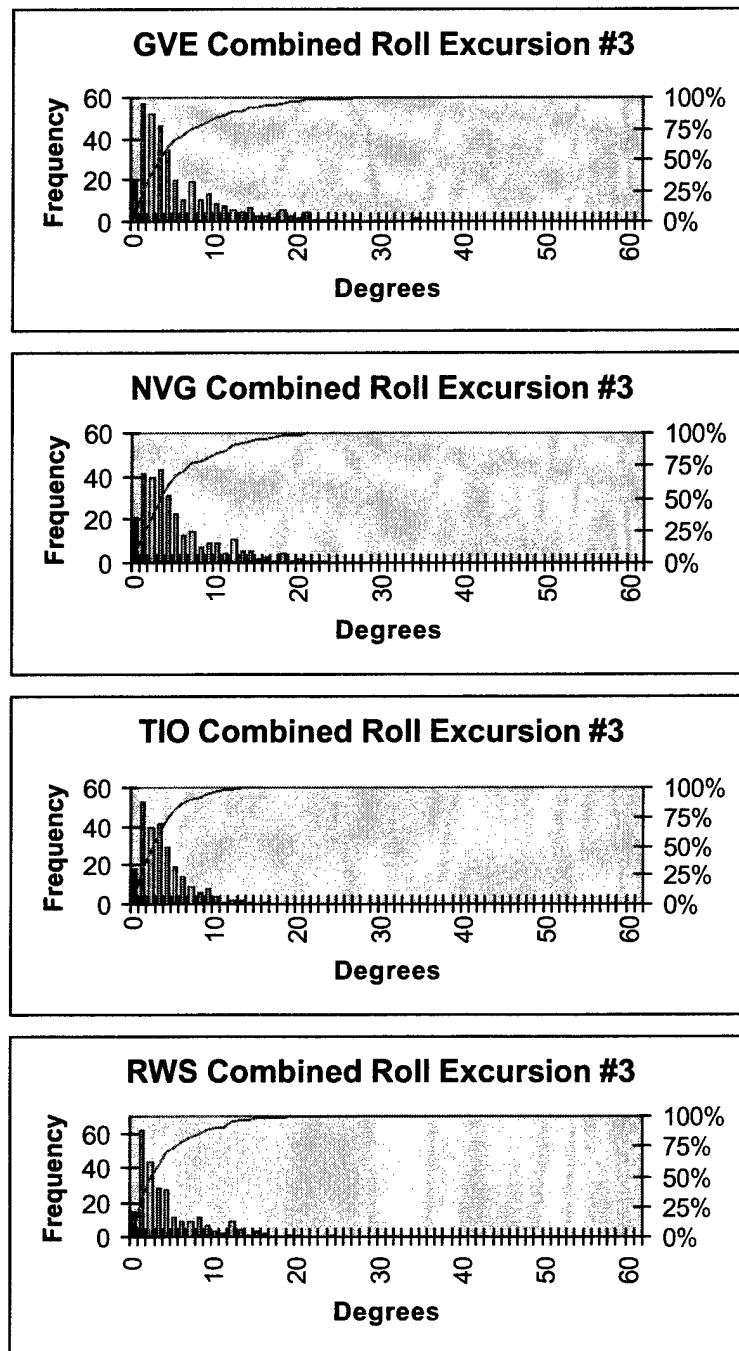
Figure 17. Subject #3 combined excursion histograms by flight type with cumulative frequency curve.

29
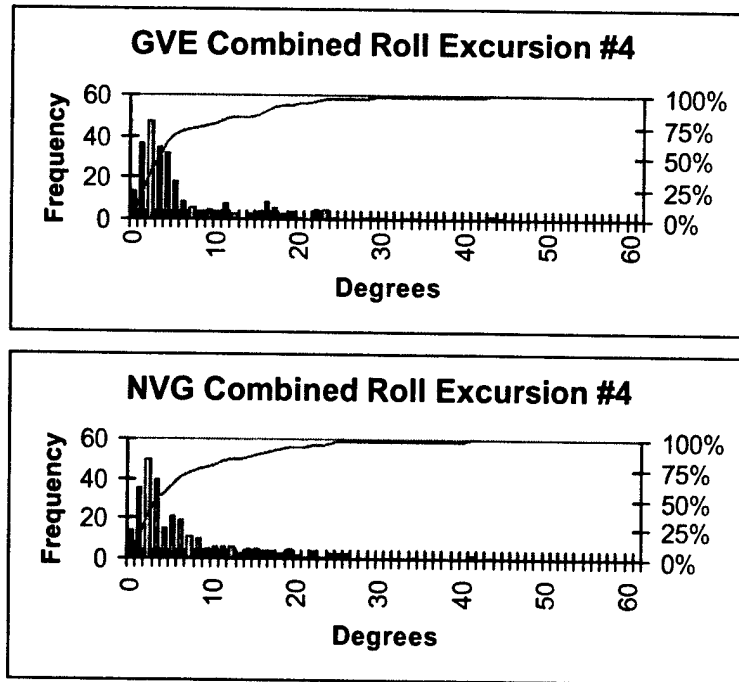
Figure 18. Subject #4 combined excursion histograms by flight type with cumulative frequency curve.
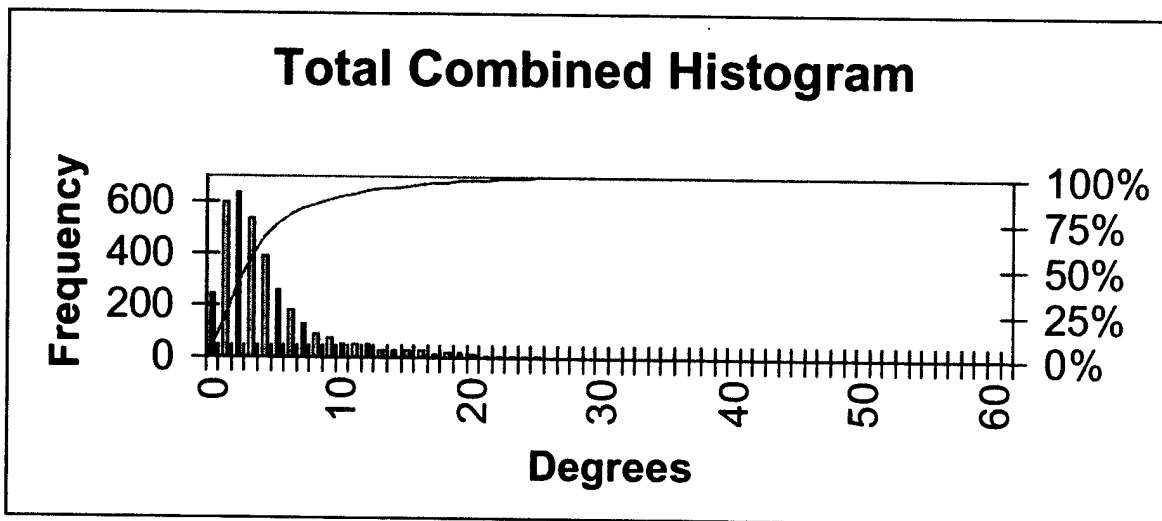
Figure 19. Overall excursion histogram for all subjects, for all visual environments.

Table 7.
Cumulative excursion percentile values (expressed in degrees).

Subject	Flight Environment	25%	50%	95%	99%
Subject #1	GVE	2	4	16	2
	NVG	2	4	2	1
	TIO	1	2	6	10
	RWS	1	2	5	8
Subject #2	GVE	2	4	19	27
	NVG	2	4	14	20
	TIO	1	3	8	11
	RWS	1	2	6	9
Subject #3	GVE	2	4	18	24
	NVG	2	4	16	1
	TIO	1	3	9	13
	RWS	1	3	13	19
Subject #4	GVE	2	4	23	43
	NVG	2	4	22	41
	TIO	None			
	RWS				

Velocity

For these analyses, all velocity values were expressed as positive in nature. There was no attempt to separate velocities of motions (tilt or roll) to the left or to the right. Velocity values were calculated from the time-sequenced elevation position data using an algorithm based on the central derivative (Bloch, 2000). The algorithm calculated the instantaneous velocities at the middle of a moving three-point interval of the time-sequenced data. Velocities at the initial and final data points were not calculated. An inspection of the resulting velocities verified there were no artifacts introduced by the derivative process.

Velocity distribution histograms

As with head position data, the use of histograms to represent the velocity distributions is a fundamental technique in the understanding of head motion. The histograms presented herein use 1-degree per second (°/sec) intervals. Also, as with the position data, for the combinations of four subjects, four visual environments and two LOAs, there were 103 roll velocity distributions available for analysis.

Individual velocity distributions. Subject #1 has a total of 25 velocity histograms that represent the various combinations of LOA, run type and visual environment; subject #2 has 24

31

histograms; subject #3 has 34 histograms; and subject #4 has 20 histograms. The resulting individual velocity histograms, with cumulative frequency curves overlaid, are presented in Appendix H. Examining these individual histograms for general characteristics and trends for each subject and visual condition yields the following:

<u>Subject #1</u>. The individual GVE head velocity distributions for subject #1 (Figure H-1) present the following characteristics: a) Cumulative frequency curves become asymptotic at velocities approximately 20°/sec to 30°/sec, and b) the beginning slopes of the cumulative frequency curves generally are not very steep, implying that the low velocity values are spread out.

NVG head velocity distributions for subject #1 (Figure H-2) present the following characteristics: a) Cumulative frequency curves become asymptotic at velocities approximately 15°/sec to 25°/sec, and b) the beginning slopes of the cumulative frequency curves are steeper than for the GVE visual.

TIO head velocity distributions for subject #1 (Figure H-3) present the following characteristics: a) Cumulative frequency curves become asymptotic at velocities near 15°/sec, and b) the beginning slopes of the cumulative frequency curves are steeper than for the GVE and NVG visual conditions.

RWS head velocity distributions for subject #1 (Figure H-4) present the following characteristics: a) Cumulative frequency curves become asymptotic at velocities near 15°/sec, and b) the beginning slopes of the cumulative frequency curves are steeper than for the GVE and NVG visual conditions comparably as steep as the TIO visual environment.

<u>Subject #2</u>. The GVE head velocity distributions for subject #2 (Figure H-5) present the following characteristics: a) Cumulative frequency curves become asymptotic at velocities approximately 25°/sec to 35°/sec and b) the beginning slopes of the cumulative frequency curves have a gradual rise implying that the frequency of the low velocity values are spread out over a larger range.

NVG head velocity distributions for subject #2 (Figure H-6) present the following characteristics: a) Cumulative frequency curves become asymptotic at velocities approximately 15°/sec to 20°/sec, and b) the beginning slopes of the cumulative frequency curves are steeper than for the GVE visual condition.

TIO head velocity distributions for subject #2 (Figure H-7) present the following characteristics: a) Cumulative frequency curves become asymptotic at velocities approximately 15°/sec, and b) the beginning slopes of the cumulative frequency curves are steeper than the GVE, but similar to NVG visual conditions.

RWS head velocity distributions for subject #2 (Figure H-8) present the following characteristics: a) Cumulative frequency curves become asymptotic at velocities

32

approximately 12-15°/sec , and b) the beginning slopes of the cumulative frequency curves are steeper than for the GVE and NVG, but slightly steeper than TIO.

Subject #3. The GVE head velocity distributions for subject #3 (Figure H-9) present the following characteristics: a) Cumulative frequency curves are not consistent and become asymptotic at velocities between 20-25°/sec, and b) the beginning slopes of the cumulative frequency curves vary, but in general have a gradual rise implying that the frequency of the low velocity values are spread out over a larger range.

NVG head velocity distributions for subject #3 (Figure H-10) present the following characteristics: a) Cumulative frequency curves become asymptotic at velocities between 25°/sec and 35°/sec, and b) the beginning slopes of the cumulative frequency curves are even more gradual than for the GVE visual condition.

TIO head velocity distributions for subject #3 (Figure H-11) present the following characteristics: a) Cumulative frequency curves become asymptotic at velocities between 15-20°/sec, and b) the beginning slopes of the cumulative frequency curves are steeper than for GVE and NVG.

RWS head position distributions for subject #3 (Figure H-12) present the following characteristics: a) Cumulative frequency curves become asymptotic at velocities between 15-25°/ sec, and b) the beginning slopes of the cumulative frequency curves for RWS are not as steep as for TIO.

Subject #4. The GVE head velocity distributions for subject #4 (Figure H-13) present the following characteristics: a) Cumulative frequency curves become asymptotic at velocities between 20-25°/sec, and b) the beginning slopes of the cumulative frequency curves are generally not very steep, implying that the low velocity values are spread out.

NVG head velocity distributions for subject #4 (Figure H-14) present the following characteristics: a) Cumulative frequency curves become asymptotic at velocities of between 20-25°/sec, and b) the beginning slopes of the cumulative frequency curves are similar to the GVE visual condition.

Note: Head position data for subject #4 were not available for TIO and RWS visual environments.

Combined velocity histograms. As with the position data, it is argued that combined velocity histograms are more useful in understanding the general (average) nature of head velocities present in the shalom course flown in this study. Figures 20-23 present the combined velocity distributions by subject and visual environment. Note that head velocity data for subject #4 were available for only two visual environments, GVE and NVG. As with the individual distributions, these combined distributions can be examined visually for general characteristics and trends. The following observations are made:

33

Subject #1. The combined GVE head velocity distribution for subject #1 (Figure 20) present the following characteristics: a) The cumulative frequency curve becomes asymptotic near 32°/sec, and b) the 50-percent velocity value is 6°/sec.

The combined NVG head velocity distribution for subject #1 (Figure 20) shows: a) The cumulative frequency curve becomes asymptotic at around 25°/sec, and b) the 50-percent velocity value is 4°/sec.

The combined TIO head velocity distribution for subject #1 (Figure 20) shows: a) The cumulative frequency curve becomes asymptotic near 20°/sec, and b) the 50-percent velocity value is 3°/sec.

The combined RWS head velocity distribution for subject #1 (Figure 20) shows: a) the cumulative frequency curve becomes asymptotic near 18°/sec, and b) the 50-percent velocity value is 3°/sec.

Subject #2. The combined GVE head velocity distribution for subject #2 (Figure 21) present the following characteristics: a) The cumulative frequency curve becomes asymptotic near 36°/sec, and b) the 50-percent velocity value is 5°/sec.

The combined NVG head velocity distribution for subject #2 (Figure 21) present the following characteristics: a) The cumulative frequency curve become asymptotic near 24°/sec, and b) the 50-percent velocity value is 4°/sec.

The combined TIO head velocity distribution for subject #2 (Figure 21) shows: a) The cumulative frequency curve becomes asymptotic near 20°/sec, and b) the 50-percent velocity value is 4°/sec.

The combined RWS head velocity distribution for subject #2 (Figure 21) shows: a) The cumulative frequency curve becomes asymptotic near 18°/sec, and b) the 50-percent velocity value is 3°/sec.

Subject #3. The combined GVE head velocity distribution for subject #3 (Figure 22) present the following characteristics: a) The cumulative frequency curve becomes asymptotic near 28°/sec, and b) the 50-percent velocity value is 5°/sec.

The combined NVG head velocity distribution for subject #3 (Figure 22) present the following characteristics: a) The cumulative frequency curve becomes asymptotic near 30°/sec, and b) the 50-percent velocity value is 5°/sec.

The combined TIO head velocity distribution for subject #3 (Figure 22) shows: a) The cumulative frequency curve becomes asymptotic near 24°/sec, and b) the 50-percent velocity value is 4°/sec.

Head Roll Velocity GVE Total

Head Roll Velocity NVG Total

Head Roll Velocity TIO Total

Head Roll Velocity RWS Total
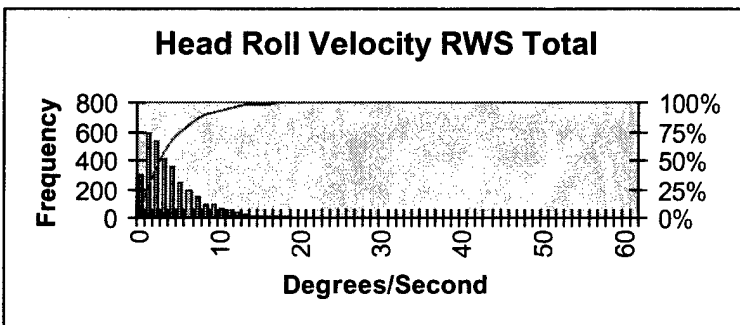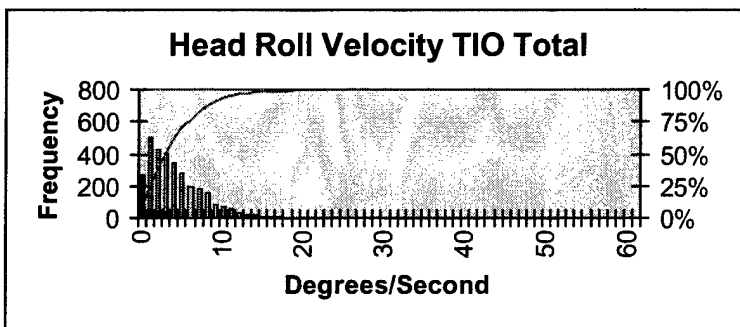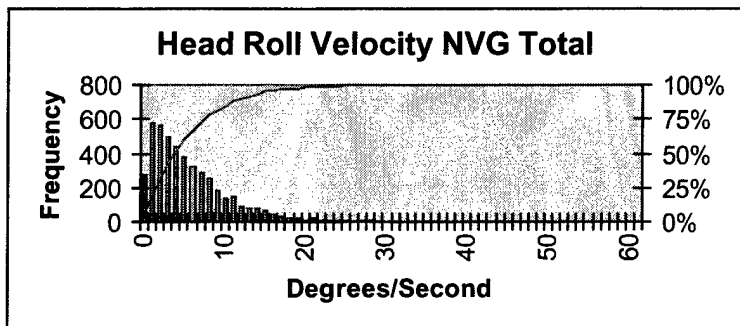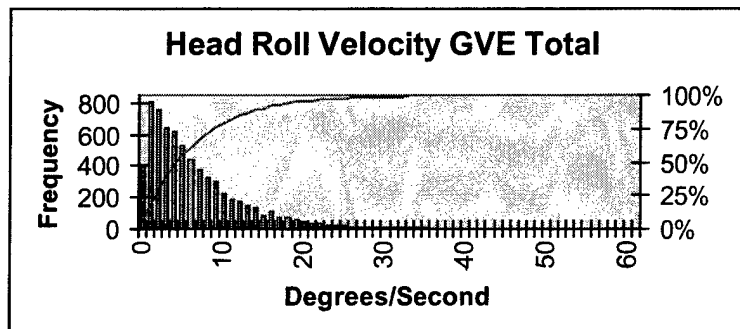
Figure 20. Combined velocity histograms for subject #1.
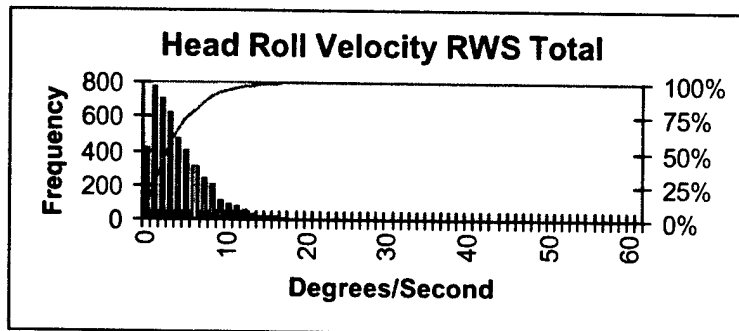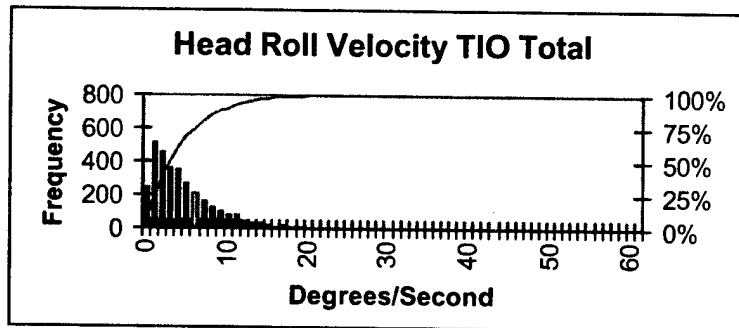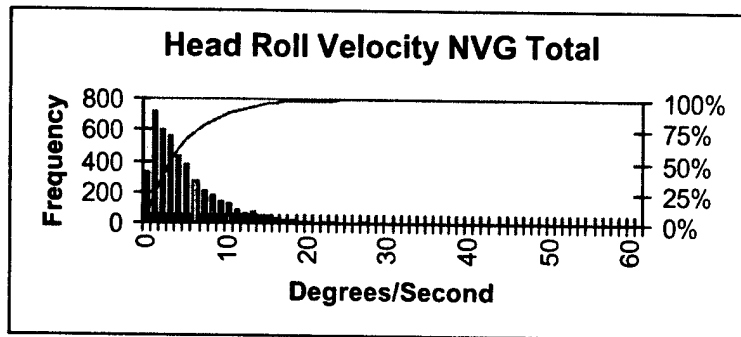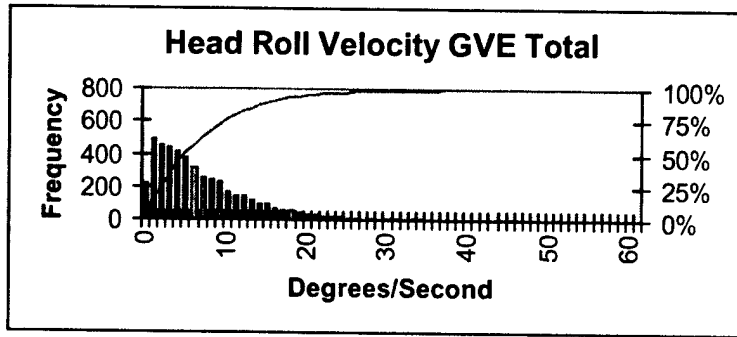
Figure 21. Combined velocity histograms for subject #2.
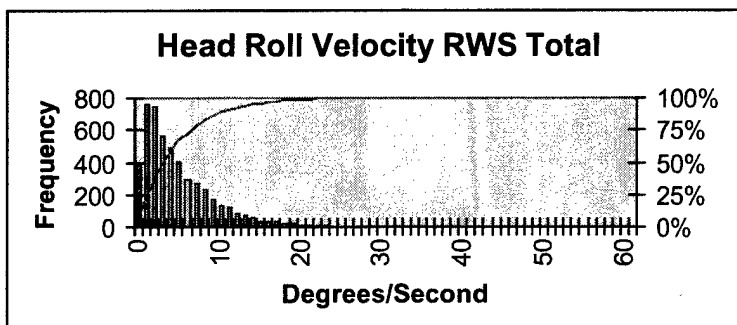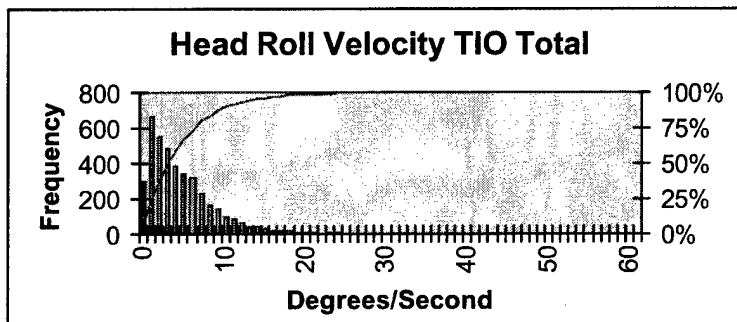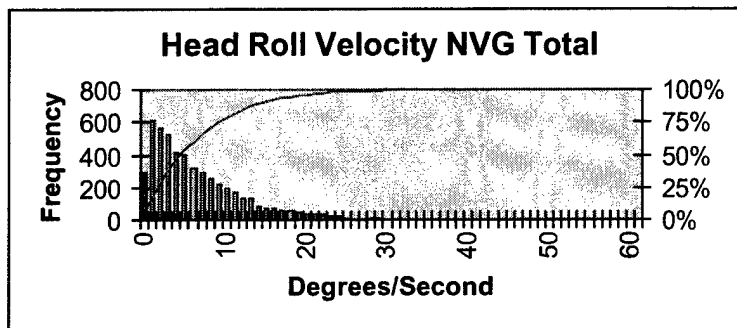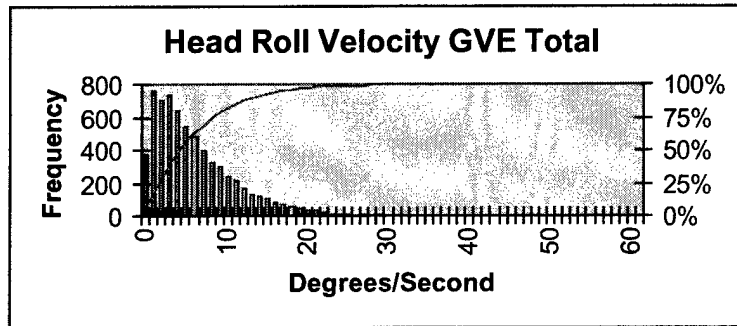
Figure 22. Combined velocity histograms for subject #3.

Head Roll Velocity GVE Total

[Chart: Frequency (0 to 800) vs Degrees/Second (0 to 60), with cumulative frequency curve on right axis 0% to 100%]

Head Roll Velocity NVG Total

[Chart: Frequency (0 to 800) vs Degrees/Second (0 to 60), with cumulative frequency curve on right axis 0% to 100%]
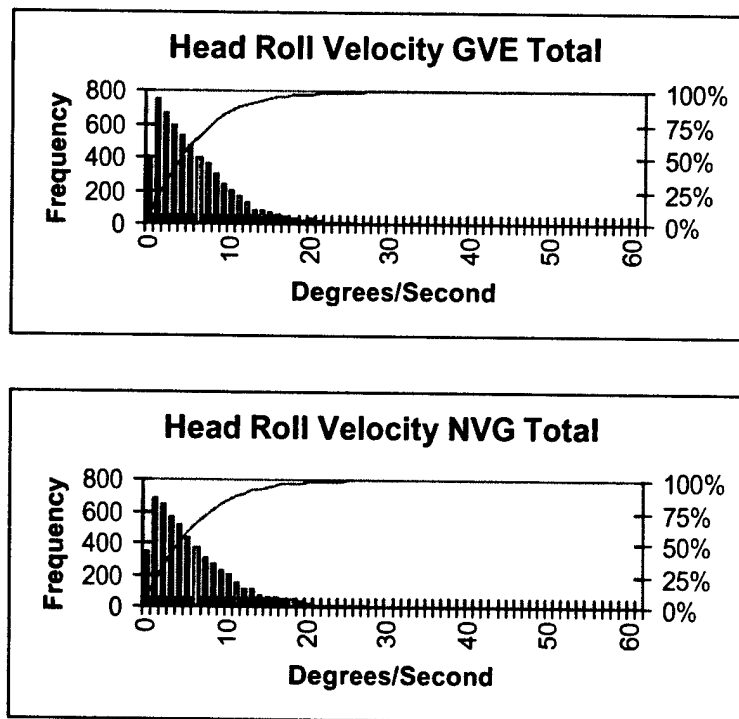
Figure 23. Combined velocity histograms for subject #4.

The combined RWS head velocity distribution for subject #3 (Figure 22) shows: a) The cumulative frequency curve asymptotic near 22°/sec, and b) the 50-percent velocity value is 4°/sec.

Subject #4. The combined GVE head velocity distribution for subject #4 (Figure 23) present the following characteristics: a) The cumulative frequency becomes asymptotic at around 27°/sec, and b) the 50-percent velocity value is 4°/sec.

The combined NVG head velocity distribution for subject #4 (Figure 23) present the following characteristics: a) The cumulative frequency curve becomes asymptotic at around 25°/sec, and b) the 50-percent velocity value is 4°/sec.

When the above observations are examined across subjects, the 50-percent velocity values range from 3-6°/sec for all visual conditions. In general, the asymptotic velocity values are greater for the GVE and NVG visual conditions. For subjects #1-3, the standard deviations in the roll velocity values are greater for the GVE and NVG conditions than for the two HMD conditions (TIO and RWS).

As with excursions, it was useful to construct a histogram that represents all velocities exhibited by all pilots during all runs (Figure 24). This overall distribution has the following statistics: mean of 5.7°/sec, median of 4°/sec, standard deviation of 5.5°/sec, and IQR of 6°/sec. An overlaid cumulative frequency curve indicates that 50% of all velocities were 4°/sec or less.

The 95% and 99% velocity values were 16°/sec and 25°/sec, respectively. The largest (maximum) roll velocity exhibited by any pilot during any run was 119°/sec.
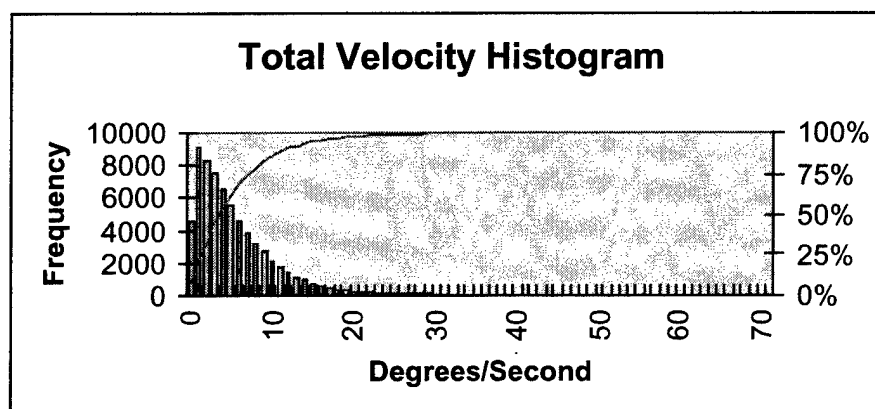
Figure 24. Overall roll velocity histogram for all subjects, for all visual environments.

Velocity distribution statistics

While distribution shape provides a basic understanding of the ongoing head motion, the semi-quantitative nature of distribution histograms does not allow for comprehensive comparison. For this reason, distributions often are described further by the distribution's moments and other additional statistics. For the velocity distributions presented herein, the maximum, mean, median, standard deviation, and IQR have been calculated.

Summary individual and combined distribution moments and statistics tables for all subjects, grouped by visual environment, are provided in Appendix I. However, following the previous arguments that comparisons can be based on the combined distributions, a summary of the calculated distribution moments and statistics by subject and visual environment for the combined distributions only is presented in Table 8. Provided in parentheses beside each value is the within subject rank of that value for the selected statistic.

To investigate the trend in ranking amongst the various velocity statistics, Tables 9 and 10 present the Spearman rank-correlation coefficients for two measures of central tendency, mean and median, and two measures of dispersion, standard deviation and IQR. While remembering that correlation coefficients involving subject #4 should be given less weight because only GVE and NVG data were available, the Spearman rank-correlation tests showed a weak to moderate association between the visual environment and the mean, median, standard deviation, and IQR. In other words, roll velocity distributions failed to provide a methodology for discriminating roll head motion between the four visual environments. However, it may be noted that the values of these four statistics were consistently higher for the two nonHMD visual environments, GVE and NVG.

39

Table 8.
Combined roll velocity summary by subject and visual environment.
Time expressed in seconds; other dimensional statistics expressed in °/sec, ranks within subject given in ( ).

Subject	Visual Environment	Time	Max	Mean	Median	S.D.	IQR
1	GVE	690.6	62.0	8.2 (1)	6.0 (1)	7.8 (1)	3.0 to 11.0 (1)
1	NVG	467.2	43.0	5.8 (2)	4.0 (2)	5.1 (2)	2.0 to 8.0 (2)
1	TIO	315.8	45.0	4.3 (3)	3.0 (3.5)	3.9 (4)	2.0 to 6.0 (4)
1	RWS	328.2	95.0	4.0 (4)	3.0 (3.5)	4.2 (3)	1.0 to 6.0 (3)
2	GVE	480.4	119.0	7.4 (1)	5.0 (1)	7.3 (1)	3.0 to 10.0 (1)
2	NVG	452.0	63.0	5.0 (2)	4.0 (2.5)	5.0 (2)	2.0 to 7.0 (2.5)
2	TIO	320.7	34.0	4.6 (3)	4.0 (2.5)	4.2 (3)	2.0 to 6.0 (4)
2	RWS	465.8	46.0	4.1 (4)	3.0 (4)	3.6 (4)	1.0 to 6.0 (2.5)
3	GVE	677.7	53.0	6.3 (2)	5.0 (1.5)	5.8 (2)	2.0 to 9.0 (1.5)
3	NVG	525.1	63.0	6.8 (1)	5.0 (1.5)	6.4 (1)	2.0 to 9.0 (1.5)
3	TIO	414.4	37.0	4.9 (3.5)	4.0 (3.5)	4.6 (3.5)	2.0 to 7.0 (3.5)
3	RWS	497.8	40.0	4.9 (3.5)	4.0 (3.5)	4.6 (3.5)	2.0 to 7.0 (3.5)
4	GVE	582.0	106.0	5.9 (1.5)	4.0 (1.5)	5.7 (1)	2.0 to 8.0 (1.5)
4	NVG	557.3	39.0	5.9 (1.5)	4.0 (1.5)	5.2 (2)	2.0 to 8.0 (1.5)
4	TIO				None		
4	RWS						

Table 9.
Spearman rank-correlation coefficients for roll velocity mean and median.

	Mean						Median			
	#1	#2	#3	#4			#1	#2	#3	#4
#1		+1.0	+0.75	+0.5		#1		+0.85	+0.95	+0.5
#2			+0.75	+0.5		#2			+0.75	+0.5
#3				+0.5		#3				+1.0
#4						#4				

Table 10.
Spearman rank-correlation coefficients for roll velocity standard deviation and IQR.

	S.D.						IQR			
	#1	#2	#3	#4			#1	#2	#3	#4
#1		+0.8	+0.75	+1.0		#1		+0.95	+0.9	+0.5
#2			+0.75	+1.0		#2			+0.75	-0.25
#3				-1.0		#3				+1.0
#4						#4				

Graphical comparison

Graphical comparisons are based on a 5-number summary box plot employed in the SPSS for Windows™ statistical software. The box plot technique provides a visual summary of a data set by emphasizing a select set of statistic values, e.g., median, quartiles, and IQR. Box-plots for combined roll velocity distributions for all subjects are presented in Figures 25-28. Individual box plots for all subjects by visual environment are presented in Appendix J. It should also be noted that extreme values have been removed to provide a less cluttered graphical representation.

From the box plots for subject #1 in Figure 25, the following characteristics and trends can be observed: a) The GVE has the slightly largest IQR and median, b) GVE and NVG have similar characteristics, and c) TIO and RWS also show similarities.

From the box plots for subject #2 in Figure 26, the following characteristics and trends can be observed: a) GVE box plot has the largest IQR, median and range, and b) TIO and RWS are the most similar.

From the box plots for subject #3 in Figure 27, the following characteristics and trends can be construed: a) GVE and NVG are similar in median, IQR and range, and b) TIO and RWS have similar characteristics.

From the box plots for subject #4 in Figure 28, the following characteristics and trends can be construed: Box plots for GVE and NVG are virtually identical.

Across all subjects, a graphical comparison via box plots for the four visual conditions failed to show any significant differences, other than greater similarities between the two nonHMD conditions, GVE and NVG, and the two HMD conditions, TIO and RWS.
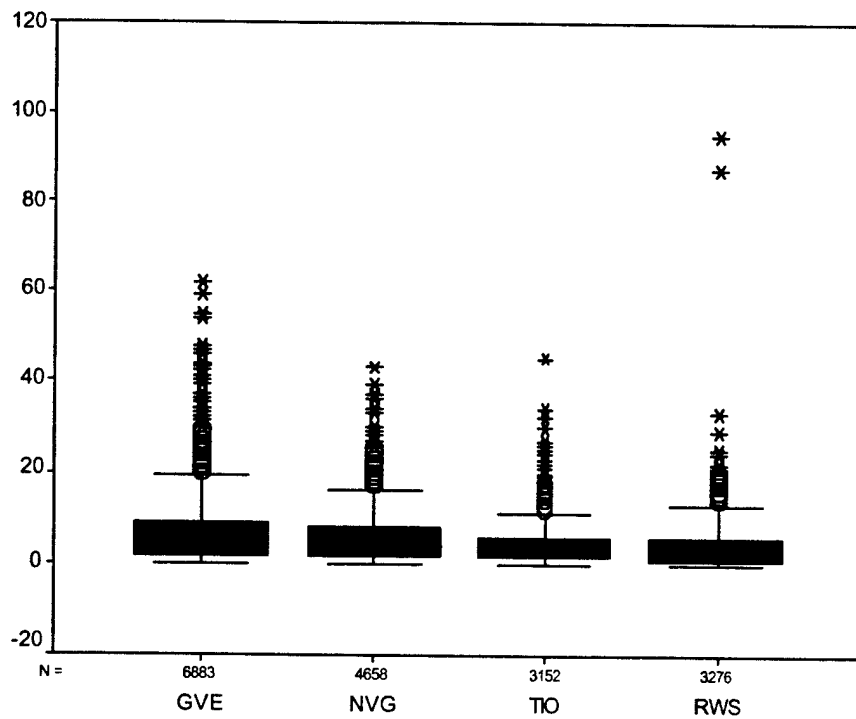
Figure 25. Combined roll velocity box plots for subject #1.
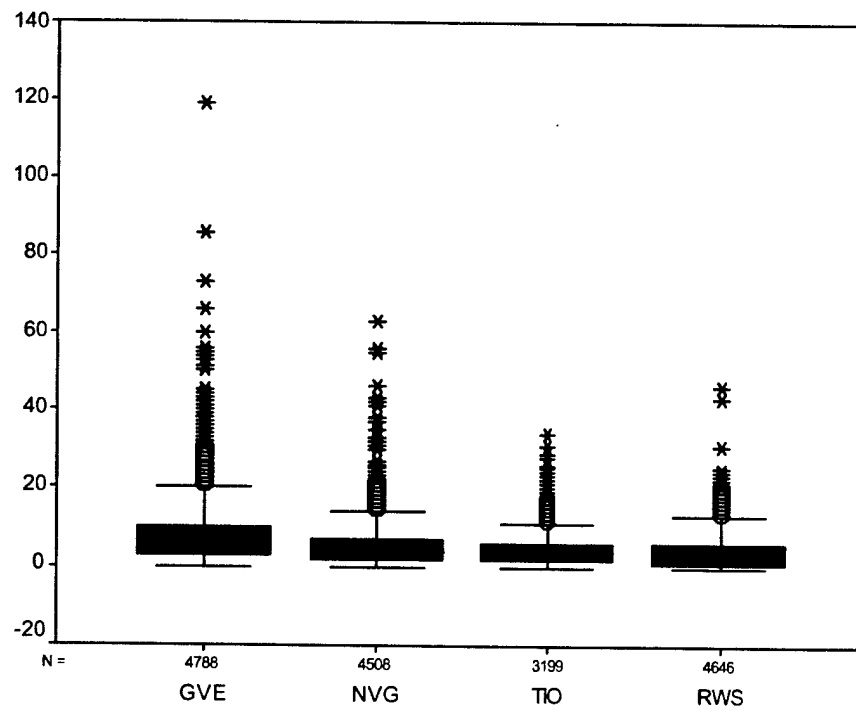
Figure 26. Combined roll velocity box plots for subject #2.
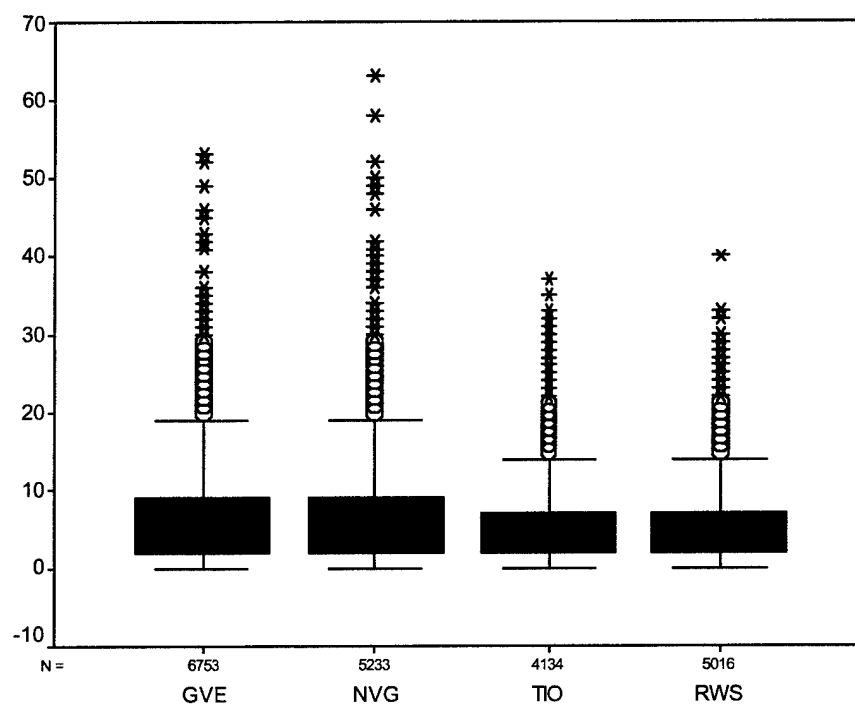
*Note: Extreme values are excluded to allow for better visual representation.
Figure 27. Combined roll velocity box plots for subject #3.
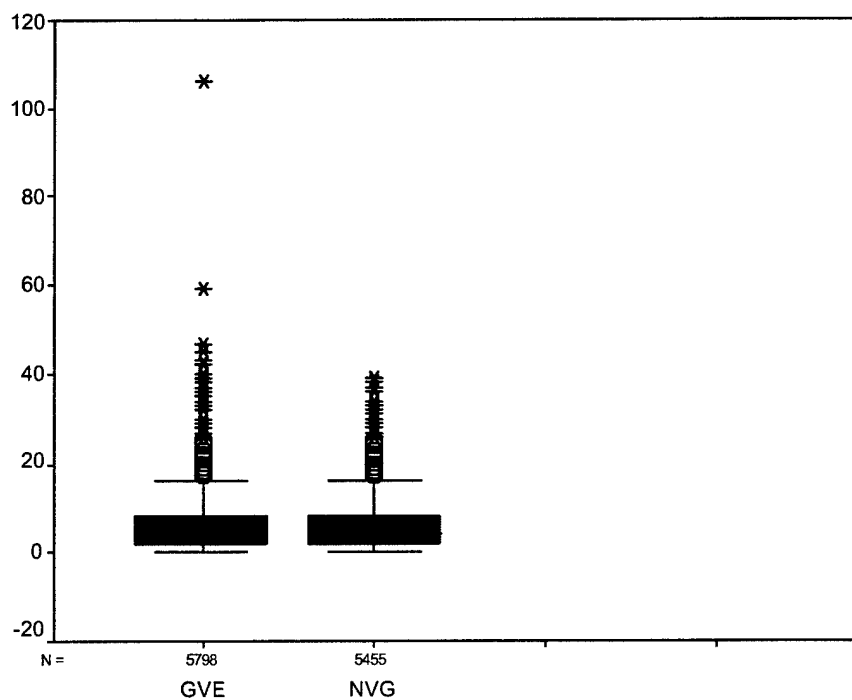
*Note: Extreme values are excluded to allow for better visual representation.
Figure 28. Combined roll velocity box plots for subject #4.

Discussion

For the previous azimuth and elevation head motion analyses (Rostad et al., 2001; Rostad and Rash, 2002), the roles of these two types of head motion are inherently recognized. Head azimuth motion allows aviators to perform such tasks as clearing obstacles on opposite sides of the aircraft, or performing target detection within a horizontal angle of approximately ±90°. Head elevation motion is used to perform the same obstacle avoidance and target detection tasks, as well as viewing overhead or panel-mounted displays. The role of roll (tilt) head motion is perhaps not as well defined. There are at least three reasons why head roll would be used by an aviator. First, cockpit transparency (window) shapes, sizes and locations may require semi-contortionist head and body movements to allow viewing outside the aircraft; the ability to tilt or roll the head is extremely advantageous for this task. Second, the brain prefers to view imagery properly oriented with the horizon. Therefore, since during flight the aircraft can take unusual attitudes, head roll, along with head elevation, can help in maintaining proper orientation of the horizon. And lastly, head roll is one aspect of combined head motion that can assist the aviator in localizing sound sources outside of the aircraft.

Verona et al. (1986) identified two major factors that influence head motion characteristics in rotary-wing flight. The first factor is aircraft configuration, which encompasses crewstation design, seating configuration (tandem vs. side-by-side), seat adjustment (fore/aft and up/down), and transparency (window) locations. The second factor is the flight task/environment, which encompasses the flight maneuver, terrain/route familiarity, and threat level. The introduction of HMDs (to include NVGs) into the cockpit with their reduced FOVs is an additional element of the flight task/environment factor. However, it would be expected that these factors would have a lesser impact on roll head motion than azimuth and elevation head motion. The one exception is the role of transparency size and location.

For the data analyzed herein, the aircraft had side-by-side seating and the subject was in the left seat; 0° in roll position was associated with the pilot holding his head in an upright position, inline with the earth's gravitational force. The exact angular subtenses of the transparencies are not available. However, an inspection of Figure 5 leads to the following observations: The two-part forward transparency subtended an angle of approximately -40° (left) to +60° (right) with respect to the subject (depending on seat adjustment) with a narrow (~4°) obstructing center rail at approximately +20° with respect to the subject pilot: The right forward transparency subtended an angle between approximately +25° to +60°: There were two side-door windows subtending approximately -75° to -40° on the left and +65° to +80° on the right (but blocked by the safety pilot). While dependent on seat height adjustment and pilot height, the upward vertical visibility is extremely limited. The lower forward vertical visibility is limited by the extended nose of the aircraft and FLIR sensor mount. Two small rectangular side windows, one on each side, are located approximately at the position of the pilot's feet.

Understanding roll head motion may be of particular importance in aviation scenarios involving HMDs. HMD systems, where pilotage imagery is provided by nose-mounted sensors, have historically not compensated for roll head motion. Task and Kocian (1995) report that the addition of roll information which can provide the capability of keeping the imagery aligned with

44

the aircraft structure may be desirable. Such availability of roll compensation is considered to be an advantage and would reduce workload. Roll compensation is intrinsic to systems such as NVG, where the sensor is head-mounted. In see-through HMDs, where the imagery may be used for daytime flights, roll compensation would prevent misregistration between the imagery of the outside world. Also, as wider FOV HMDs are developed, the displayed imagery will become more compelling and may require roll compensation (Haworth, 1997).

For the current investigation, the baseline GVE condition (across all subjects) (Figure 29) resulted in a roll (tilt) position range of approximately –35° to +26°, while 95% of the time head tilt was between –16° and +20°. The major peak in roll position in the current investigation occurred at approximately 0°; the pilots head remained essentially in an untilted position.

The maximum GVE roll velocity for the current investigation was 119°/sec; 50% of the roll velocity values were 4°/sec; and 90% were less than 14°/sec. A combined GVE velocity distribution for all subjects is presented in Figure 30.
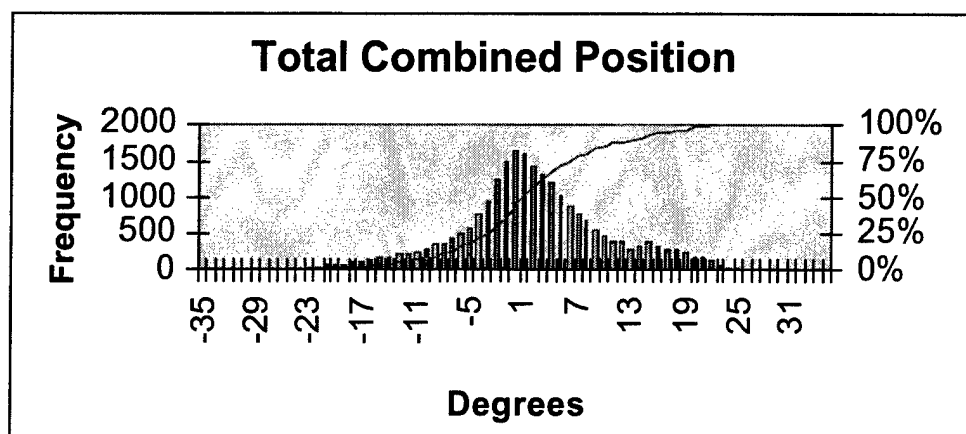
Figure 29. Frequency histogram for current study GVE roll position combined for all subjects.
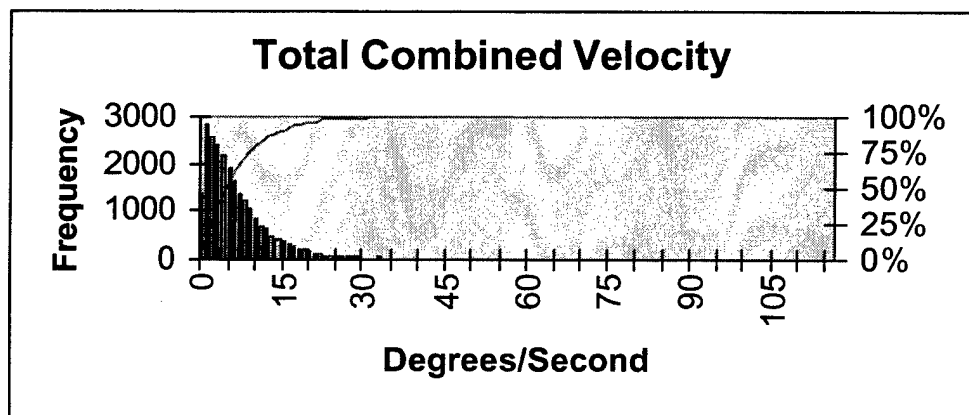
Figure 30. Frequency histogram for current study GVE roll velocity combined for all subjects.

Summary

Position analyses

As was found with the analysis of both azimuth and elevation head motion (Rostad et al., 2001; Rostad and Rash, 2002), there was considerable variability in roll head position data, both within and between subjects. The rationale for this variability, as before, is supported by Verona et al, (1986), which asserted that even for the same pilot flying the same course back-to-back under the same conditions, head motion will be different. However, it is reasonable to expect that certain trends in head motion may be present for a given set of conditions. This is the argument put forth herein and in the previous azimuth and elevation analyses.

Rostad et al. (2001) had shown that the IQR spread statistic was a useful discriminator between visual environments for azimuth head position. This finding did not continue for the investigation of elevation head position. It was suggested that this failure was due to the sensitivity of elevation position due to the repeatability of helmet fit (Rostad and Rash, 2002). The investigation, herein, of roll head position found that all three distribution spread statistics (IQR, range, standard deviation (SD)) could serve as discriminators between roll position distributions for the four visual environments.

Identified general characteristics and trends in the roll head position data include:
- Almost all roll head positions distributions were unimodal.
- GVE roll head position distributions generally had the largest spread.
- TIO and RWS distributions were most similar and presented the smallest spread.

Rate analyses

With regard to rate of change in roll head position across the four visual environments, three parameters were investigated: reversal rates, excursions, and velocities. Reversal rates, which attempted to quantify the number of times pilots reversed head motion direction, failed to show significant differences between the visual environments.

Excursions were used as an additional measure of the angular roll movement of the head by the pilots between reversal points, expressed in degrees. Histograms of excursion sizes showed roll movements as large as 44°. However, none of the distribution histograms, for any of the pilots, for any of the visual environments, showed any high degree of similarity. An analysis of all excursions collapsed across all runs, indicated that 50% of all excursions were less than 3° in size; 95% were less than 16°.

Velocities exhibited for the four visual environments failed to show any difference. Neither the mean, median or IQR statistics could be used to discriminate between the visual environments. In addition, there was no clear trend between subjects for which visual environments exhibited the highest velocities. However, the velocity statistics for the GVE and NVG conditions were higher than for the two nonHMD environments (TIO and RWS).

An analysis of all velocity values collapsed across all runs (Figure 24), indicated that 50% of all roll velocities were less than 4°/sec; 95% were less than 16°/sec. The largest roll velocity exhibited by any pilot during any run was 119°/sec.

The Spearman rank-correlation tests failed to show more than a weak association between the visual environment and the mean, median, standard deviation and IQR. Therefore, none of these velocity statistics could be used for discriminating between visual environments.

Conclusions

As with the previous azimuth and elevation head motion studies, this investigation of roll head motion had two objectives. The first was to expand the understanding of the head motion of (Army) pilots in an operational rotary-wing environment, especially while wearing various HMD configurations. The second objective was to identify which characteristics of head motion position and velocity data could be used to differentiate between head motion distributions (e.g., different visual flight environments).

The first objective was met via the construction of frequency histograms for the measured head positions, excursions, and velocities for four different visual flight conditions, i.e., GVE, NVG, TIO, and RWS. These distributions were defined by the calculation of their moments (i.e., mean, standard deviation, skewness, and kurtosis) as well as additional statistics (e.g., minimum, maximum, median, IQR, etc.).

The position distributions for roll showed strong trends, as were found in the previous azimuth analysis. Head roll position was fully contained within the range of approximately -35° (left) and +28° (right), a total of 63°. When the spread of roll head position values was examined by visual environment, the GVE and NVG environments generally produced the greatest IQR, range, and SD for each subject.

Similarly, the roll velocity data showed no real trends. The maximum roll velocity exhibited by any pilot for any visual environment was 119°/sec. However, 50% of all velocities were less than 4°/sec; 95% were 16°/sec or less; and over 99% of all velocities were less than 25°/sec. The mean and median velocities were 5.7°/sec and 4.0°/sec, respectively. When velocity distributions were compared by visual environment, no single visual environment consistently produced any predominant characteristics.

The second objective to identify one or more distribution statistics to allow discrimination between roll head motion in the various visual environments was achieved by the finding that all three spread distribution statistics could be used to differentiate between head roll position distributions, but none of the statistics were found to be useful in discriminating between head velocity distributions.

In conclusion, the data suggest that for roll head position, the three spread distribution statistics (IQR, range, and SD) could serve as discriminators between the four visual environments. For roll head motion, none of the distribution statistics could be used as discriminators.

References

Azuma, R., and Bishop, G. 1995. A frequency-domain analysis of head-motion prediction. <u>Computer Graphics Proceedings</u>, 401-408. SIGGRAPH 95, Los Angeles, CA, August 6-11 401-408.

Bloch, S. C. 2000. <u>Excel for engineers and scientists</u>. New York: John Wiley and Sons. 69-74.

Borah, J. 1989. <u>Helmet mounted eye tracking for virtual panoramic display systems. Vol. II: Eye tracker specification and design approach</u>. Wright Patterson Air Force Base, OH: Armstrong Aerospace Medical Research Laboratory. AAMRL-TR-89-019.

Borah, J. 1998. Technology and application of head based control. Proceedings of Research and Technology Organization, Lecture Series 215, Alternative Control Technologies: Human Factors Issues, RTO-EN-3, 6-1 to 6-12.

Cameron, A. A., Trythall, S., and Barton, A. M. 1995. Helmet trackers – The future. <u>Helmet- and head-mounted displays and symbology design requirements II</u>, <u>Proceedings of SPIE</u>, Vol. 2465, 281-295.

Craig, G. L., Jennings, S. A., and Swail, C. P. 2000. Head roll compensation in a visually coupled HMD: Considerations for helicopter operations. <u>Aviation Space and Environmental Medicine</u>. 71:476-84.

Crowley, J. S. 1998. <u>Simulating a degraded visual environment in the Lynx helicopter</u>. Farnborough: DERA. DERA Report No. DERA/CHS/PP5/CR9780005/1.0.

Curtis, W., and Sowizral, H. 1994. A note on dynamics of human head motions and on predictive filtering of head-set orientations. <u>SPIE Proceedings: Telemanipulator and telepresence technologies</u>, vol. 2351. Boston, MA. 23-58.

Gauthier, G. M., Martin, B. J., and Stark, L. W. 1986. Adapted head- and eye-movement responses to head inertia. <u>Aviation, Space, and Environmental Medicine</u>. 57:336-42.

Haworth, L. A. 16 Dec 1997. Conversation (telephone communication) concerning roll compensation, Aeroflightdynamics Directorate, Ames Research Center, Moffett Field, CA.

Kocian, D. F., and Task, H. L. 1995 "Visually coupled systems hardware and the human interface" In Barfield, W., and Furness, T. A., (Eds) <u>Virtual environments and advanced interface design</u>. New York: Oxford University Press.

Melzer, J. E., and Moffitt, K. 1997. <u>Head mounted displays: Designing for the user</u>. New York: McGraw Hill.

Michael, P. R., Jardine, T. E., and Goom, M. K. 1978. Visual effects of helicopter maneuver on weapon aiming performance. Operational Helicopter Aviation Medicine, AGARD, pp. 25/1-25/15.

Phillips, C. A., and Petrofsky, J. S. 1983. Neck muscle loading and fatigue: Systematic variation of headgear weight center-of-gravity. Aviation, space, and environmental medicine. 54(10):901-905.

Rash, C. E. Editor. 1999. Helmet-mounted display: Design issues for rotary-wing aircraft. Fort Rucker, AL: U. S. Army Aeromedical Research Laboratory.

Robinson, R. M. , and Wetzel, P. A. 1989. Eye tracker development in the fiber optic helmet mounted display. Helmet-mounted displays, Proceedings of SPIE Vol. 1116, 102-108.

Rostad, R. J. , and Rash, C. E. 2002. Elevation head motion in rotary-wing flight with helmet-mounted displays. Helmet-and head-mounted displays VI, Proceedings of SPIE Vol. 4711, 115-129.

Rostad, R. J. , Rash, C. E., Crowley, J. S., Briley, J. K., and Mora, J. C. 2001. Analysis of azimuth head motion in rotary-wing flight using various helmet-mounted display configurations. Helmet-and head-mounted displays VI, Proceedings of SPIE Vol. 4361, 115-129.

Rostad, R.J. et al, 2003. Analysis of head motion in rotary wing flight using various helmet-mounted display configurations (part I. Azimuth). Fort Rucker, Alabama; U.S. Army Aeromedical Research Laboratory, USAARL Report No. 2003-07

Task, H. L., and Kocian, D. F. 1995. Design and integration issues of visually-coupled systems (VCS). Wright-Patterson AFB, OH:Armstrong Laboratory. AL/CF-SR-1995-0004.

Verona, R.W., Rash C. E., Holt, W. R., and Crosley, J. K. 1986. Head movements during contour flight. Ft. Rucker, AL: U.S. Army Aeromedical Research Laboratory. USAARL Report No. 87-1.

Appendix A.

Roll position distributions.

51

Figure A-1. Subject #1 GVE head position data.

Figure A-2. Subject #1 NVG head position data.

Figure A-3. Subject #1 TIO head position data.

Figure A-4. Subject #1 RWS head position data.
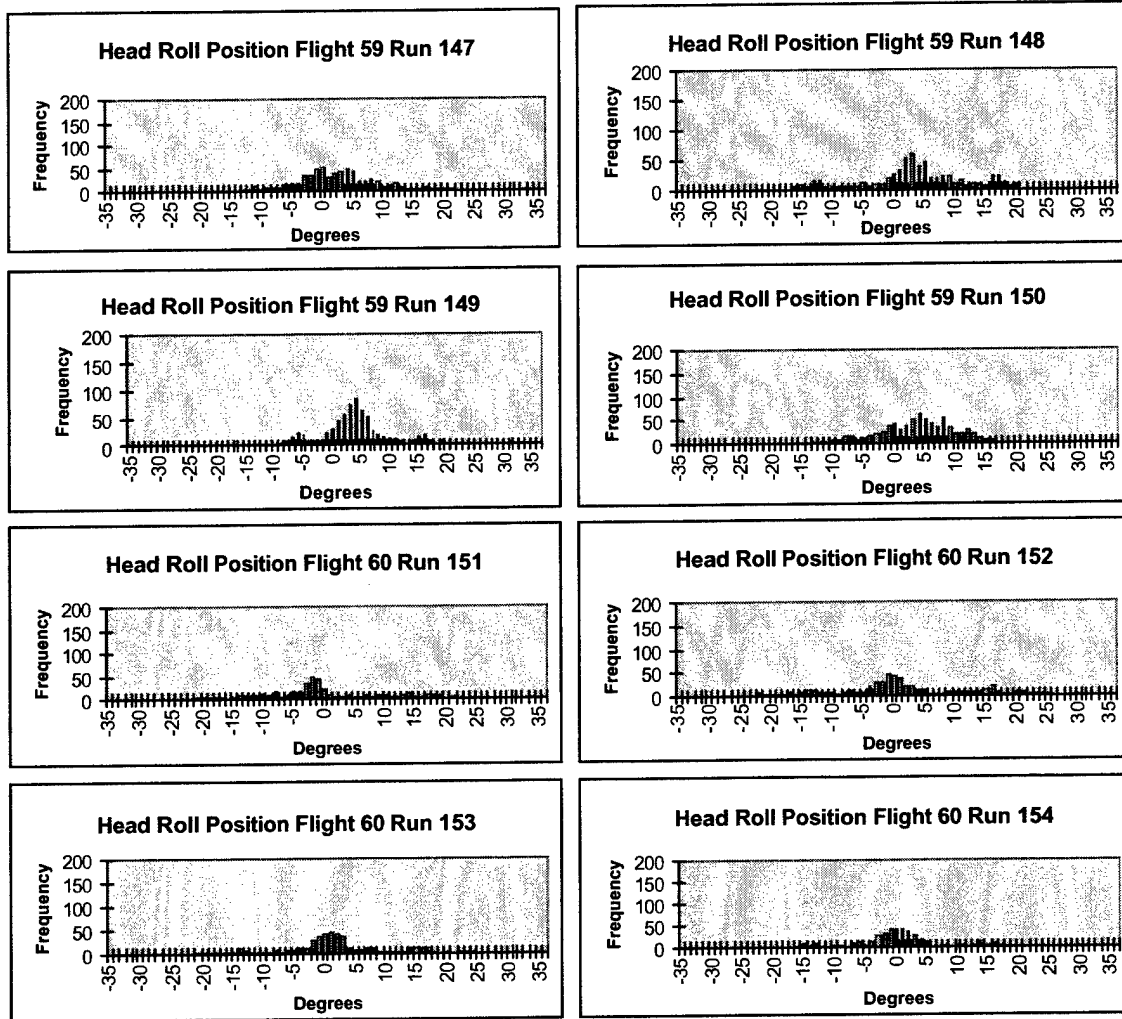
Figure A-5. Subject #2 GVE head position data.
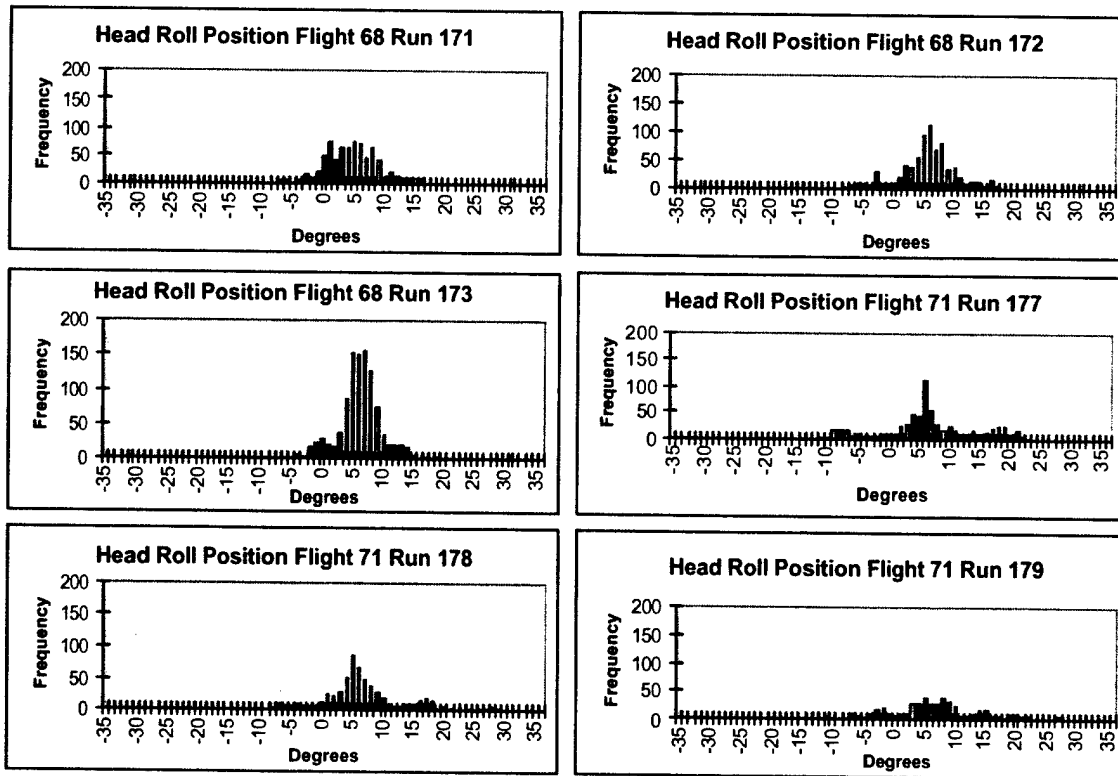
Figure A-6. Subject #2 NVG head position data.
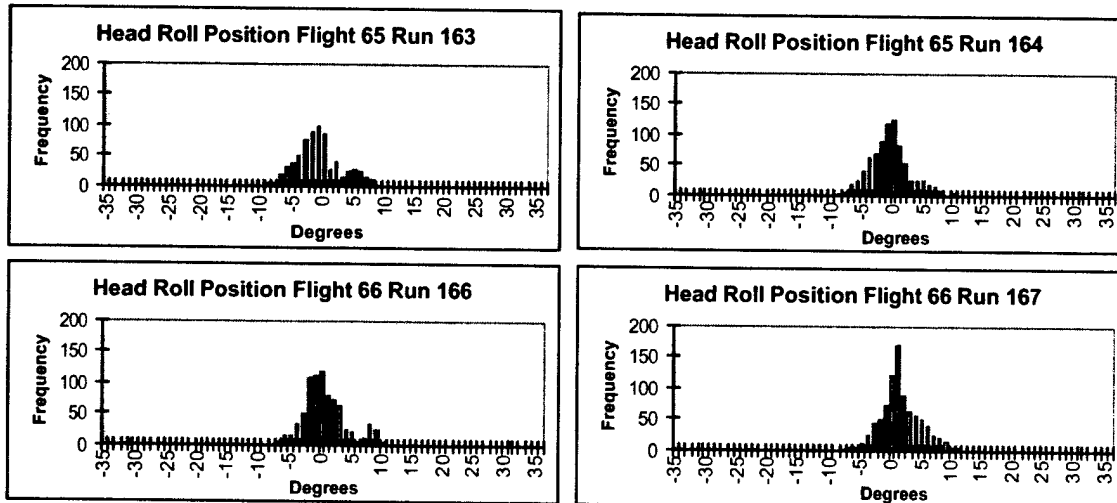
Figure A-7. Subject #2 TIO head position data.
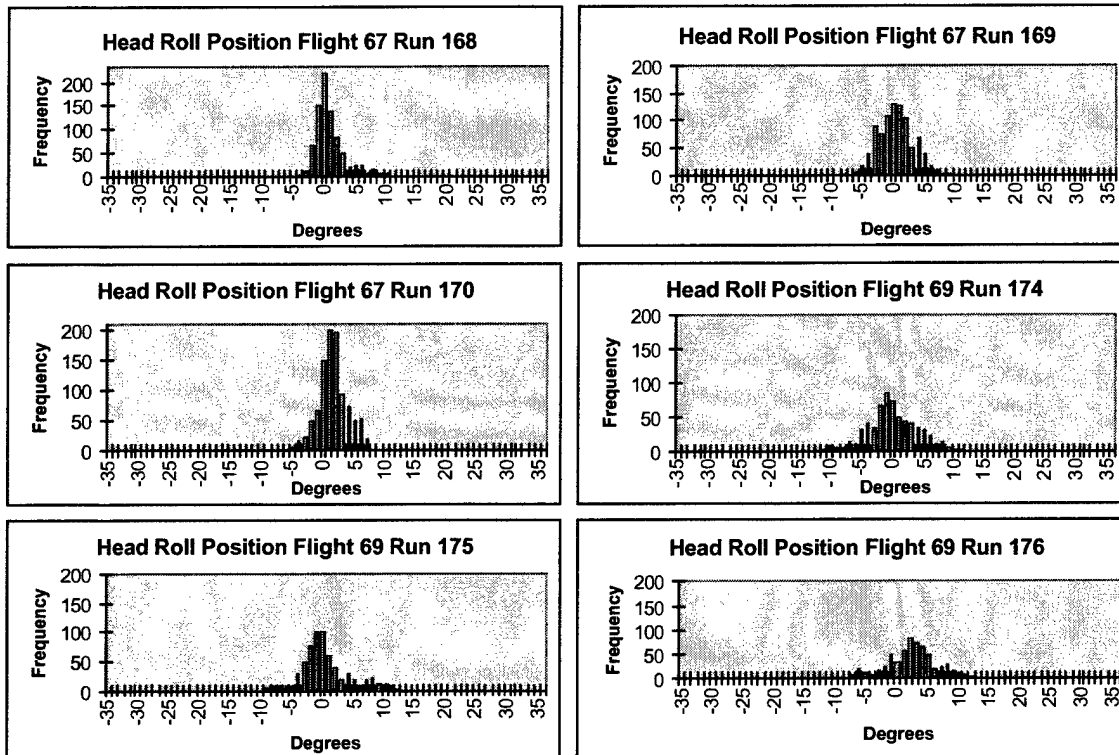
Figure A-8. Subject #2 RWS head position data.
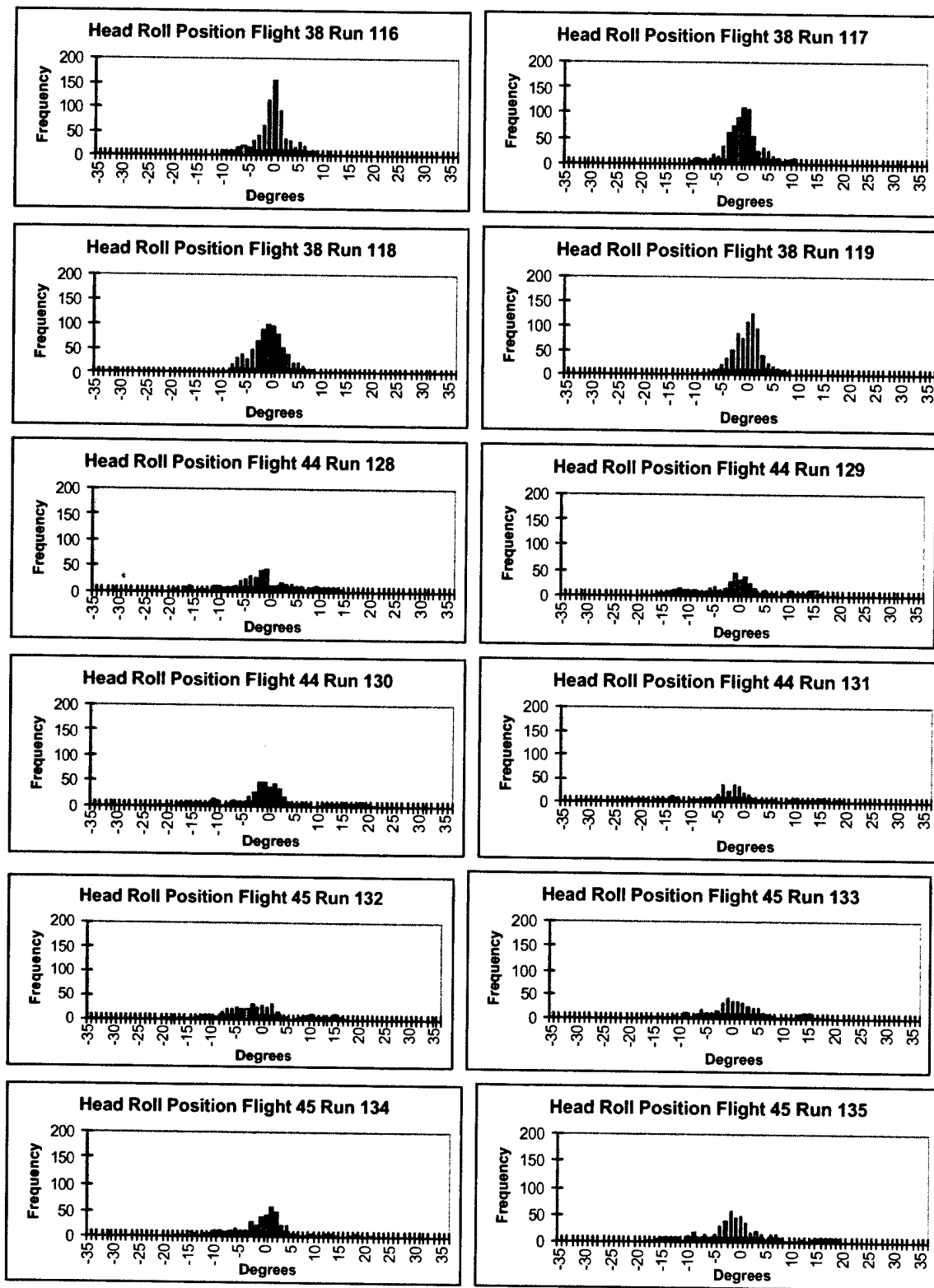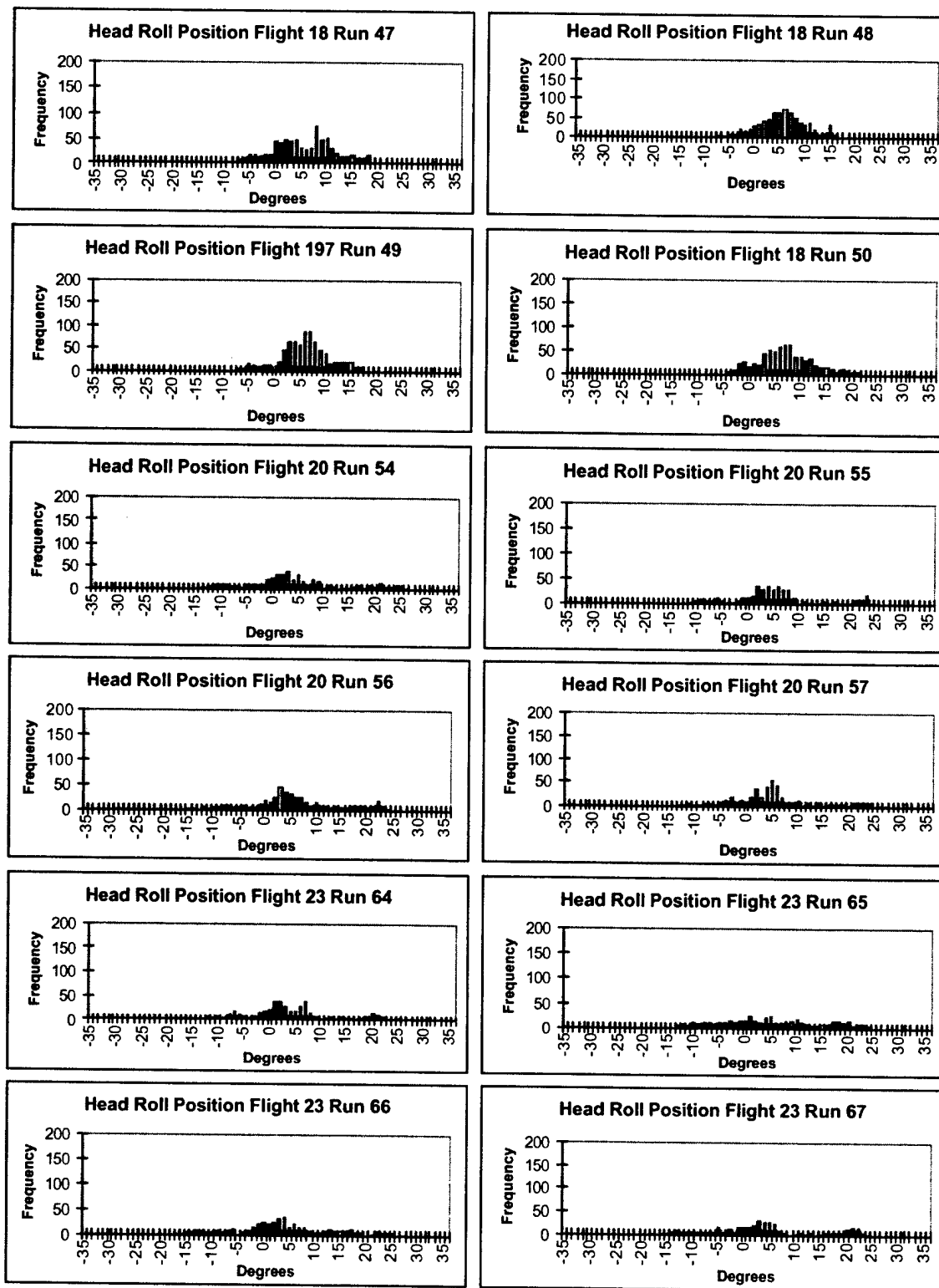
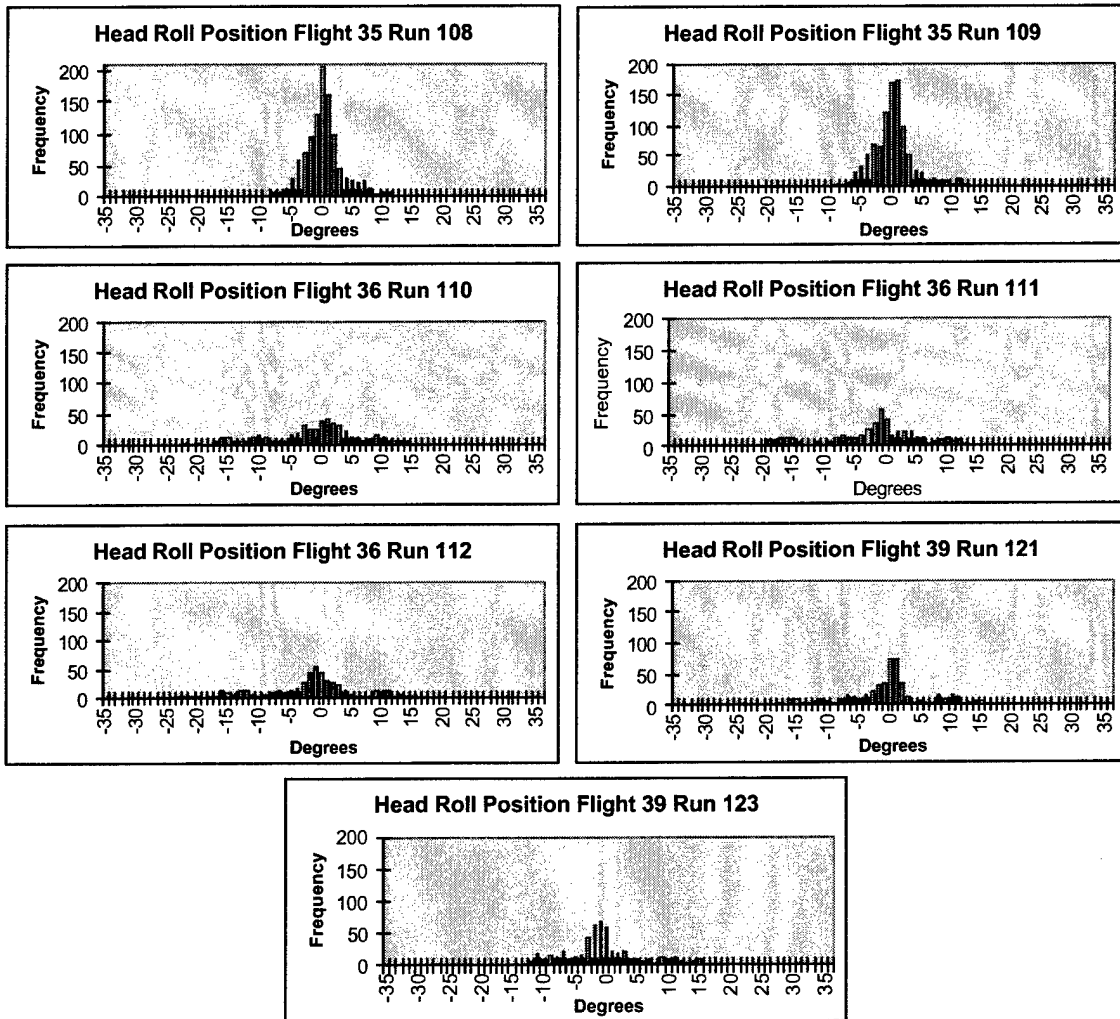Figure A-9. Subject #3 GVE head position data.
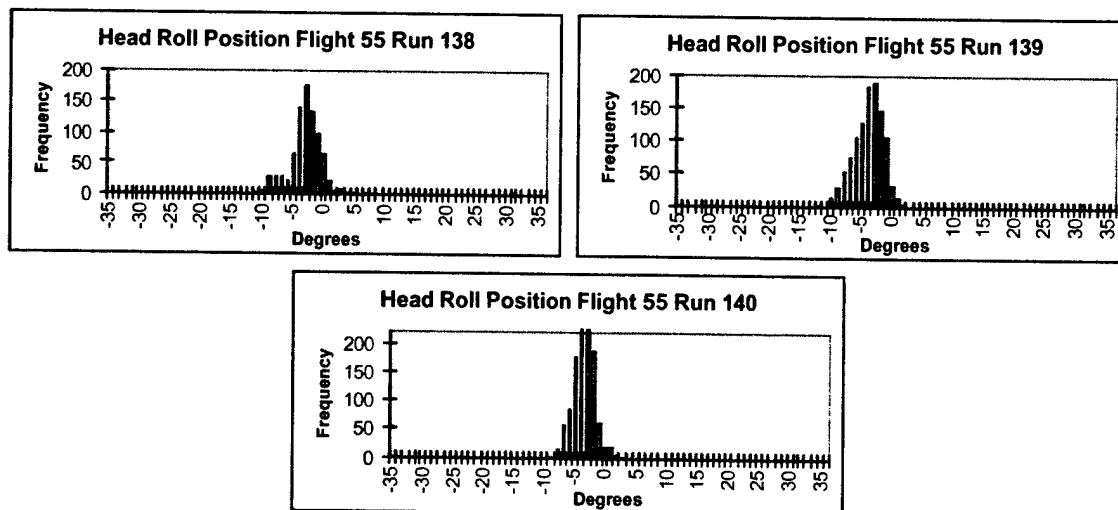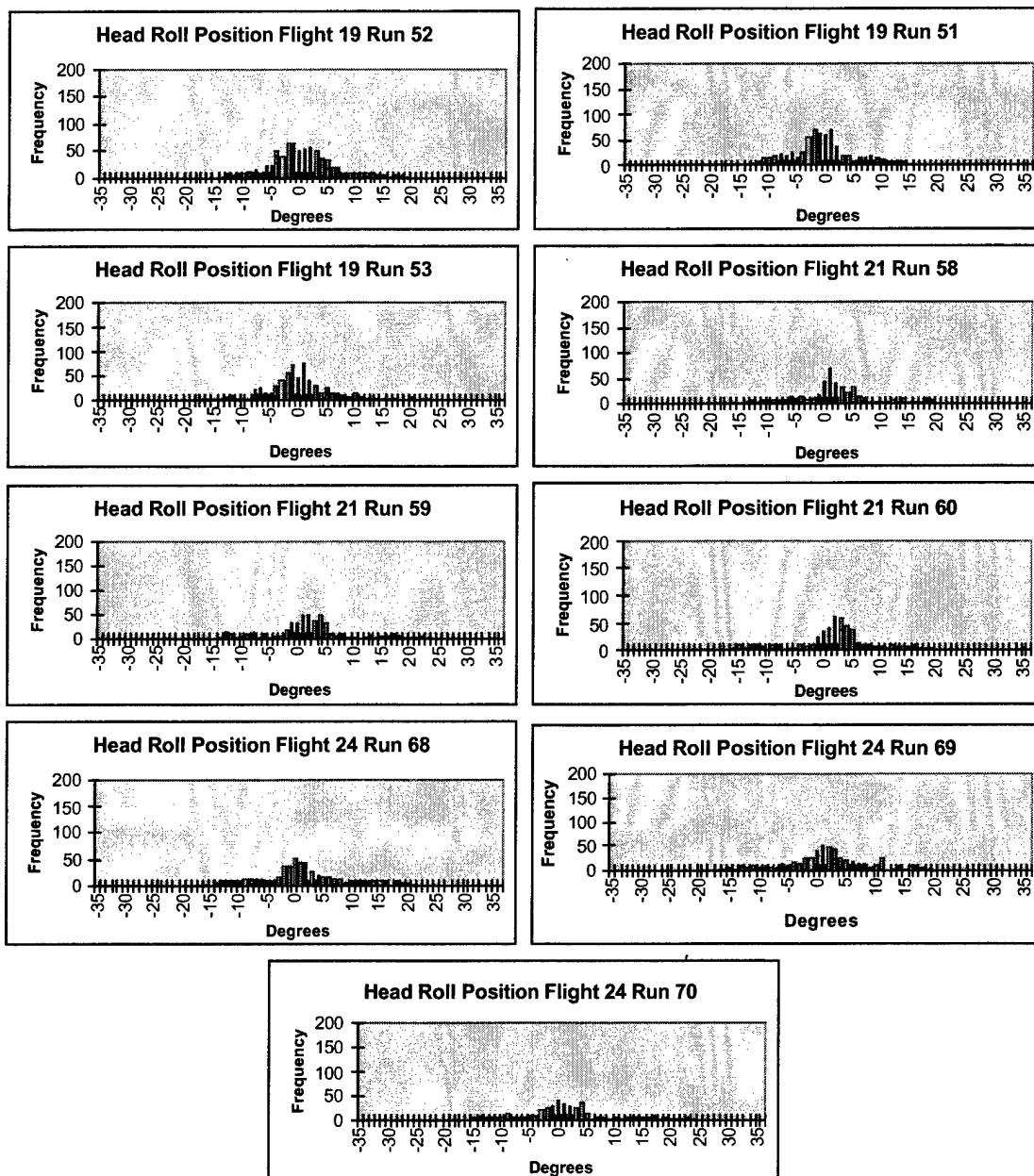
Figure A-10. Subject #3 NVG head position data.

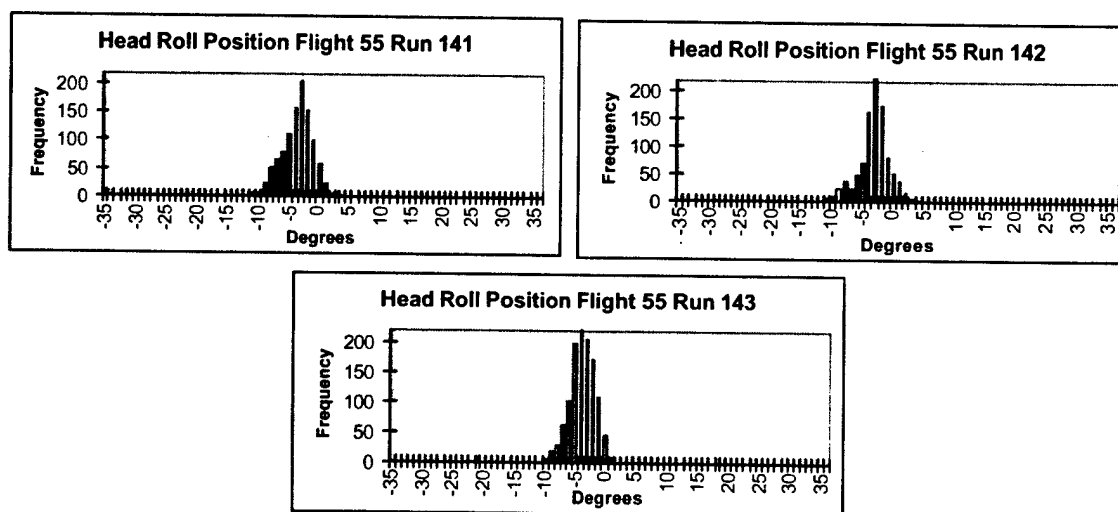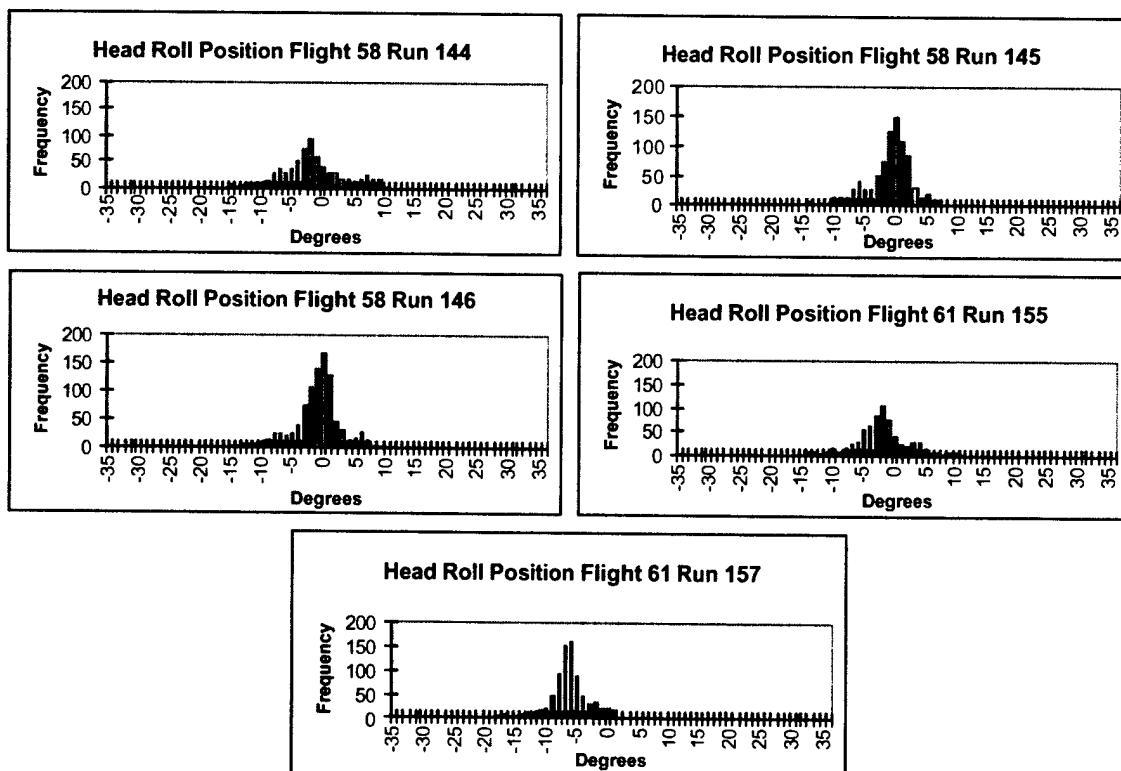Figure A-11. Subject #3 TIO head position data.
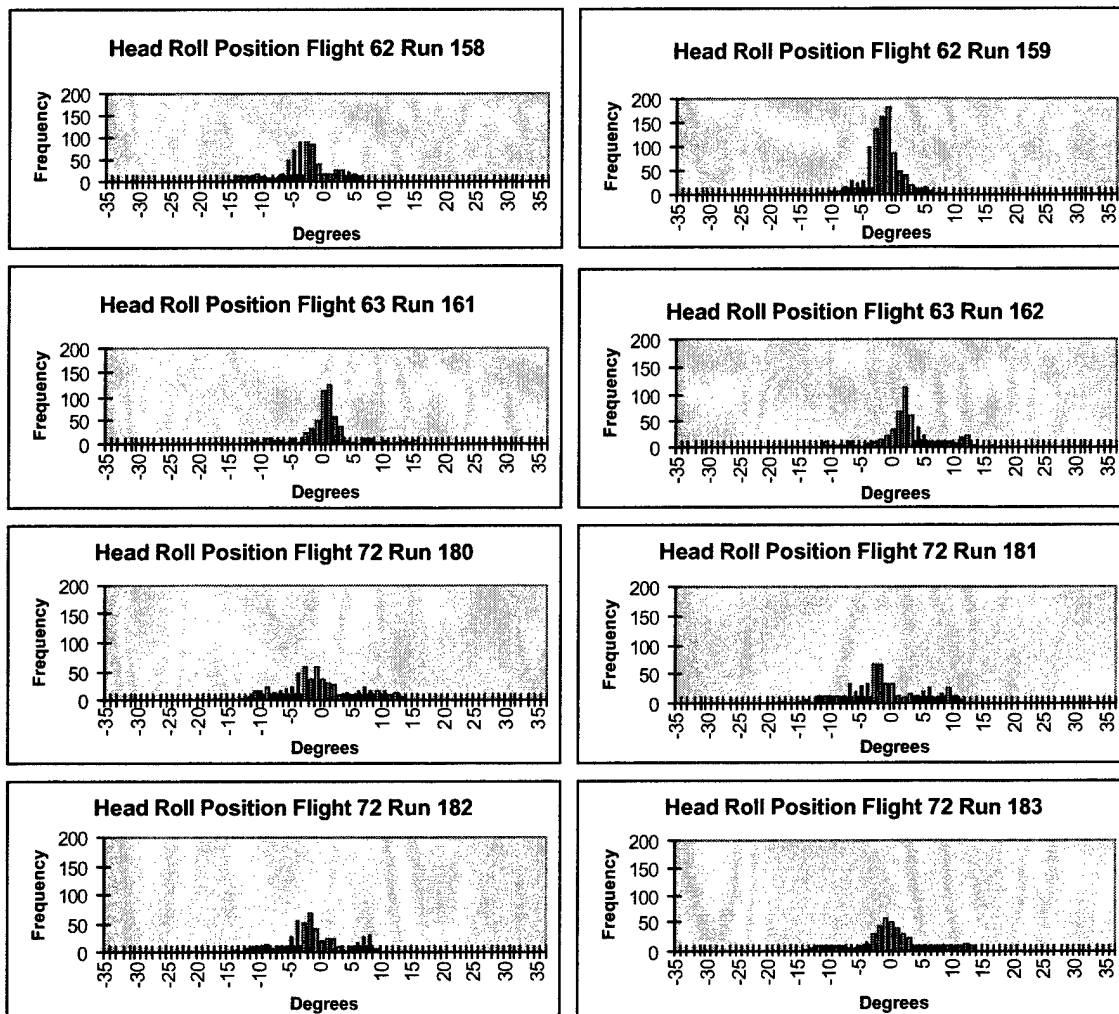
Figure A-12. Subject #3 RWS head position data.
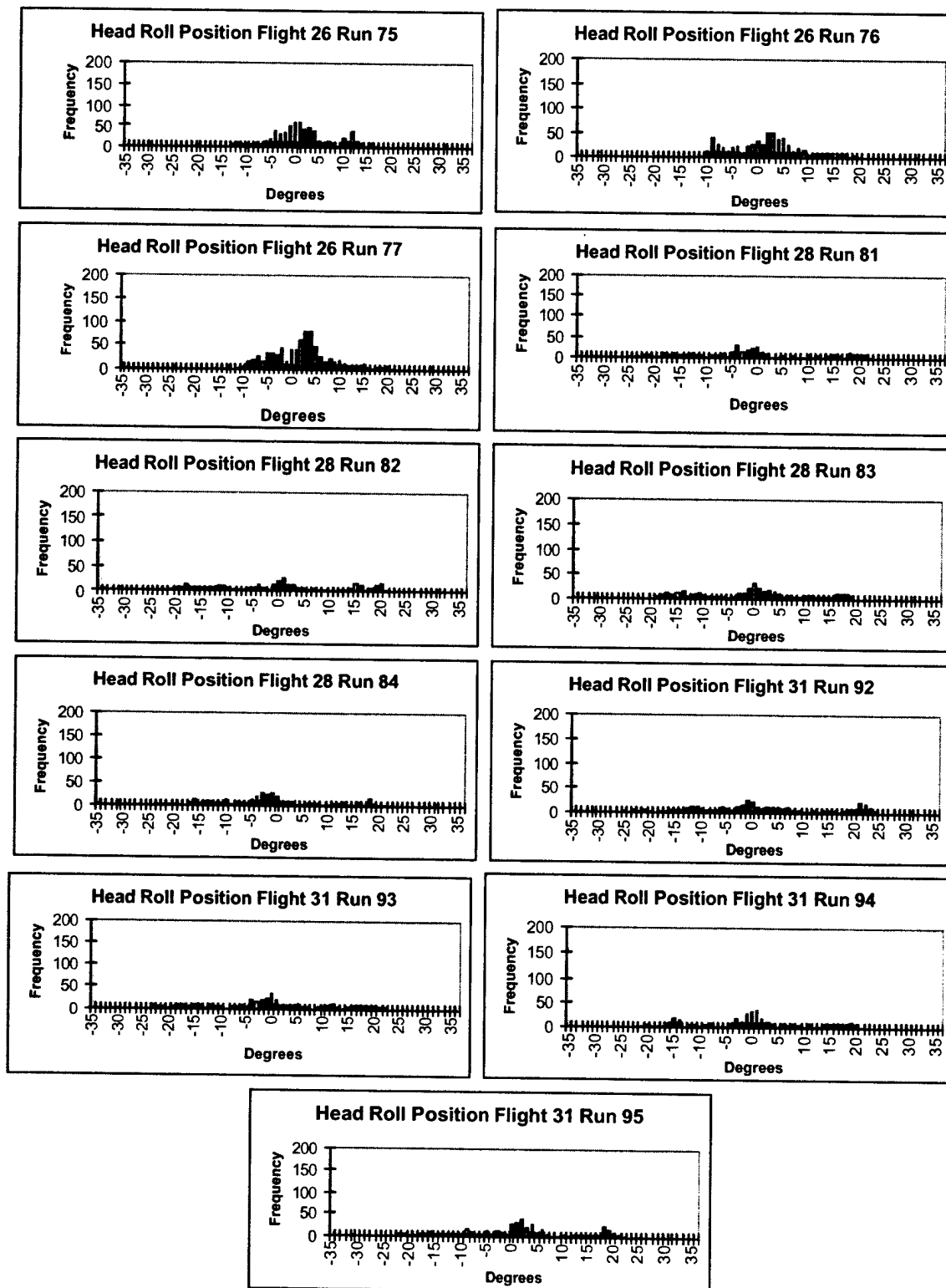
Figure A-13. Subject #4 GVE head position data.
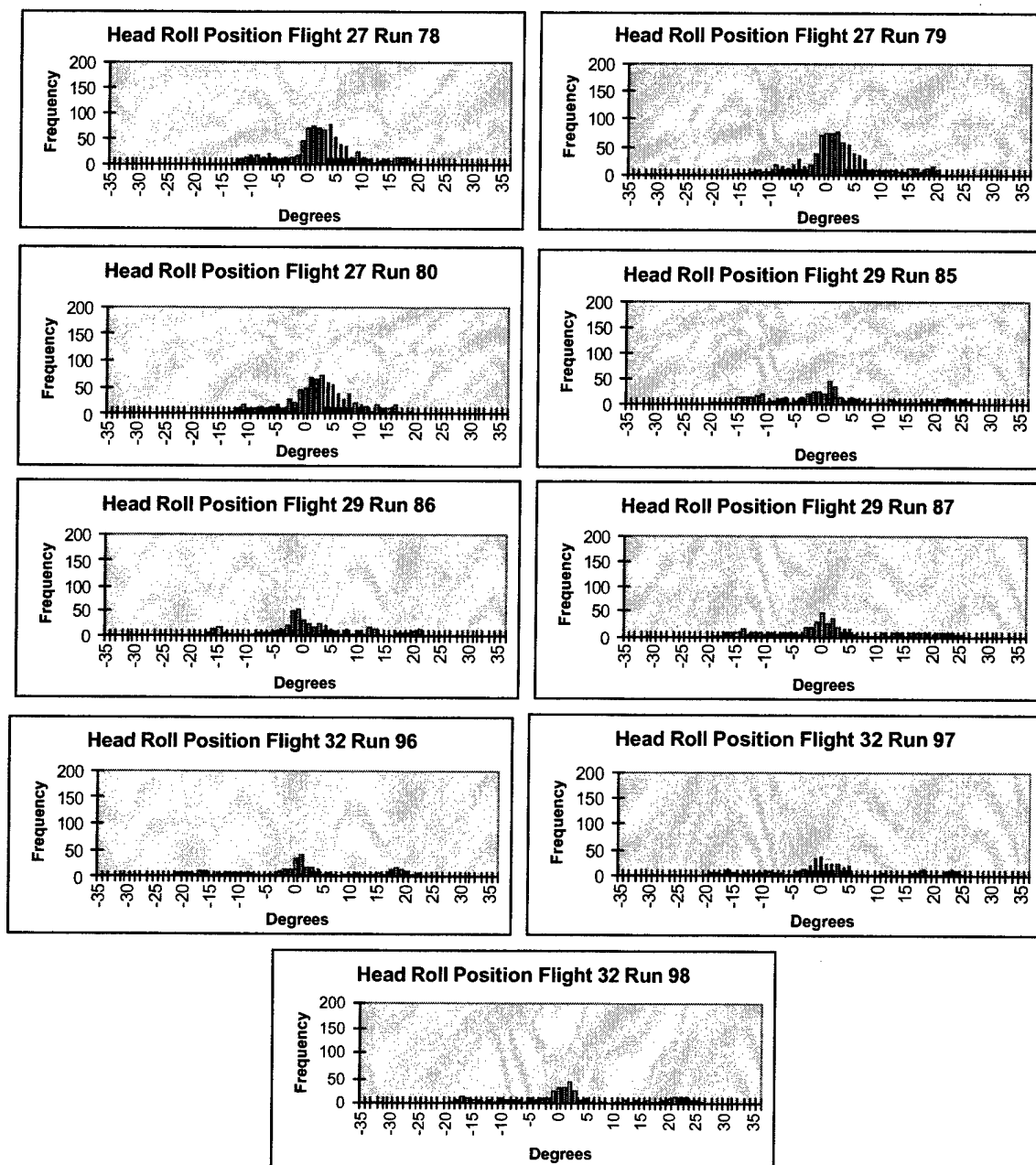
Figure A-14. Subject #4 NVG head position data.

Appendix B.

Summary tables of roll position distributions by visual environment.

Table B-1.
Summary of moments and statistics for roll position, slalom course, GVE.
(roll values expressed in degrees)

Subject	Run	Time	Min	Max	Mean	Median	S.D.	IQR	Skew	Kurt
1	116	76.9	-13.4	10.4	-1.0	-0.8	3.8	-2.7 to .6	-0.2	0.7
1	117	75.7	-11.9	10.4	-0.6	-0.7	-2.7	-2.7 to 1.1	0.1	0.8
1	118	76.9	-9.7	8.6	-1.5	-1.4	3.5	-3.6 to .6	0.1	-0.1
1	119	76.0	-11.6	8.3	-0.6	-0.4	3.1	-2.5 to 1.2	-0.2	0.9
1	128	45.2	-24.1	13.9	-2.6	-2.6	7.7	-6.4 to 2.0	-0.1	0.0
1	129	48.1	-21.1	18.9	-1.5	-1.3	8.3	-6.9 to 2.2	0.2	-0.3
1	130	48.6	-25.8	21.2	-1.2	-1.3	8.8	-4.7 to 1.7	0.2	0.5
1	131	43.8	-35.4	19.0	-4.2	-3.0	11.5	-9.8 to 1.0	-0.3	-0.1
1	132	45.6	-22.8	17.2	-1.6	-2.0	7.9	-6.3 to 1.7	0.2	0.1
1	133	49.8	-19.9	17.3	0.1	-0.2	7.2	-3.8 to 3.8	0.0	0.2
1	134	51.1	-22.7	21.3	-1.1	-0.6	7.5	-5.0 to 1.9	0.2	0.8
1	135	52.9	-19.1	19.1	-0.7	-1.6	7.7	-4.4 to 2.1	0.5	0.6
Combined		**690.6**	**-35.4**	**21.3**	**-1.3**	**-1.1**	**6.8**	**-4.1 to 1.4**	**-0.2**	**2.1**
2	147	68.4	-17.6	20.2	1.8	1.6	6.9	-2.5 to 5.7	0.1	0.1
2	148	65.1	-17.6	21.2	3.1	2.9	8.6	-.5 to 8.2	-0.3	-0.2
2	149	71.7	-13.1	21.9	3.6	3.3	6.2	.5 to 5.9	0.4	0.4
2	150	73.9	-13.5	17.0	3.3	3.5	6.1	-.7 to 7.5	-0.3	-0.3
2	151	47.0	-25.6	20.7	-0.5	-2.0	9.8	-6.1 to 6.8	0.2	-0.5
2	152	52.2	-22.9	25.0	0.3	-0.7	9.9	-4.4 to 4.7	0.2	-0.2
2	153	51.7	-21.6	23.6	0.8	0.3	9.2	-3.0 to 4.9	0.1	0.1
2	154	50.4	-19.4	26.3	1.4	0.1	8.9	-3 to 4.2	0.5	0.3
Combined		**480.4**	**-25.6**	**26.3**	**1.9**	**1.7**	**8.2**	**-2.5 to 6.6**	**0.0**	**0.2**
3	47	74.8	-15.6	18.5	5.1	5.4	6.0	.7 to 9.2	0.0	-0.4
3	48	75.7	-9.9	17.5	5.2	5.3	4.9	2.2 to 8.3	0.0	-0.2
3	49	78.8	-7.4	17.3	5.3	5.5	4.9	2.6 to 8.1	-0.2	0.1
3	50	73.2	-10.1	23.5	6.6	6.3	5.5	3.0 to 10	0.3	0.0
3	54	44.6	-21.9	25.6	4.2	2.7	9.4	-1.0 to 8.2	0.4	-0.1
3	55	47.6	-13.3	24.5	5.0	4.2	8.5	.7 to 7.6	0.4	0.0
3	56	46.5	-15.4	24.8	5.5	4.4	8.5	1.1 to 9.9	0.2	-0.2
3	57	49.0	-14.7	26.2	5.0	4.2	8.4	.5 to 8.0	0.5	0.2
3	64	50.6	-16.1	24.9	3.5	2.2	8.8	-1.5 to 7.1	0.4	-0.2
3	65	46.8	-18.2	23.6	4.6	4.1	9.7	-2.6 to 11.3	0.1	-0.9
3	66	46.7	-17.4	25.1	3.4	2.8	9.3	-1.7 to 8.3	0.1	-0.2
3	67	43.4	-22.5	23.5	3.7	2.9	10.32	-3.1 to 9.1	0.2	-0.6
Combined		**677.7**	**-22.5**	**26.2**	**4.9**	**4.5**	**7.7**	**0.5 to 8.8**	**0.1**	**0.3**
4	75	72.4	-15.4	17.9	1.1	0.4	6.7	-3.0 to 4.7	0.2	-0.3
4	76	69.0	-13.1	20.9	1.6	1.5	7.5	-4.1 to 5.6	0.3	-0.4
4	77	79.8	-12.8	21.2	1.9	2.0	6.5	-2.8 to 4.7	0.5	0.3
4	81	42.0	-25.6	22.4	-1.2	-1.9	12.5	-10.0 to 9.5	0.1	-0.9
4	82	42.6	-25.9	21.4	-0.5	-0.4	12.3	-11 to 9.5	0.1	-1.0
4	83	46.0	-22.5	21.1	-0.2	.00	10.8	-9.7 to 7.1	0.0	-0.9
4	84	45.0	-25.2	21.9	-0.9	-2.1	10.8	-8.2 to 6.6	0.2	-0.6
4	92	44.4	-32.1	24.0	1.7	-0.2	12.6	-6.7 to 11.1	0.0	-0.7
4	93	43.6	-24.4	21.8	-.3	-0.6	11.9	-7.5 to 8.9	0.0	-0.7
4	94	48.0	-22.5	21.7	0.1	-0.1	11.1	-7.6 to 7.6	0.0	-0.7
4	95	49.2	-23.3	21.4	0.7	1.0	10.9	-6.7 to 6.4	0.0	-0.6
Combined		**582**	**-32.1**	**24.0**	**0.6**	**0.3**	**10.1**	**-5.2 to 6.4**	**0.0**	**-0.3**
All Subjects		**2251.7**	**-35.4**	**26.3**	**1.4**	**0.1**	**2.5**	**-6.3 to 8.3**	**0.0**	**-0.5**

65

Table B-2.
Summary of moments and statistics for roll position, slalom course, NVG.
(roll values expressed in degrees, time in seconds)

Subject	Run	Time	Min	Max	Mean	Median	S.D.	IQR	Skew	Kurt
1	108	105.7	-9.0	10.8	-0.2	-0.4	3.2	-2.2 to 1.2	0.6	1.0
1	109	98.2	-10.1	11.7	-0.3	-0.3	3.4	-2.2 to 1.1	0.6	1.6
1	110	51.3	-24.9	13.7	-1.7	-0.7	7.7	-5.4 to 2.8	-0.5	-0.1
1	111	51.7	-22.0	15.1	-2.5	-1.6	7.8	-6.6 to 2.3	-0.4	-0.2
1	112	51.1	-24.7	15.1	-2.3	-1.4	7.8	-6.3 to 1.8	-0.3	0.1
1	121	54.0	-21.1	15.1	-1.2	-0.6	7.0	-4.2 to 1.5	-0.2	0.3
1	123	55.2	-14.0	15.3	-0.8	-1.5	6.2	-3.8 to 1.7	0.6	0.2
Combined		**467.2**	**-24.9**	**15.3**	**-1.1**	**-0.7**	**6.0**	**-3.4 to 1.5**	**-0.5**	**1.5**
2	171	80.0	-9.5	17.1	4.2	4.2	4.7	0.9 to 7.2	0.1	0.2
2	172	80.9	-8.7	16.6	5.0	5.3	4.9	2.8 to 7.6	-0.3	0.5
2	173	103.2	-4.9	19.2	5.8	5.9	3.5	4.1 to 7.7	0.0	1.3
2	177	70.6	-12.4	22.1	6.3	5.7	7.7	2.8 to 10.6	-0.1	-0.2
2	178	63.0	-8.6	28.5	6.4	5.4	6.8	3.2 to 8.8	0.7	1.0
2	179	54.3	-9.2	27.7	7.0	6.3	7.8	2.3 to 11.8	0.4	-0.2
Combined		**452.0**	**-12.4**	**28.5**	**5.7**	**5.4**	**5.9**	**2.8 to 8.1**	**0.4**	**1.2**
3	51	71.8	-19.4	18	-0.9	-1.3	6.1	-4.3 to 1.8	0.3	0.1
3	52	73.9	-14.5	19.5	0	-0.5	6.1	-3.6 to 3.0	0.5	0.7
3	53	68.2	-18.3	23.0	-0.3	-0.8	6.7	-3.7 to 2.5	0.6	1.7
3	58	50.5	-17.3	18.8	1.1	0.7	7.4	-2.6 to 4.4	0.2	0.2
3	59	51.9	-14.9	22.5	1.6	1.2	7.8	-1.8 to 4.3	0.4	0.4
3	60	52.6	-17.0	18.7	1.4	1.8	7.3	-1.1 to 4.4	-0.3	0.5
3	68	53.6	-17.1	22.6	0.9	0.3	7.6	-2.8 to 4.7	0.3	0.1
3	69	53.8	-16.9	18.5	1.2	1.1	7.1	-2.3 to 4.7	0	0.2
3	70	48.8	-18.1	23.9	1.1	0.2	8.8	-3.5 to 4.1	0.5	0.1
Combined		**525.1**	**-19.4**	**23.9**	**0.6**	**0.4**	**7.2**	**-3.2 to 3.8**	**0.3**	**0.5**
4	78	85.3	-15.3	19.3	1.9	1.9	6.7	-1.1 to 5.0	0.1	0.3
4	79	81.9	-16.7	19.7	1.5	0.9	6.8	-1.8 to 4.3	0.5	0.7
4	80	83.9	-14.4	20.3	2.1	2.1	6.6	-1.4 to 5.7	0	0.2
4	85	52.7	-20.4	26.9	0.3	0.2	11.7	-7.2 to 7.5	0.4	-0.6
4	86	56.0	-19.6	21.6	1.0	-0.4	9.7	-3.5 to 7.1	0.2	-0.3
4	87	49.8	-21.2	24.9	1.8	0.4	11.0	-3.5 to 8.7	0.3	-0.5
4	96	44.6	-22.5	22.5	1.0	0.4	11.9	-7.2 to 10.4	-0.1	-0.8
4	97	47.0	-20.8	24.4	1.7	0.2	11.4	-4.1 to 7.9	0.2	-0.5
4	98	46.1	-19.7	25.9	2.0	0.7	12.0	-5.2 to 10.6	0.3	-0.7
Combined		**547.3**	**-22.5**	**26.9**	**1.6**	**1.0**	**9.4**	**-2.9 to 5.8**	**0.2**	**0.1**
All Subjects		**1991.6**	**-24.9**	**28.5**	**1.5**	**0.4**	**2.4**	**-4.2 to 7.6**	**-0.4**	**0.2**

Table B-3.
Summary of moments and statistics for roll position, slalom course, TIO.
(roll values expressed in degrees, time in seconds)

Subject	Run	Time	Min	Max	Mean	Median	S.D.	IQR	Skew	Kurt
1	138	85.7	-15.3	6.3	-3.5	-3.4	2.7	-4.8 to −2.0	-0.2	1.3
1	139	109.7	-14.1	1.7	-4.5	-4.2	2.4	-6.1 to −2.8	-0.4	0.0
1	140	120.4	-9.9	3.0	-4.1	-4.0	1.8	-5.2 to −3.0	0.1	0.8
Combined		**315.8**	**-15.3**	**6.3**	**-4.1**	**-3.9**	**2.3**	**-5.3 to −2.7**	**-0.1**	**1.1**
2	163	70.0	-10.8	9.0	-1.3	-1.7	3.7	-3.7 to 0.6	0.4	-0.1
2	164	82.5	-9.5	9.4	-1.1	-1.2	3.4	-3.2 to 0.7	0.4	0.3
2	166	80.1	-8.0	9.4	0.1	-0.5	3.5	-2.2 to 1.8	0.7	0.3
2	167	88.1	-8.5	10.7	1.0	0.6	3.4	-0.9 to 3.0	0.3	0.2
Combined		**320.7**	**-10.8**	**10.7**	**-0.3**	**-0.6**	**3.6**	**-2.6 to 1.6**	**0.4**	**0.1**
3	144	70.9	-15.8	10.1	-2.4	-2.6	5.2	-5.6 to 0.5	0.1	-0.1
3	145	89.3	-15.5	7.7	-1.8	-1.1	3.9	-3.5 to 0.7	-0.8	1.0
3	146	97.9	-15.1	8.5	-1.7	-1.3	4.0	-3.4 to 0.4	-0.6	1.2
3	155	71.9	-14.7	11.5	-2.6	-2.7	4.6	-5.1 to −0.4	0.2	0.7
3	157	84.4	-20.6	1.0	-7.0	-6.9	3.5	-8.3 to −5.4	-0.7	1.7
Combined		**414.4**	**-20.6**	**11.5**	**-3.1**	**-2.6**	**4.7**	**-6.3 to −0.2**	**-0.2**	**0.4**
4	None									
All Subjects		**1050.9**	**-20.6**	**11.5**	**-2.4**	**-2.1**	**2.0**	**-3.6 to −1.1**	**-0.8**	**0.9**

Table B-4.
Summary moments and statistics for roll position, slalom course, RWS.
(roll values expressed in degrees, time in seconds)

Subject	Run	Time	Min	Max	Mean	Median	S.D.	IQR	Skew	Kurt
1	141	106.2	-12.0	3.1	-4.1	-3.8	2.5	-5.7 to −2.4	-0.3	-.1
1	142	102.0	-11.5	18.2	-3.7	-3.5	2.6	-4.7 to −2.3	0.2	5.5
1	143	120.0	-13.4	0.8	-4.3	-4.2	2.1	-5.6 to −2.8	-0.4	0.2
Combined		**328.2**	**-13.4**	**18.2**	**-4.1**	**-3.8**	**2.4**	**-5.4 to −2.5**	**-0.1**	**2.5**
2	168	83.2	-4.6	11.2	0.4	-0.2	2.5	-1.1 to 1.3	1.4	2.1
2	169	89.1	-8.3	8.3	-0.1	-0.2	2.8	-2.1 to 1.6	0.2	0.2
2	170	101.1	-6.23	7.5	1.0	0.9	2.4	-0.4 to 2.4	0	0.1
2	174	63.6	-11.7	10.5	-0.5	-0.7	3.9	-2.7 to 2.2	0	0
2	175	65.0	-9.8	11.1	0.0	-07	4.1	-2.4 to 1.8	0.6	0.3
2	176	63.8	-9.4	12.1	1.9	2.0	4.1	-0.5 to 4.3	-0.1	0.0
Combined		**465.8**	**-11.7**	**12.1**	**0.5**	**0.3**	**3.3**	**-1.5 to 2.3**	**0.3**	**0.7**
3	158	71.2	-19.3	6.1	-3.9	-3.8	4.6	-6.0 to −1.6	-0.3	0.3
3	159	94.8	-13.9	7.6	-2.4	-2.4	2.9	-3.9 to −1.0	-0.1	1.3
3	161	61.2	-13.8	16.4	0.2	0	5.2	-1.5 to 1.6	0.4	1.6
3	162	55.3	-13.2	16.6	2.0	1.6	5.4	0 to 4.0	0	.8
3	180	59.6	-13.7	13.0	-1.1	-1.7	6.0	-4.7 to 2.3	0.3	-0.5
3	181	58.9	-18.8	12.2	-1.9	-2.6	6.1	-5.7 to 2.6	0.1	-0.4
3	182	52.9	-15.4	11.1	-1.8	-2.5	5.4	-4.7 to 1.4	0.1	-0.3
3	183	43.9	-17.2	12.8	-0.6	-0.8	6.1	-3.3 to 2.0	0	.1
Combined		**497.8**	**-19.3**	**16.6**	**-1.4**	**-1.7**	**5.4**	**-4.2 to 1.4**	**0.2**	**0.5**
4					None					
All Subjects		**1291.8**	**-19.3**	**18.2**	**-1.1**	**-0.8**	**1.5**	**-4.7 to 2.3**	**1.8**	**8.2**

68

Appendix C.

Roll position box plots.

Figure C-1. Subject #1 GVE box plots.

Figure C-2. Subject #1 NVG box plots.

70

Figure C-3. Subject #1 TIO box plots.
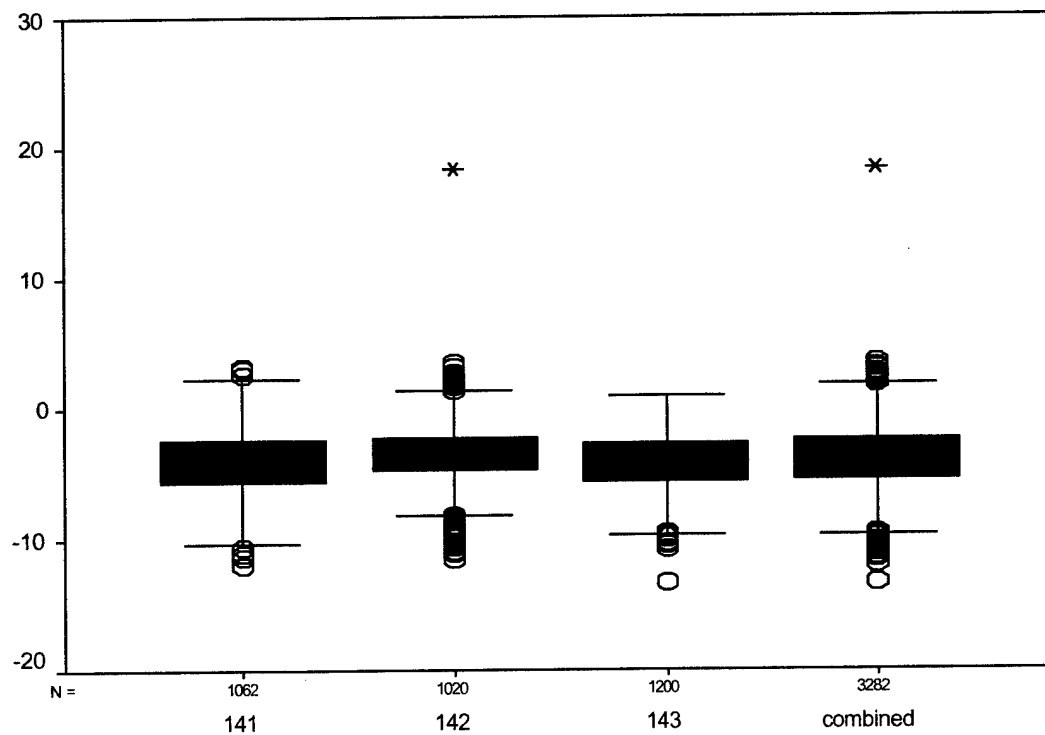
Figure C-4. Subject #1 RWS box plots.
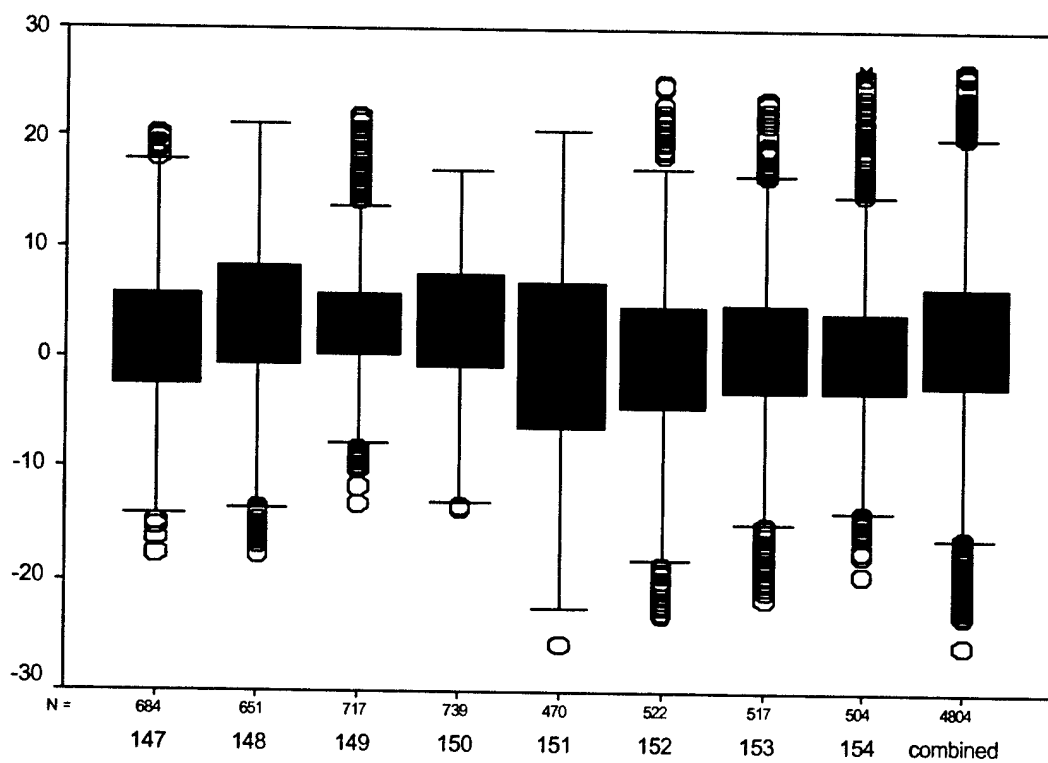
Figure C-5. Subject #2 GVE box plots.
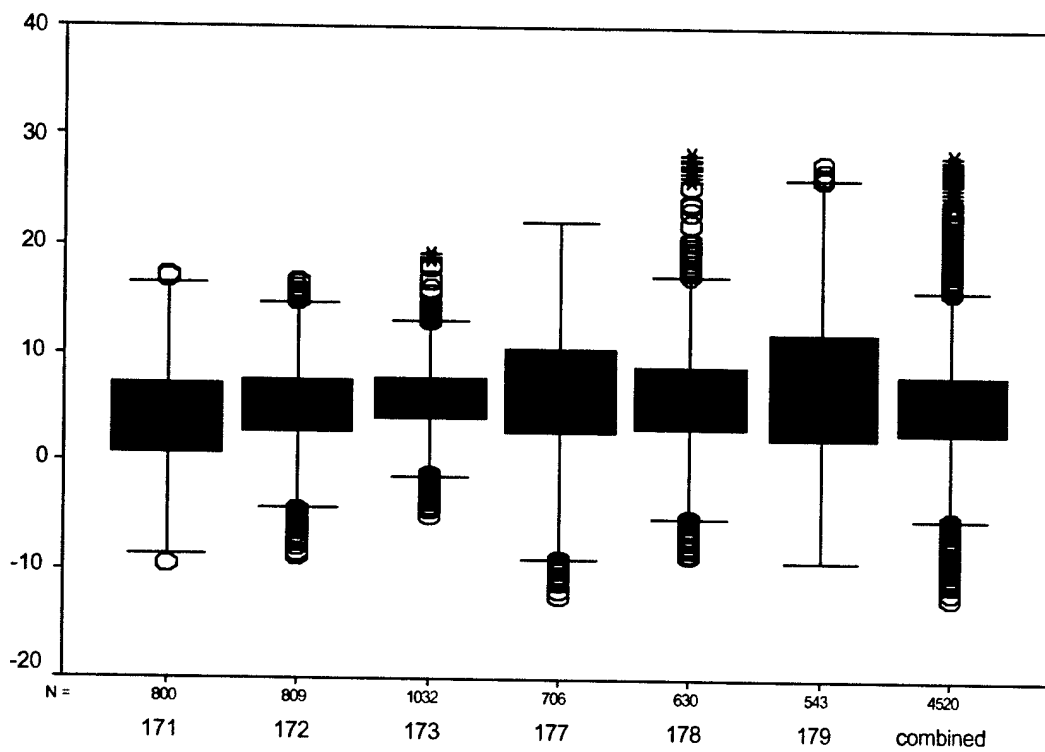
Figure C-6. Subject #2 NVG box plots.
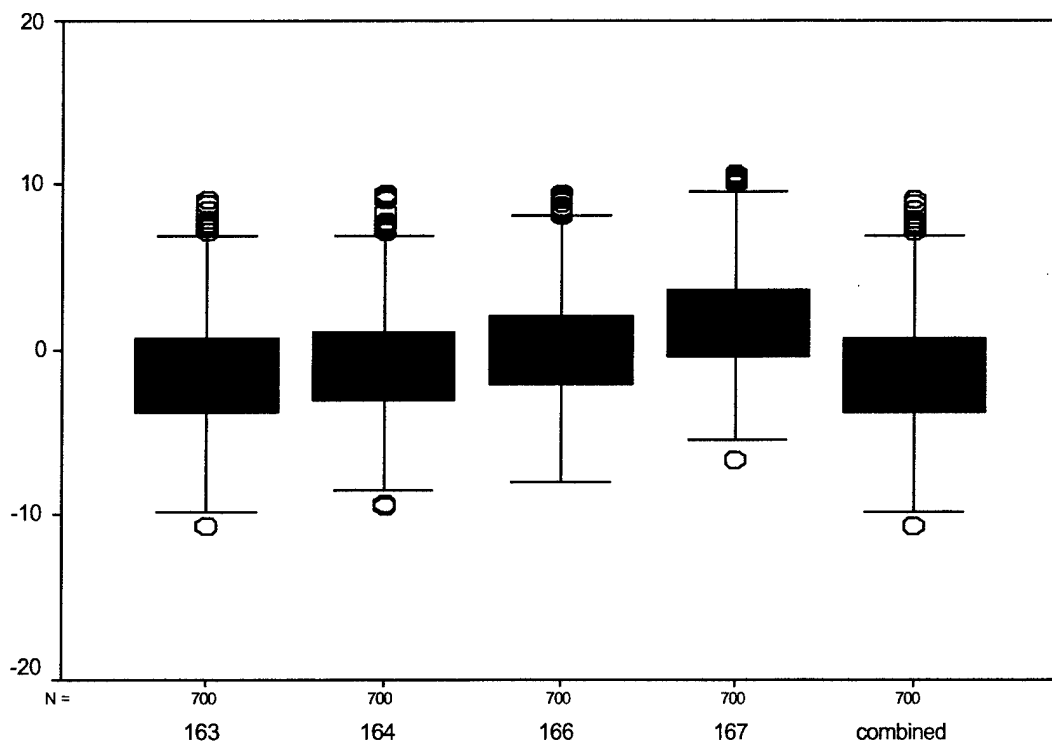
Figure C-7. Subject #2 TIO box plots.
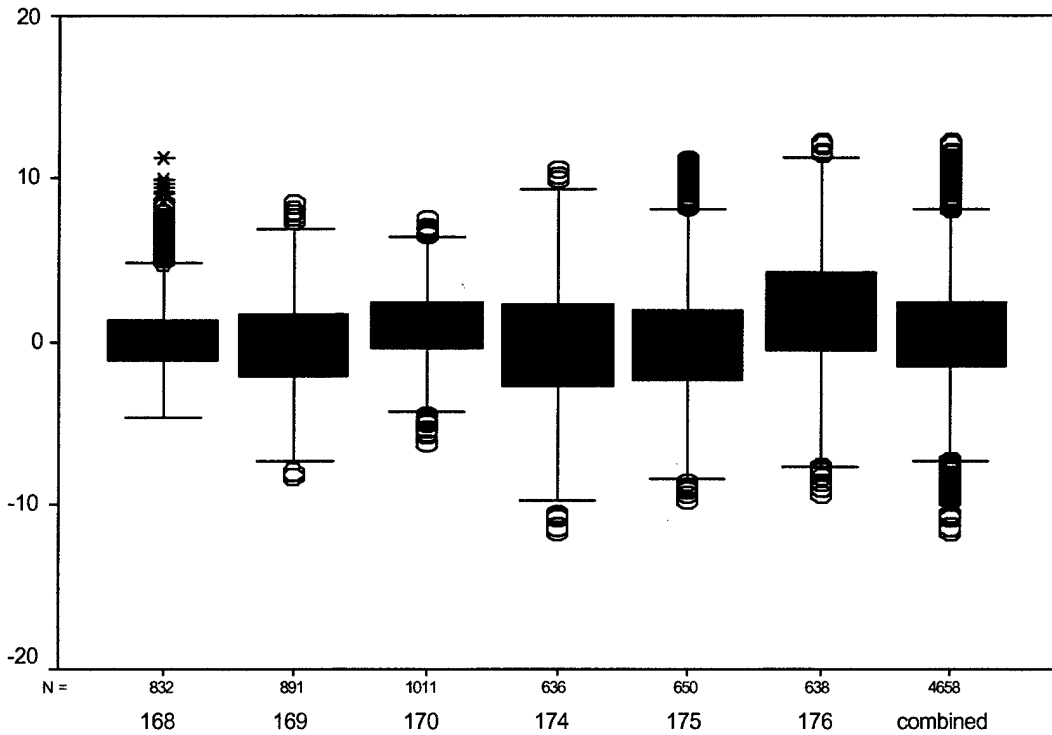
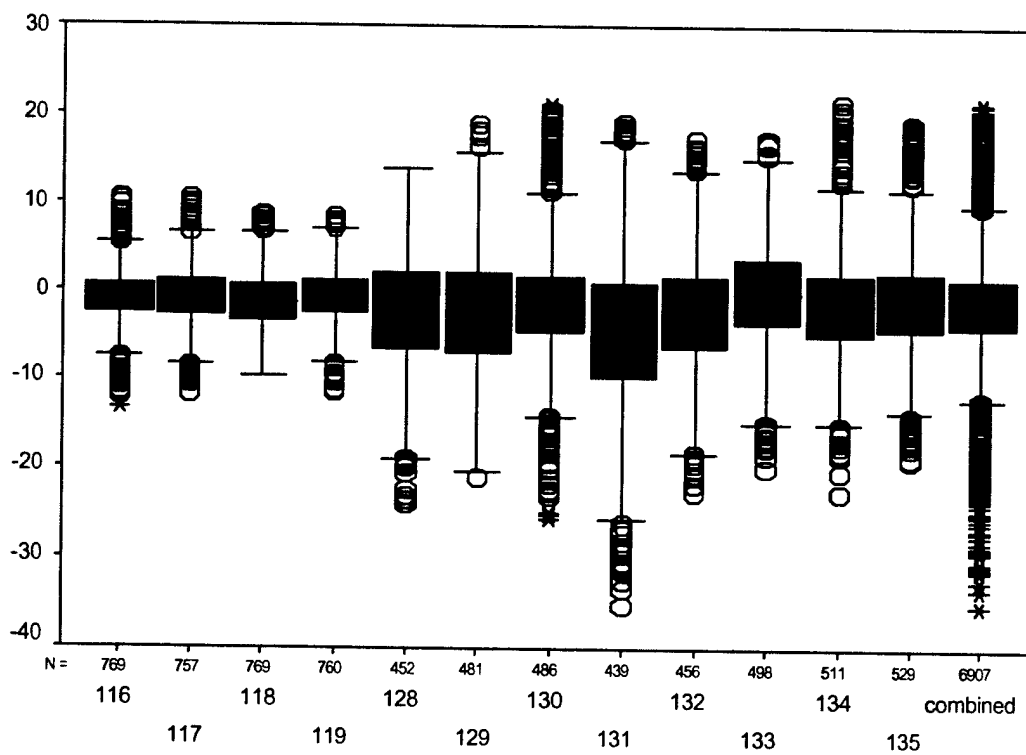Figure C-8. Subject #2 RWS box plots.
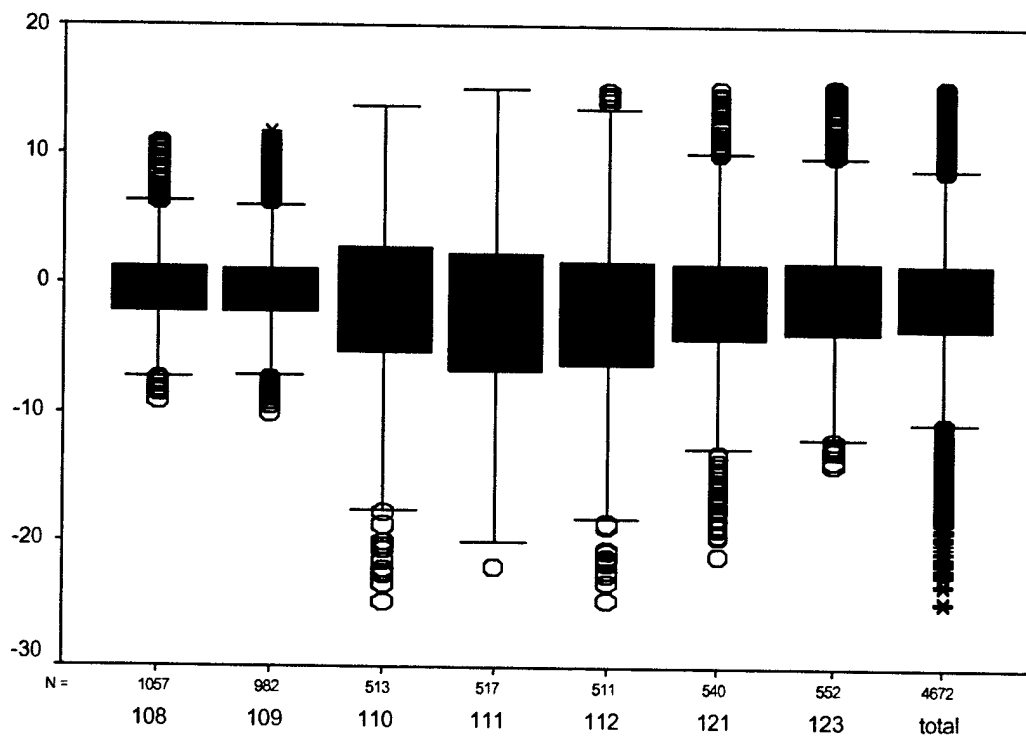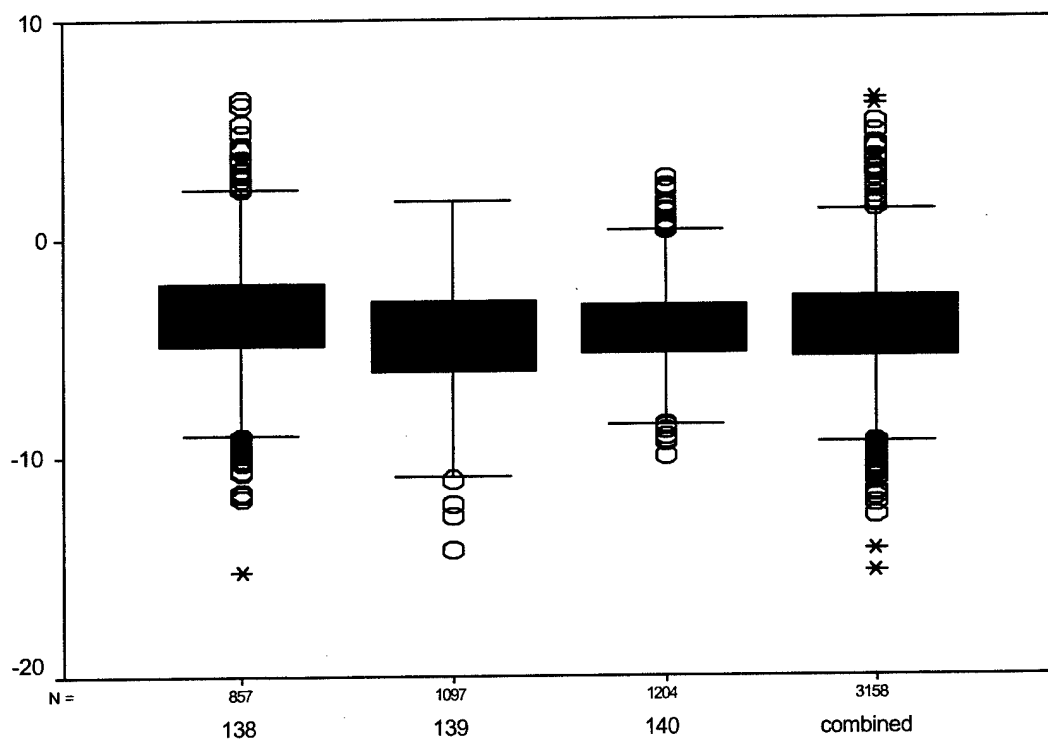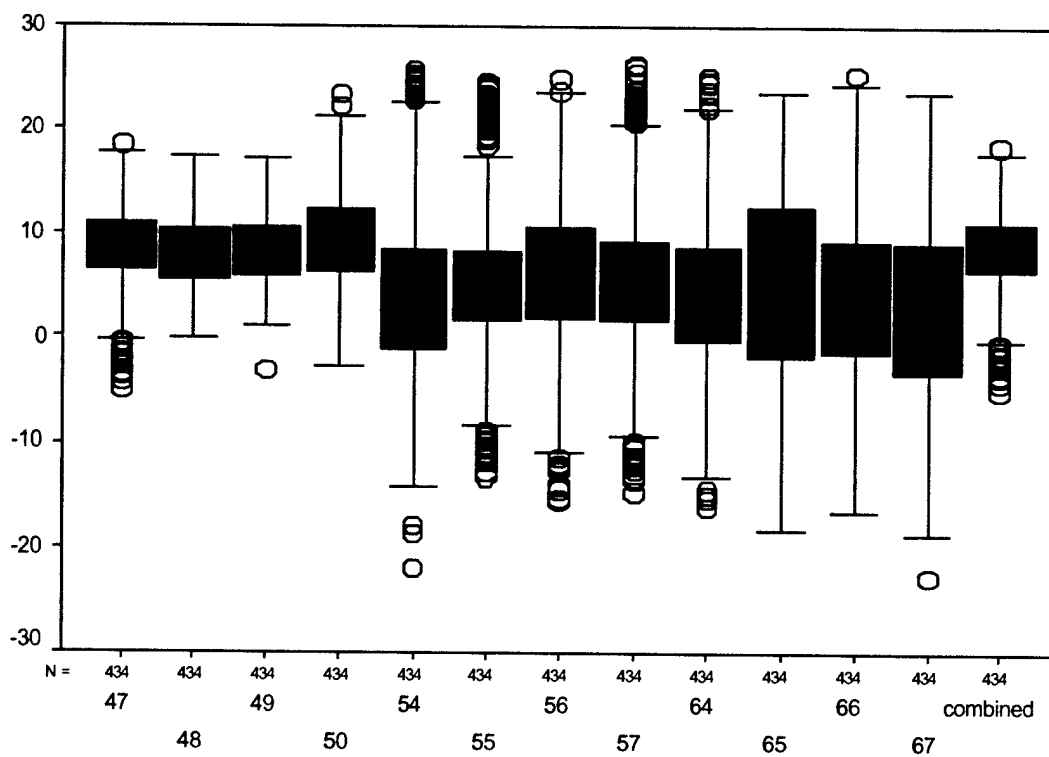
Figure C-9. Subject #3 GVE box plots.
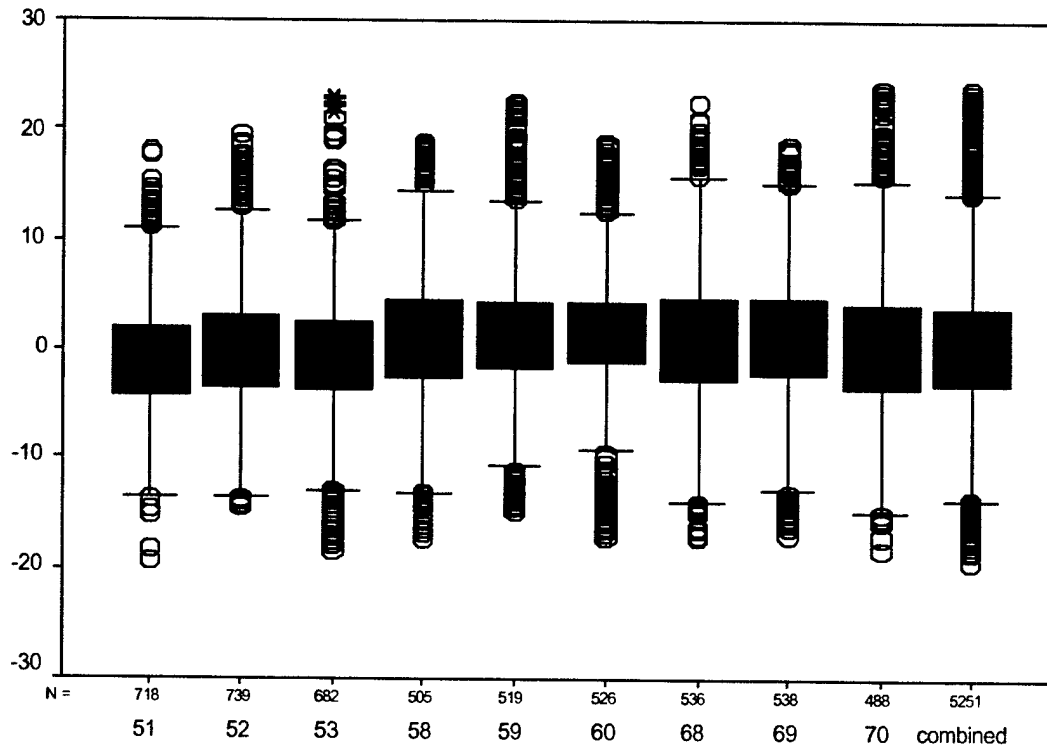
Figure C-10. Subject #3 NVG box plots.
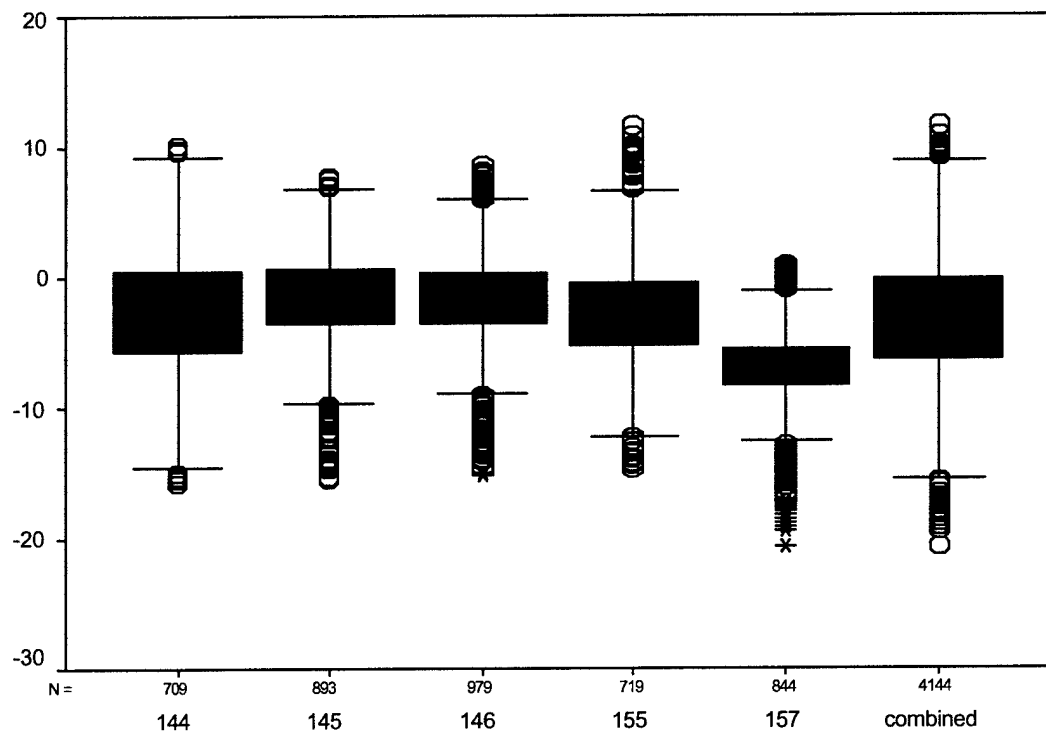
Figure C-11. Subject #3 TIO box plots.
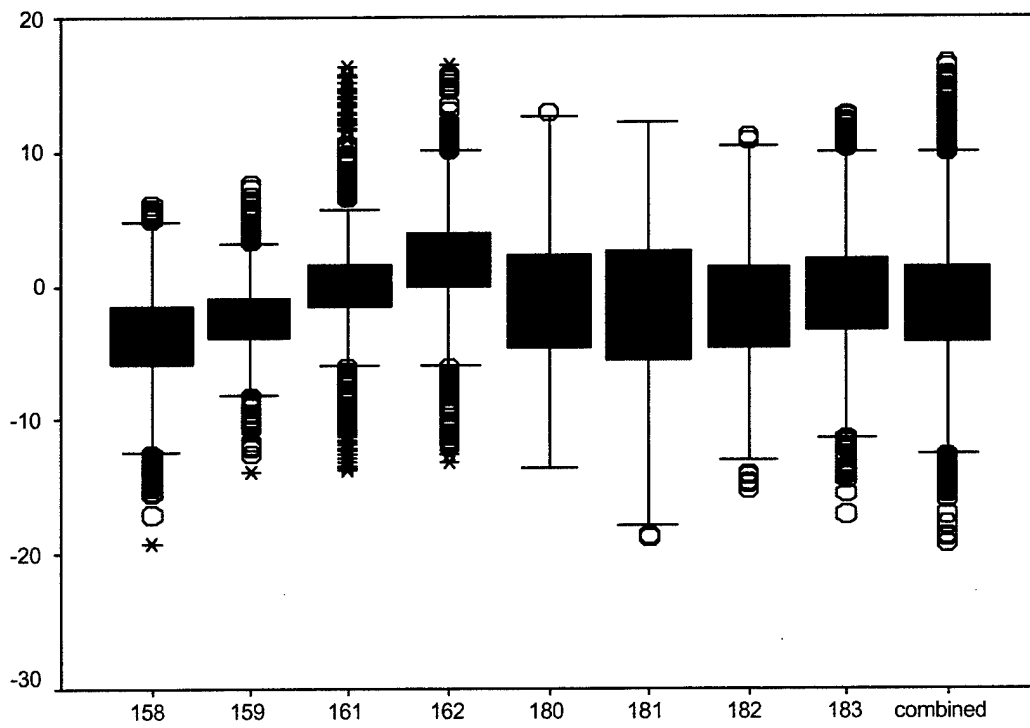
Figure C-12. Subject #3 RWS box plots.
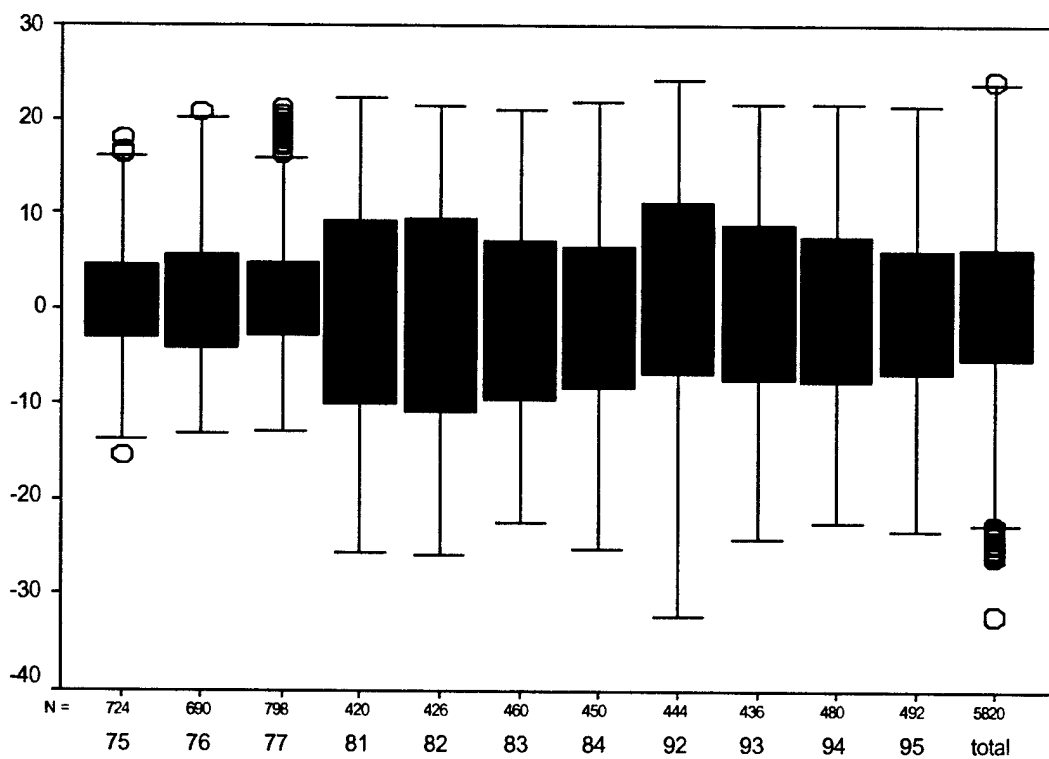
Figure C-13. Subject #4 GVE box plots.
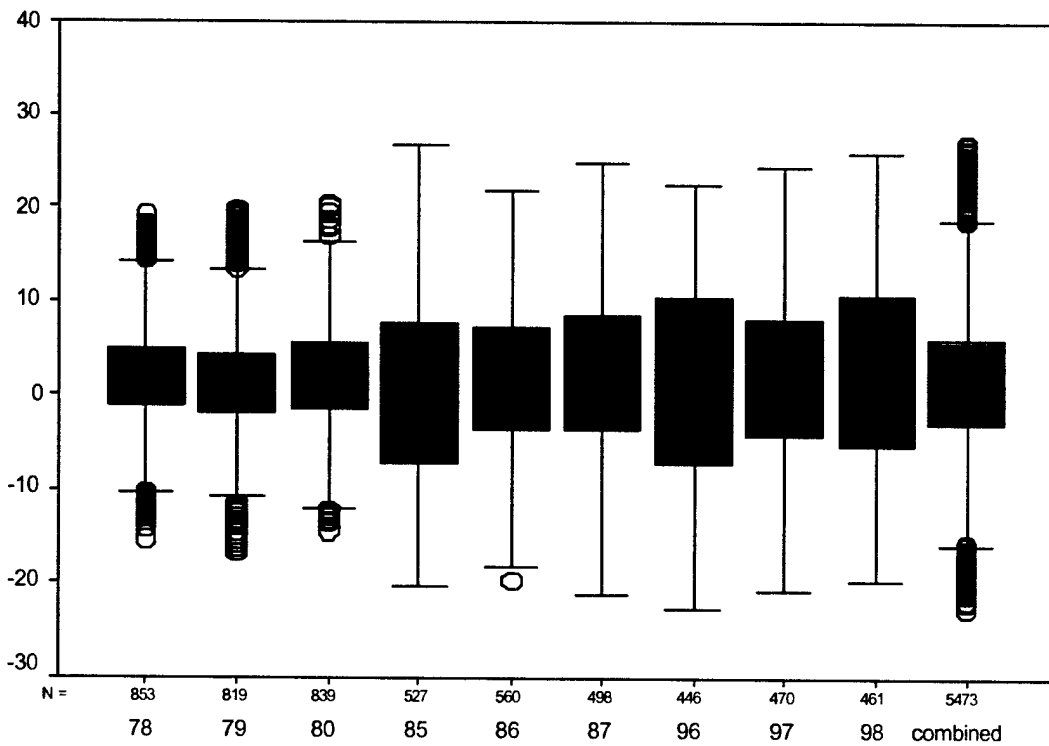
Figure C-14. Subject #4 NVG box plots.

Appendix D.

Roll reversal summary tables.

Table D-1.
Summary statistics for roll reversals, slalom course, GVE.
(expressed in degrees)

Subject	Run	Time	# of Reversals	Rev/min
1	116	76.9	53	41.4
1	117	75.7	51	40.4
1	118	76.9	47	36.7
1	119	76.0	58	45.8
1	128	45.2	31	41.2
1	129	48.1	29	36.2
1	130	48.6	29	35.8
1	131	43.8	23	31.5
1	132	45.6	24	31.6
1	133	49.8	26	31.3
1	134	51.1	32	37.6
1	135	52.9	29	32.9
Combined		690.6	432	37.5
2	147	68.4	42	36.8
2	148	65.1	45	41.5
2	149	71.7	46	38.5
2	150	73.9	44	35.7
2	151	47.0	22	28.1
2	152	52.2	31	35.6
2	153	51.7	19	22.1
2	154	50.4	31	36.9
Combined		480.4	280	35.0
3	47	74.8	36	28.9
3	48	75.7	46	36.5
3	49	78.8	51	38.8
3	50	73.2	35	28.7
3	54	44.6	24	32.3
3	55	47.6	18	22.7
3	56	46.5	20	25.8
3	57	49.0	22	26.9
3	64	50.6	25	29.6
3	65	46.8	24	30.8
3	66	46.7	23	29.6
3	67	43.4	26	35.9
Combined		677.7	350	31.0
4	75	72.4	43	35.6
4	76	69.0	45	39.1
4	77	79.8	46	34.6
4	81	42.0	12	17.1
4	82	42.6	14	19.7
4	83	46.0	20	26.1
4	84	45.0	21	28.0
4	92	44.4	16	21.6
4	93	43.6	17	23.4
4	94	48.0	17	21.3
4	95	49.2	21	25.6
Combined		582	272	28.0
All Subjects		2430.7	1334	32.9

78

Table D-2.
Summary statistics for roll reversals, slalom course, NVG.
(expressed in degrees)

Subject	Run	Time	# of Reversals	Rev / min
1	108	105.7	82	46.5
1	109	98.2	72	44.0
1	110	51.3	31	36.3
1	111	51.7	31	36.0
1	112	51.1	31	36.4
1	121	54.0	32	35.6
1	123	55.2	36	39.1
Combined		**467.2**	**315**	**40.5**
2	171	80.0	50	37.5
2	172	80.9	47	34.9
2	173	103.2	77	44.8
2	177	70.6	44	37.4
2	178	63.0	44	41.9
2	179	54.3	28	30.9
Combined		**452.0**	**290**	**38.5**
3	51	71.8	40	33.4
3	52	73.9	50	40.6
3	53	68.2	33	29.0
3	58	50.5	28	33.3
3	59	51.9	27	31.2
3	60	52.6	29	33.1
3	68	53.6	36	40.3
3	69	53.8	29	32.3
3	70	48.8	34	41.8
Combined		**525.1**	**306**	**35.0**
4	78	95.3	46	29.0
4	79	81.9	49	35.9
4	80	83.9	59	42.2
4	85	52.7	29	33.0
4	86	56.0	31	33.2
4	87	49.8	24	28.1
4	96	44.6	18	24.2
4	97	47.0	18	23.0
4	98	46.1	15	19.5
Combined		**557.3**	**289**	**31.1**
All Subjects		**2001.6**	**1200**	**36.0**

Table D-3.
Summary statistics for roll reversals, slalom course, TIO.
(expressed in degrees)

Subject	Run	Time	# of Reversals	Rev /min
1	138	85.7	67	46.9
1	139	109.7	77	42.1
1	140	120.4	70	34.9
Combined		**315.8**	**214**	**40.7**
2	163	70.0	38	32.6
2	164	82.5	46	33.5
2	166	80.1	39	29.2
2	167	88.1	49	33.4
Combined		**320.7**	**172**	**32.2**
3	144	70.9	40	33.9
3	145	89.3	52	34.9
3	146	97.9	63	38.6
3	155	71.9	48	40.1
3	157	84.4	47	33.4
Combined		**414.4**	**250**	**36.2**
4	None			
All Subjects		**1050.9**	**636**	**36.3**

Table D-4.
Summary statistics for roll reversals, slalom course, RWS.
(expressed in degrees)

Subject	Run	Time	# of Reversals	Rev /min
1	141	106.2	77	43.5
1	142	102.0	73	42.9
1	143	120.0	85	42.5
Combined		**328.2**	**235**	**43.0**
2	168	83.2	43	31.0
2	169	89.1	46	31.0
2	170	101.1	72	42.7
2	174	63.6	37	34.9
2	175	65.0	40	36.9
2	176	63.8	30	28.2
Combined		**465.8**	**268**	**34.5**
3	158	71.2	25	21.1
3	159	94.8	61	38.6
3	161	61.2	31	30.4
3	162	55.3	26	28.2
3	180	59.6	31	31.2
3	181	58.9	31	31.6
3	182	52.9	23	26.1
3	183	43.9	28	38.3
Combined		**497.8**	**256**	**30.9**
4	None			
All Subjects		**1291.8**	**759**	**35.3**

Appendix E.

Roll excursion distributions.

Figure E-1. Subject #1 GVE head position excursion histograms.

83

Head Roll Excursion Flight 35 Run 108

Head Roll Excursion Flight 35 Run 109

Head Roll Excursion Flight 36 Run 110

Head Roll Excursion Flight 36 Run 111

Head Roll Excursion Flight 36 Run 112

Head Roll Excursion Flight 39 Run 121

Head Roll Excursion Flight 39 Run 123

Figure E-2. Subject #1 NVG head position excursion histograms.

84

Head Roll Excursion Flight 55 Run 138

Head Roll Excursion Flight 55 Run 139

Head Roll Excursion Flight 55 Run 140

Figure E-3. Subject #1 TIO head position excursion histograms.

Head Roll Excursion Flight 55 Run 141

Head Roll Excursion Flight 55 Run 142

Head Roll Excursion Flight 55 Run 143

Figure E-4. Subject #1 RWS head position excursion histograms.

Figure E-5. Subject #2 GVE head position excursion histograms.

Figure E-6. Subject #2 NVG head position excursion histograms.

Figure E-7. Subject #2 TIO head position excursion histograms.

Figure E-8. Subject #2 RWS head position excursion histograms.

Figure E-9. Subject #3 GVE head position excursion histograms.
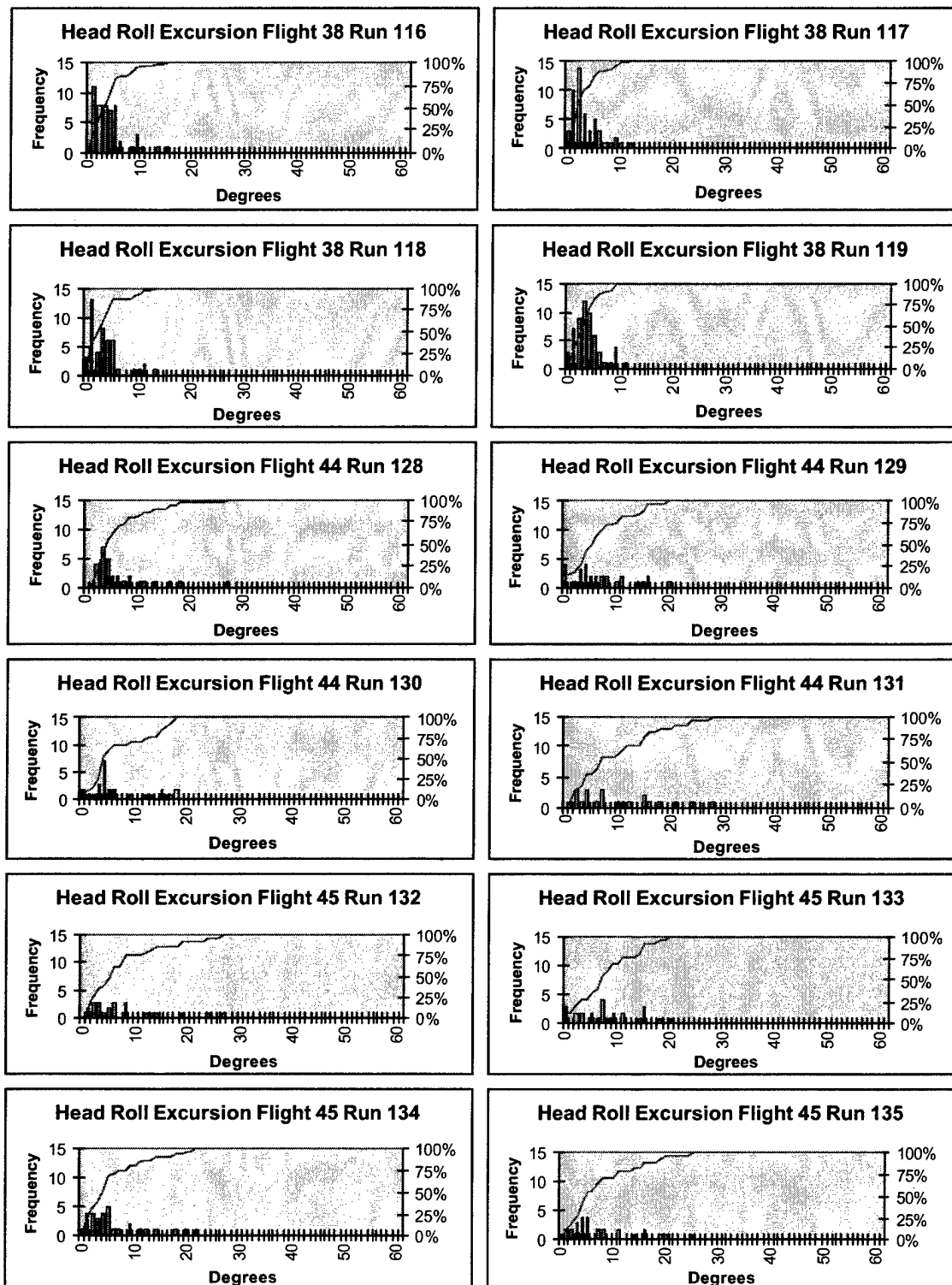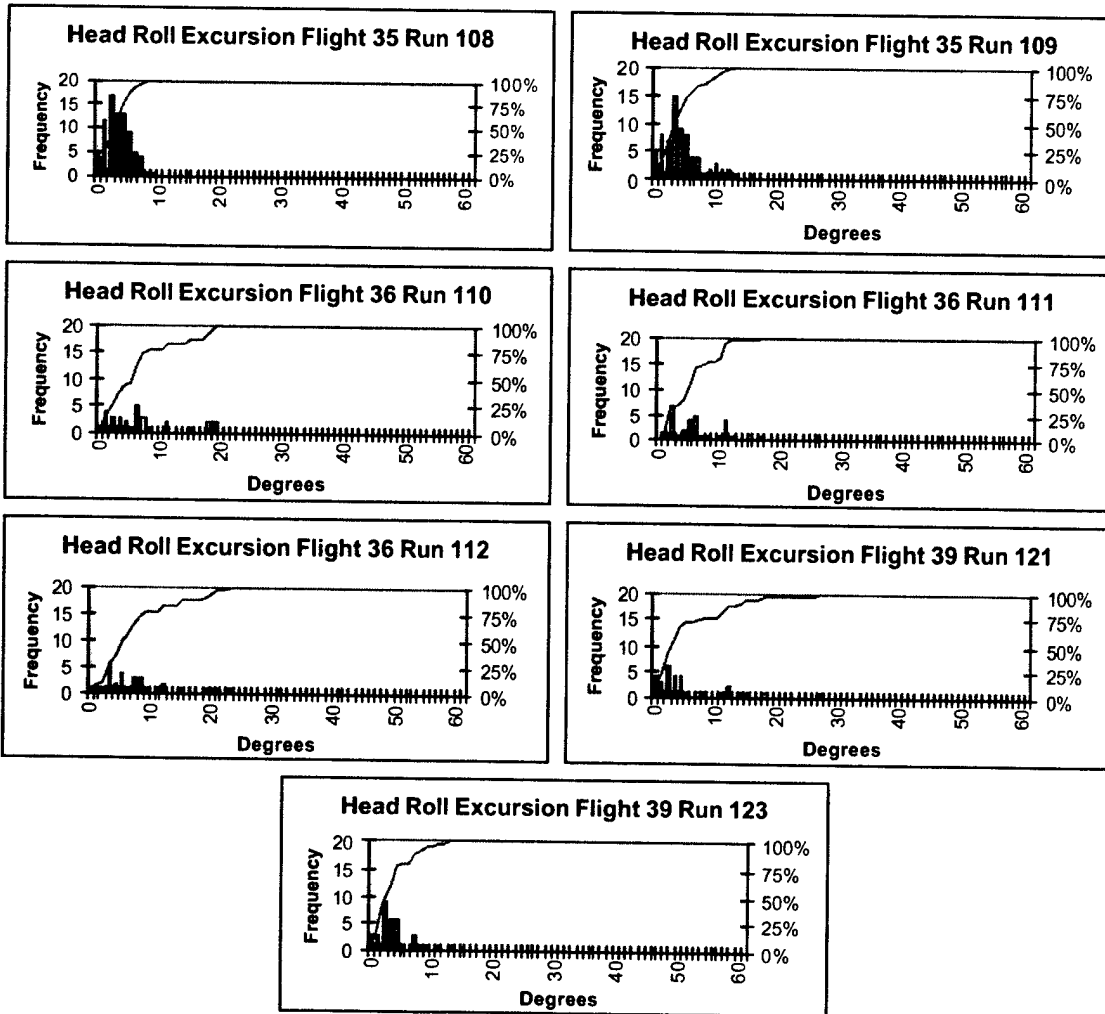
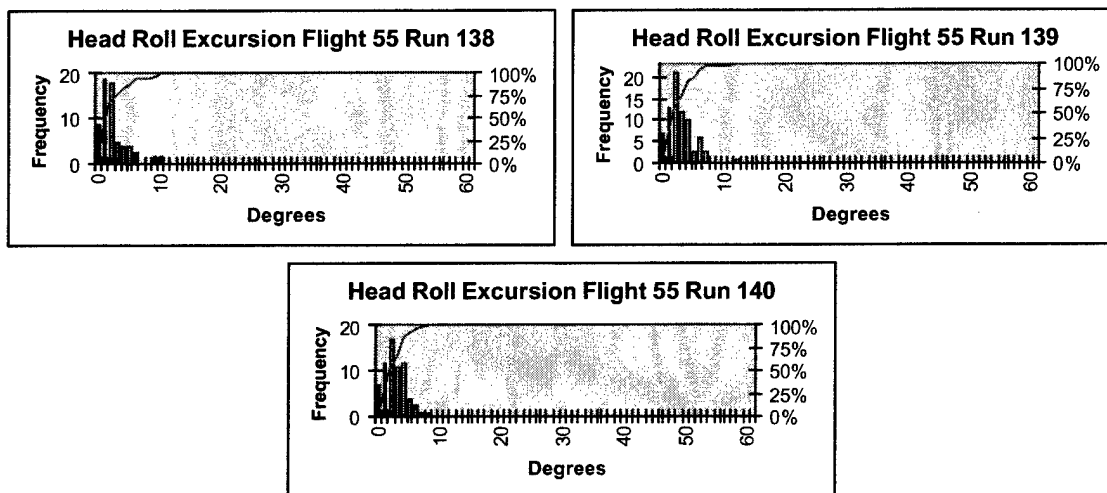Figure E-10. Subject #3 NVG head position excursion histograms.

Figure E-11. Subject #3 TIO head position excursion histograms.

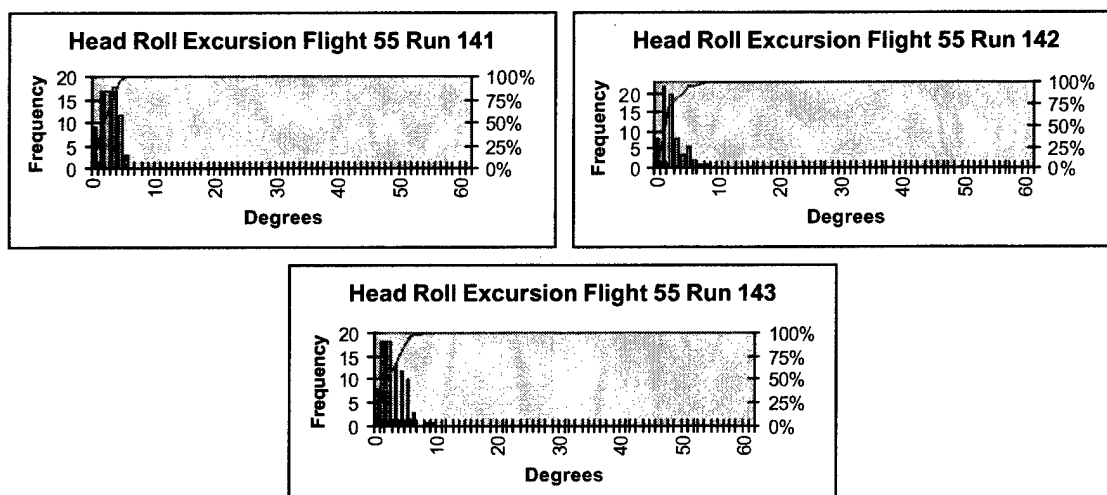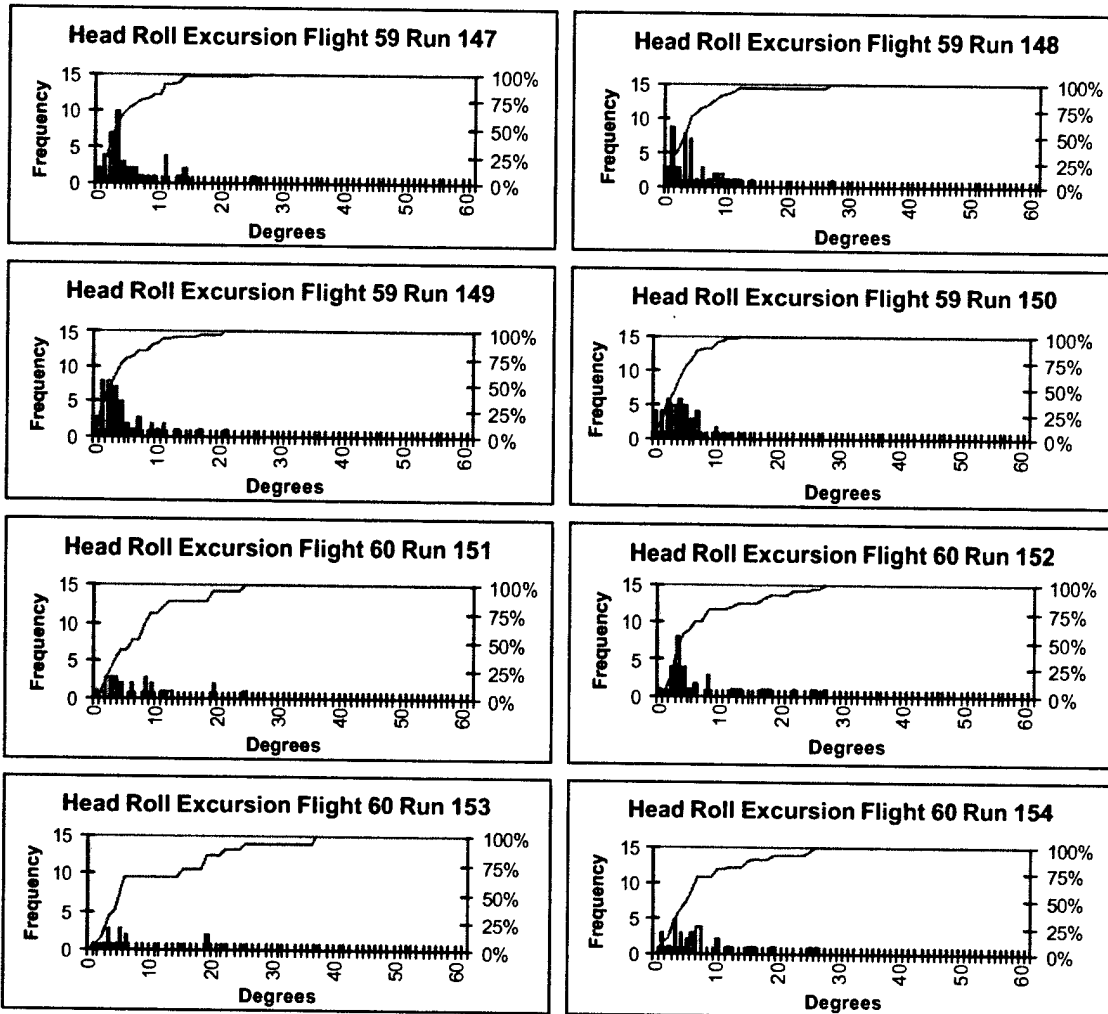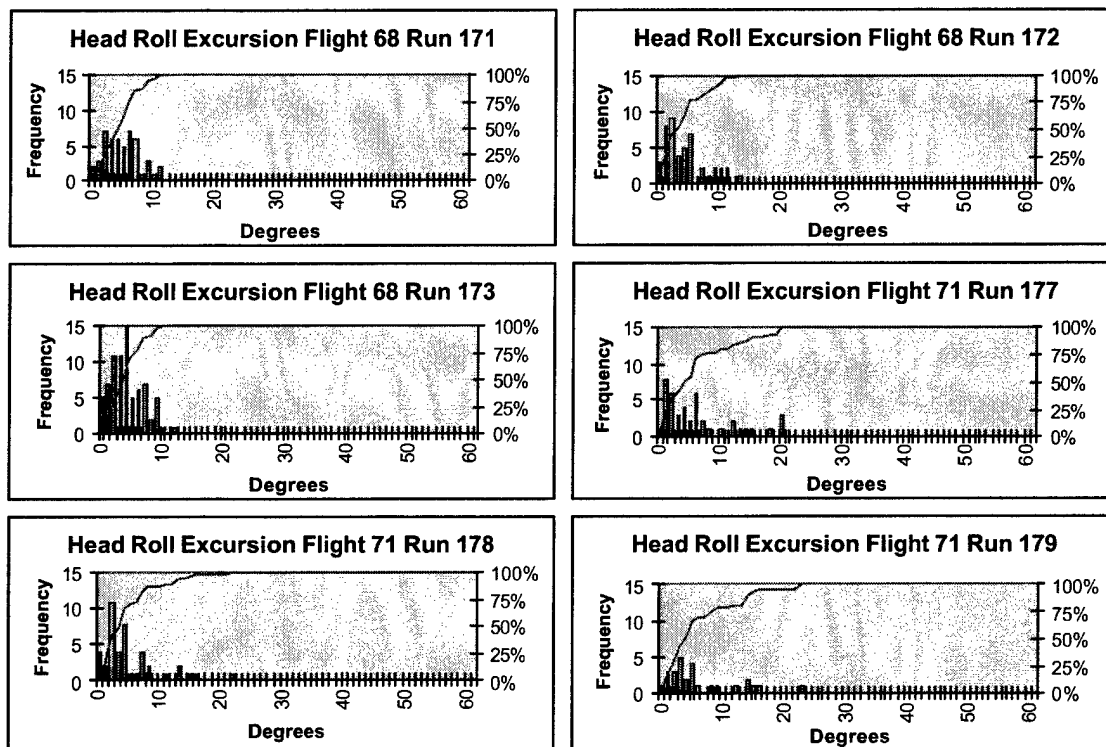Figure E-12. Subject #3 RWS head position excursion histograms.

92

Figure E-13. Subject #4 GVE head position excursion histograms.

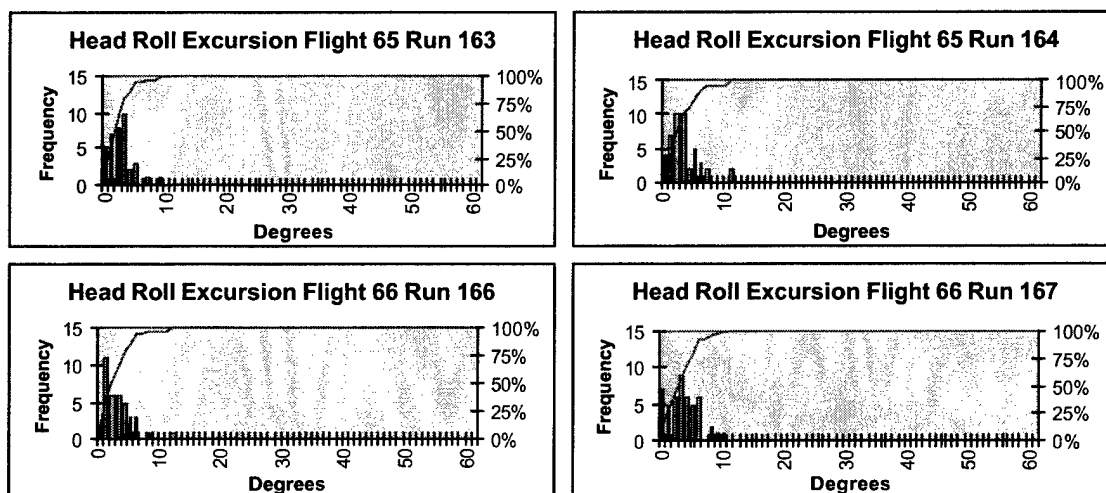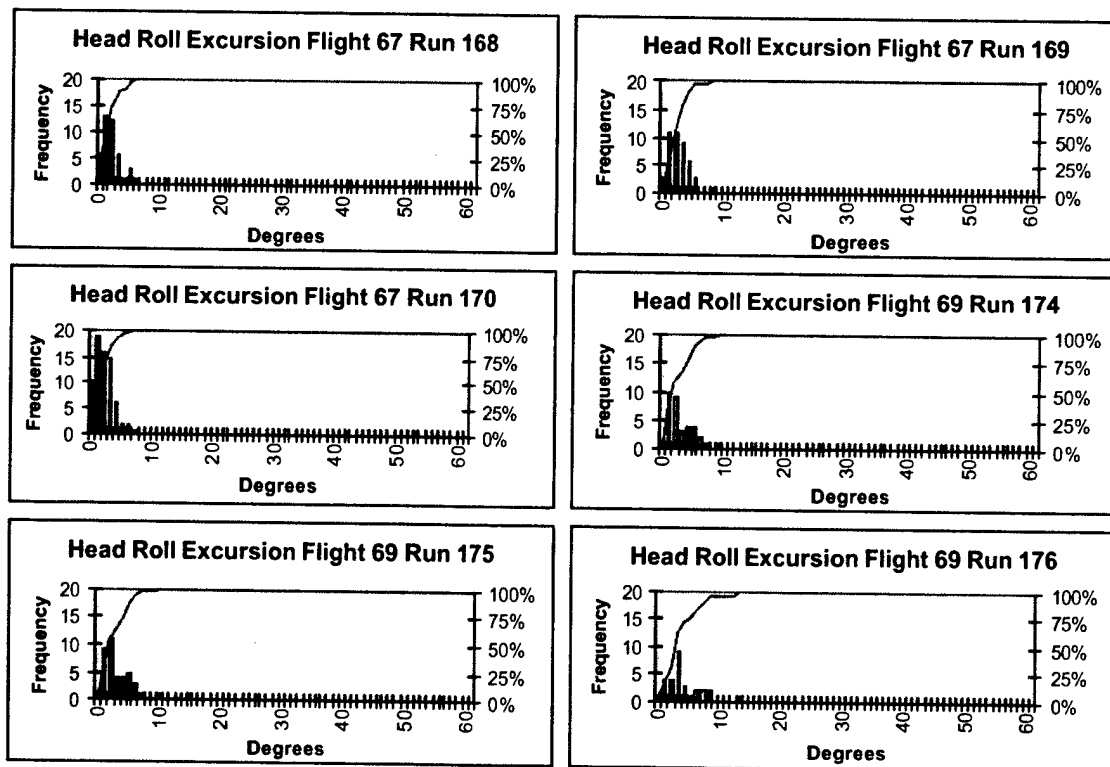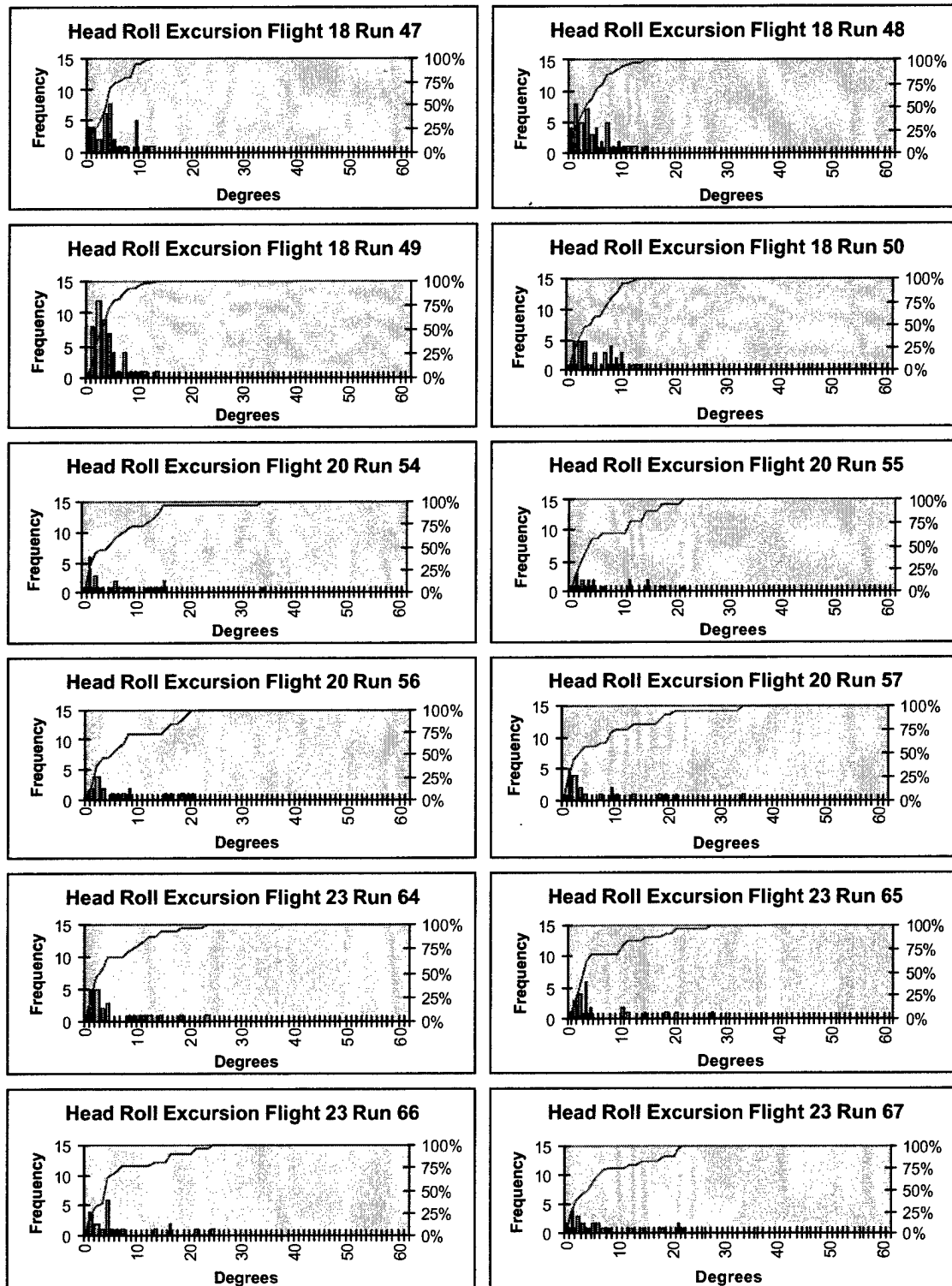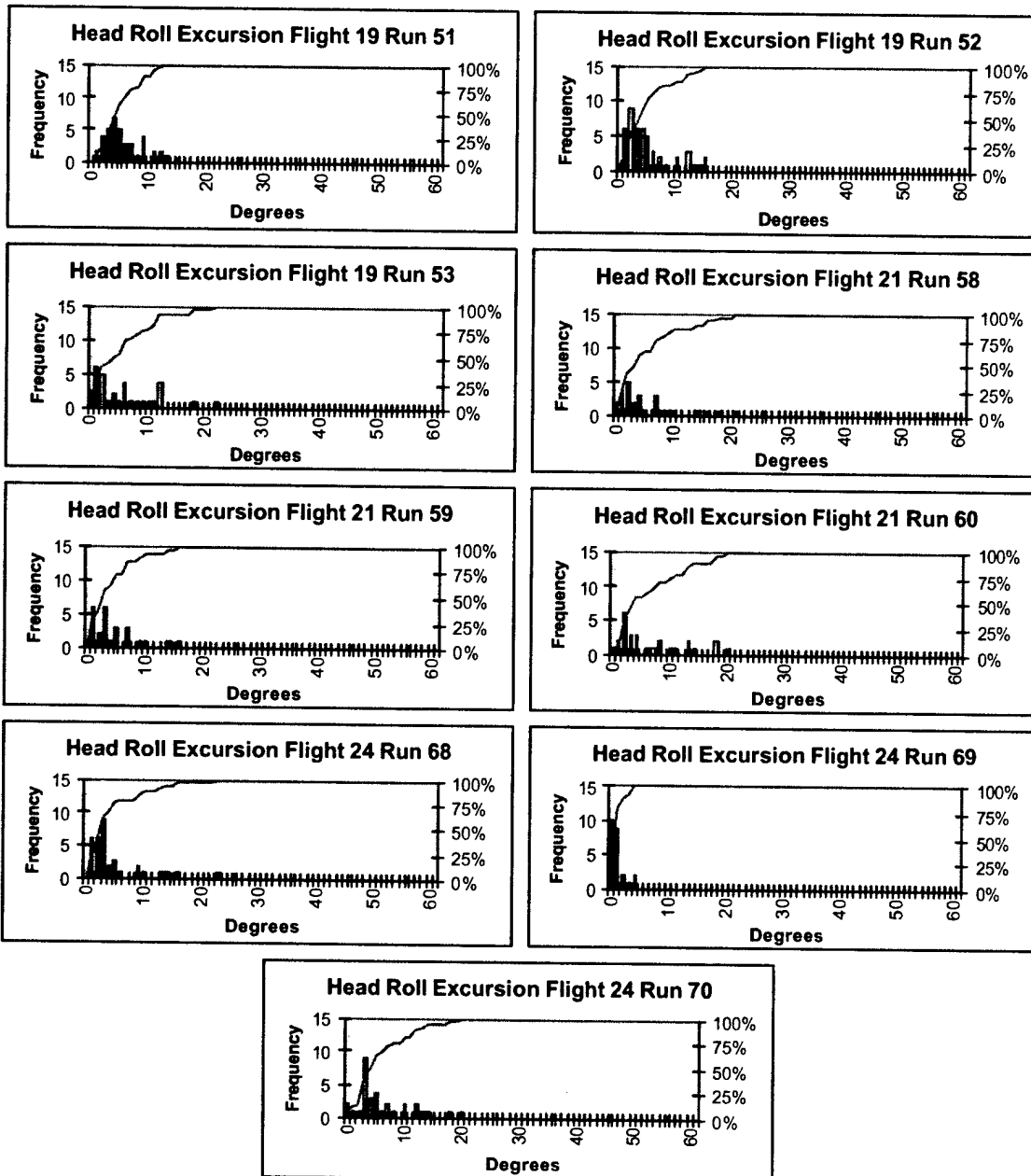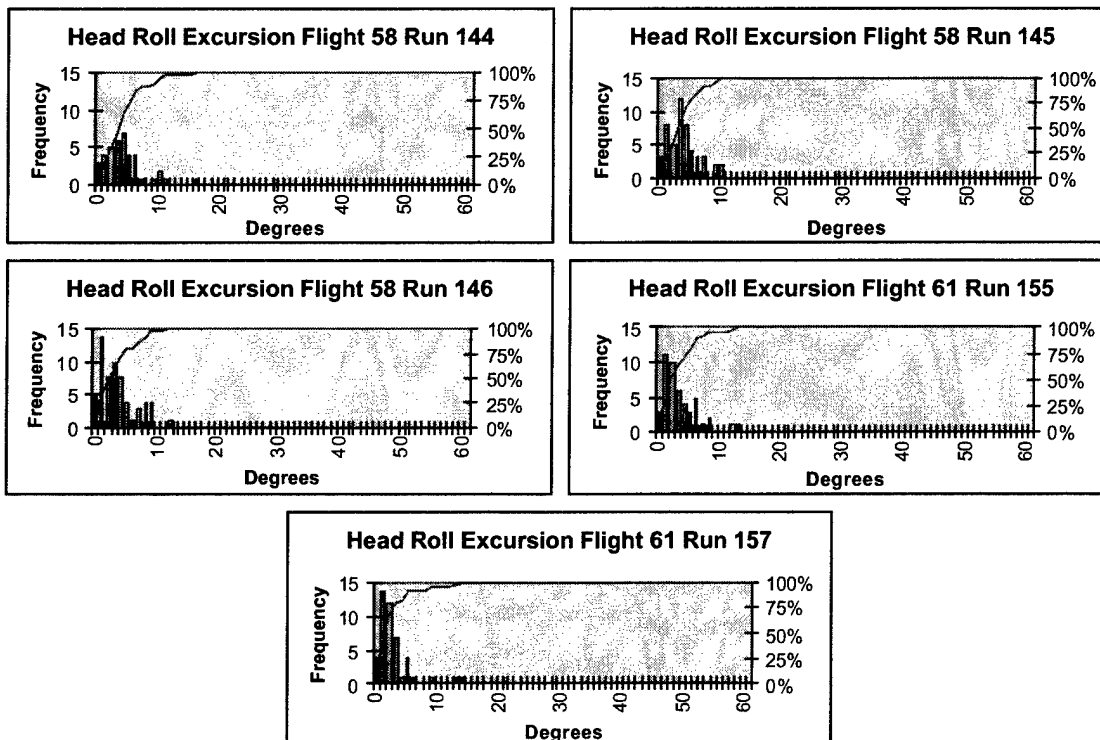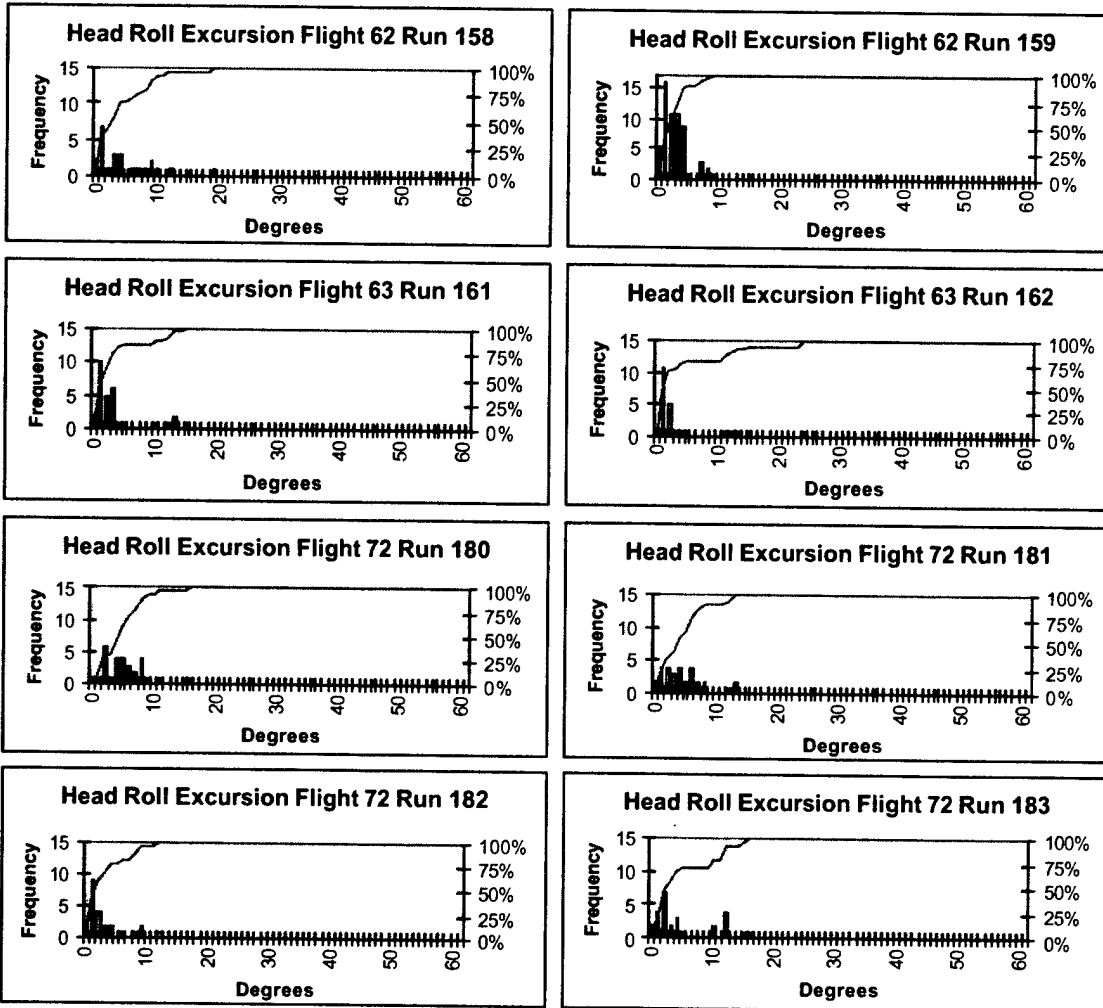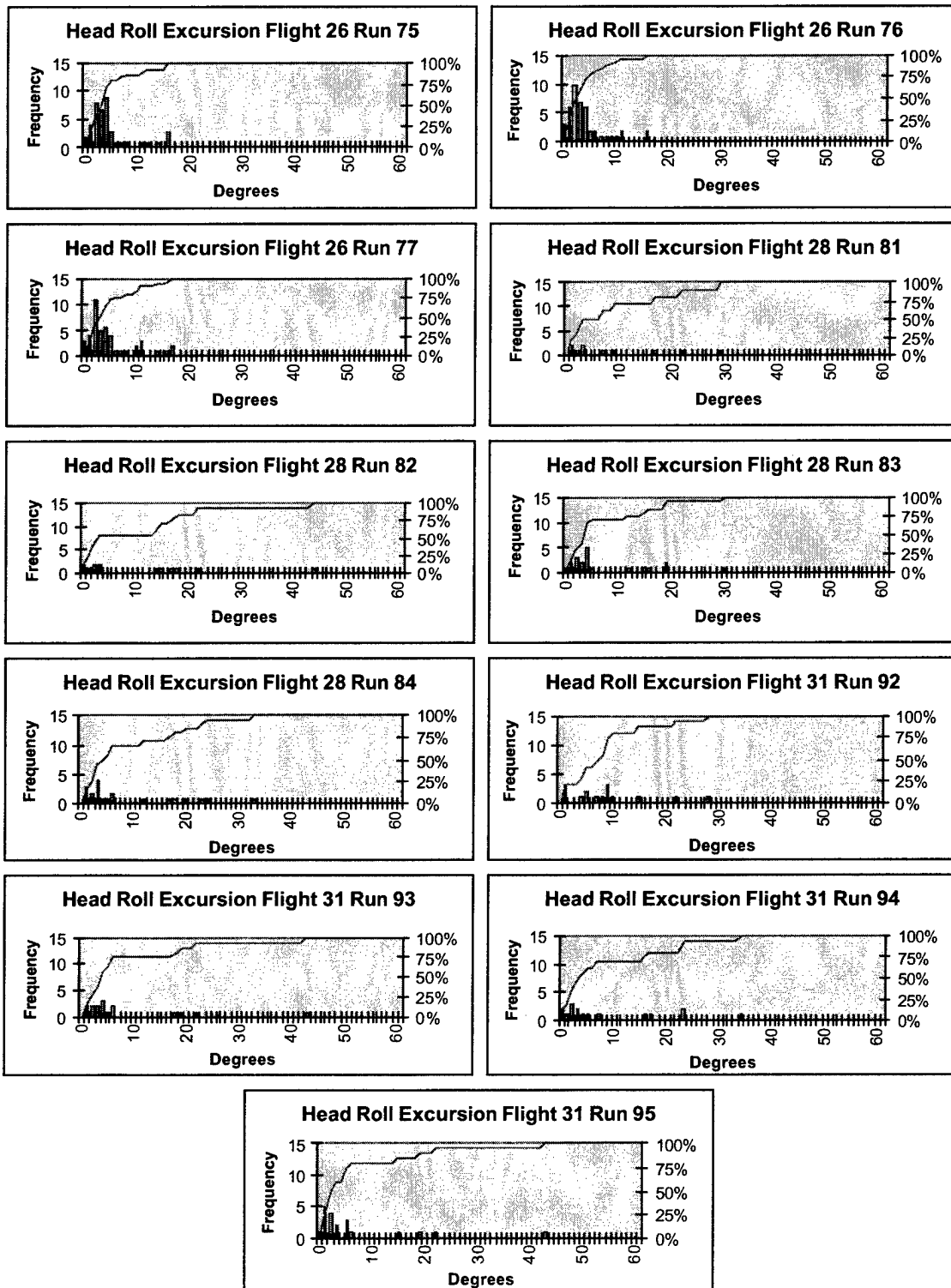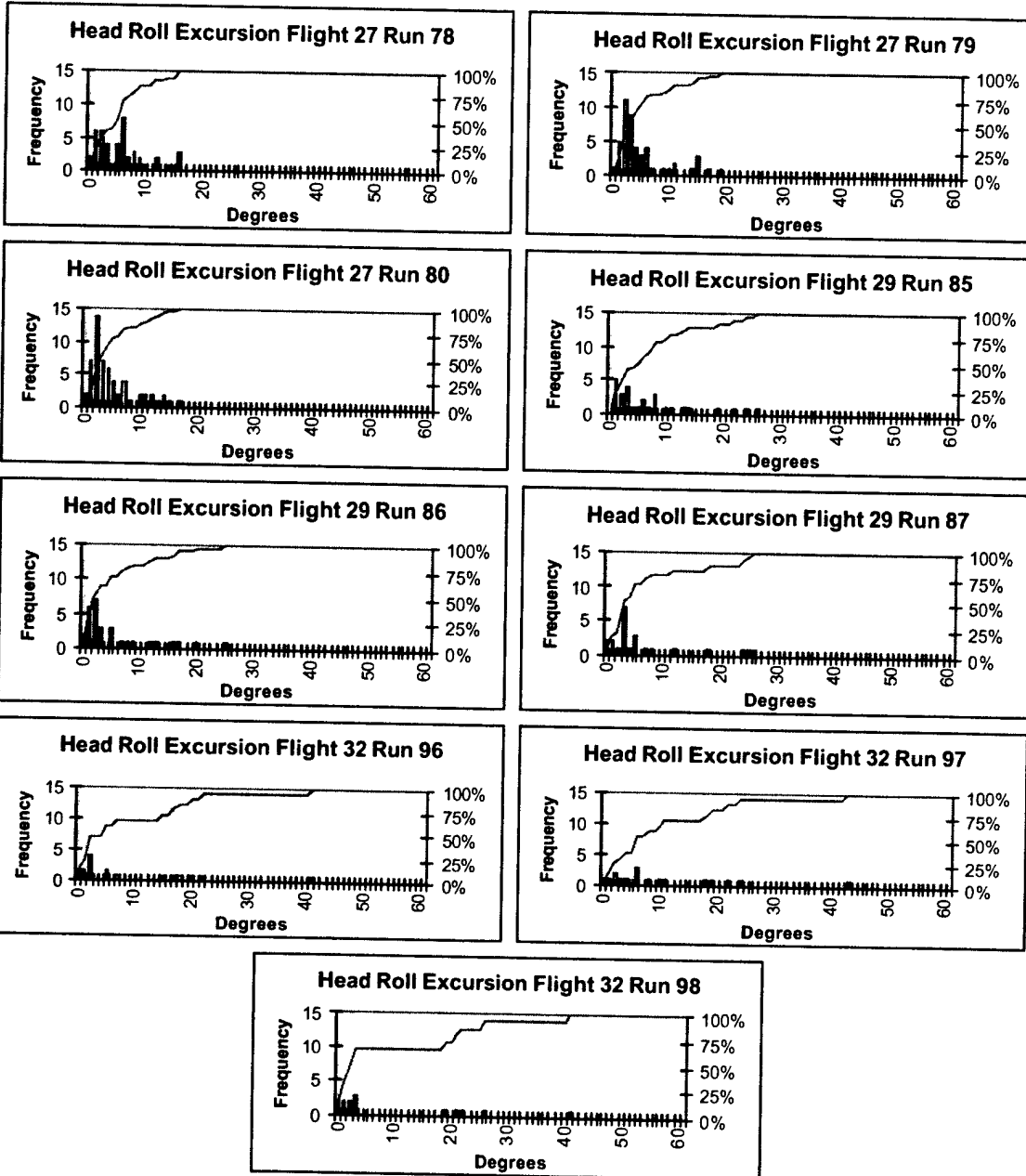Figure E-14. Subject #4 NVG head position excursion histograms.

Appendix F.

Roll excursion summary tables.

Table F-1.
Summary statistics for roll excursions, slalom course, GVE.
(excursion values expressed in degrees)

Subject	Run	Time	# of Excursions	Exc/min	Min	Max	Mean	Median	S.D.	IQR
1	116	76.9	54	42.1	0	15	4.0	3.0	3.1	2.0 to 5.0
1	117	75.7	52	41.2	0	12	3.4	2.0	2.7	1.5 to 5.0
1	118	76.9	48	37.5	0	13	3.4	3.0	3.0	1.0 to 4.5
1	119	76.0	59	46.6	0	9	3.4	3.0	2.2	2.0 to 4.0
1	128	45.2	32	42.2	2	27	6.6	4.0	5.7	3.0 to 8.0
1	129	48.1	30	37.4	0	20	7.0	6.0	5.4	3.0 to 11.0
1	130	48.6	30	37.0	0	18	7.1	4.5	5.8	3.8 to 12.3
1	131	43.8	24	32.9	1	28	9.9	7.0	7.6	4.0 to 15.0
1	132	45.6	25	32.9	1	27	7.6	5.5	7.2	2.8 to 9.0
1	133	49.8	27	32.5	0	20	7.7	7.0	5.7	3.0 to 11.0
1	134	51.1	33	38.8	0	22	6.0	4.0	5.7	2.0 to 7.5
1	135	52.9	30	34.0	0	25	7.4	5.0	6.5	3.0 to 11.0
Combined		**690.6**	**444**	**38.6**	**0**	**28**	**5.5**	**4.0**	**5.2**	**2.0 to 7.0**
2	147	68.4	43	37.7	0	25	5.3	3	5.0	2.0 to 7.0
2	148	65.1	46	42.4	0	27	4.6	3	4.8	1.0 to 6.0
2	149	71.7	47	39.3	0	21	4.6	3	4.6	2.0 to 6.8
2	150	73.9	45	36.5	0	14	4.6	4	3.6	2.0 to 6.3
2	151	47.0	23	29.4	0	24	8.3	7	6.7	3.0 to 10.5
2	152	52.2	32	36.6	0	27	7.3	4	7.2	3.0 to 8.0
2	153	51.7	20	23.2	1	37	10.1	5	9.9	3.5 to 17.0
2	154	50.4	32	38.1	1	26	7.9	6	6.8	3.0 to 10.0
Combined		**480.4**	**288**	**36.0**	**0**	**37**	**6.0**	**4**	**6.0**	**2.0 to 8.0**
3	47	74.8	37	29.7	0	12	4.4	4.0	3.4	2.0 to 6.3
3	48	75.7	47	37.3	0	14	4.3	3.0	3.4	1.3 to 6.8
3	49	78.8	52	39.6	1	13	3.8	3.0	2.8	2.0 to 5.0
3	50	73.2	36	29.5	0	13	5.2	5.0	3.6	2.0 to 8.0
3	54	44.6	25	33.6	0	34	6.8	4.0	7.7	1.0 to 9.8
3	55	47.6	19	23.9	0	21	7.3	4.0	6.8	2.0 to 13.5
3	56	46.5	21	27.1	0	20	7.2	5.0	6.7	2.0 to 9.8
3	57	49.0	23	28.2	1	34	8.2	3.5	8.9	2.0 to 12.3
3	64	50.6	26	30.8	0	23	6.3	3.0	6.5	2.0 to 10.0
3	65	46.8	25	32.1	0	27	6.1	3.0	7.1	2.0 to 10.0
3	66	46.7	24	30.8	0	24	6.3	4.0	6.8	2.0 to 6.5
3	67	43.4	27	37.3	0	22	6.6	4.0	7.1	1.0 to 8.0
Combined		**677.7**	**362**	**32.0**	**0**	**34**	**5.6**	**4.0**	**5.7**	**2.0 to 8.0**
4	75	72.4	44	36.5	0	16	4.9	4.0	4.4	2.0 to 5.0
4	76	69.0	46	40.0	0	16	4.3	3.0	3.9	2.0 to 5.0
4	77	79.8	47	35.3	0	17	4.9	3.0	4.6	2.0 to 5.8
4	81	42.0	13	18.6	1	29	10.6	7.0	10.3	2.5 to 19.5
4	82	42.6	15	21.1	0	44	10.2	3.0	12.5	2.0 to 16.5
4	83	46.0	21	27.4	0	30	7.5	4.0	8.1	2.0 to 12.8
4	84	45.0	22	29.3	1	33	9.0	4.0	9.6	2.0 to 17.0
4	92	44.4	17	23.0	1	28	9.8	8.5	8.2	4.8 to 11.3
4	93	43.6	18	24.8	1	43	8.5	4.0	11.1	2.0 to 6.0
4	94	48.0	18	22.5	0	34	8.4	3.0	10.2	2.0 to 16.0
4	95	49.2	22	26.8	0	43	7.4	3.0	10.5	1.0 to 6.0
Combined		**582.0**	**283**	**29.2**	**0**	**44**	**6.7**	**4.0**	**7.9**	**2.0 to 9.0**
All Subjects		**2430.7**	**1377**	**34.0**	**0**	**44**	**6.6**	**4.0**	**2.5**	**0.4 to 3.5**

Table F-2.
Summary statistics for roll excursions, slalom course, NVG.
(expressed in degrees)

Subject	Run	Time	# of Excursions	Exc/ min	Min	Max	Mean	Median	S.D.	IQR
1	108	105.7	83	47.1	0	9	3.2	3.0	2.0	2.0 to 4.0
1	109	98.2	73	44.6	0	13	4.4	4.0	3.2	2.0 to 6.0
1	110	51.3	32	37.4	0	19	6.6	6.0	5.7	2.0 to 7.5
1	111	51.7	32	37.1	1	17	5.9	5.0	3.9	2.0 to 7.5
1	112	51.1	32	37.6	0	23	7.6	5.0	6.1	3.0 to 8.5
1	121	54.0	33	36.7	0	27	5.5	3.0	6.2	2.0 to 7.3
1	123	55.2	37	40.2	0	13	3.8	3.0	3.0	2.0 to 4.3
Combined		**467.2**	**322**	**41.4**	**0**	**27**	**4.8**	**4.0**	**4.3**	**2.0 to 6.0**
2	171	80.0	51	38.3	0	11	4.8	5.0	2.8	3.0 to 7.0
2	172	80.9	48	35.6	0	13	4.1	3.0	3.3	2.0 to 5.0
2	173	103.2	78	45.3	0	12	4.2	4.0	2.7	2.0 to 6.0
2	177	70.6	45	38.2	0	20	6.1	4.0	5.7	2.0 to 7.3
2	178	63.0	45	42.9	0	22	5.2	4.0	4.9	2.0 to 7.0
2	179	54.3	29	32.0	0	23	6.5	4.5	5.8	2.8 to 9.8
Combined		**452.0**	**296**	**39.3**	**0**	**23**	**5.0**	**4.0**	**4.2**	**2.0 to 7.0**
3	51	71.8	41	34.3	0	13	5.5	5.0	3.3	3.0 to 7.3
3	52	73.9	51	41.1	0	15	5.1	4.0	4.1	2.0 to 6.0
3	53	68.2	34	30.0	0	22	5.9	5.0	5.4	2.0 to 9.0
3	58	50.5	29	34.5	0	21	6.1	4.0	6.0	2.0 to 8.3
3	59	51.9	28	32.4	0	19	5.0	3.0	4.9	1.5 to 7.0
3	60	52.6	30	34.2	0	20	6.6	4.0	5.8	2.0 to 10.3
3	68	53.6	37	41.4	1	23	4.9	3.0	5.0	2.0 to 5.0
3	69	53.8	30	33.5	0	4	1.0	1.0	1.2	0.0 to 1.0
3	70	48.8	35	43.0	0	20	6.4	5.0	5.0	3.0 to 10.0
Combined		**525.1**	**315**	**36.0**	**0**	**23**	**5.2**	**4.0**	**4.8**	**2.0 to 7.0**
4	78	95.3	47	29.6	0	16	5.6	5.0	4.3	2.0 to 7.8
4	79	81.9	50	36.6	0	19	5.2	3.0	4.8	2.0 to 6.0
4	80	83.9	60	42.9	0	17	5.0	3.0	4.3	2.0 to 7.0
4	85	52.7	30	34.2	1	34	8.6	6.0	8.7	2.0 to 11.0
4	86	56.0	32	34.3	0	25	5.6	3.0	6.4	1.5 to 7.5
4	87	49.8	25	30.1	0	26	7.6	3.5	8.3	3.0 to 9.0
4	96	44.6	19	25.6	0	41	9.1	4.0	11.0	2.0 to 16.5
4	97	47.0	19	24.3	0	43	11.7	7.0	11.4	3.3 to 18.8
4	98	46.1	16	20.8	0	41	11.1	3.0	13.0	1.5 to 21.5
Combined		**557.3**	**295**	**31.8**	**0**	**43**	**6.8**	**4.0**	**7.4**	**2.0 to 9.0**
All Subjects		**2001.6**	**1228**	**36.8**	**0**	**43**	**5.9**	**4.0**	**5.7**	**2.0 to 9.0**

Table F-3.
Summary statistics for roll excursions, slalom course, TIO.
(expressed in degrees)

Subject	Run	Time	# of Excursions	Exc/min	Min	Max	Mean	Median	S.D.	IQR
1	138	85.7	68	47.6	0	10	2.5	2	2.4	1.0 to 3.0
1	139	109.7	78	42.7	0	12	2.8	2	2.1	1.0 to 4.0
1	140	120.4	71	35.4	0	8	2.7	2	1.8	1.0 to 4.0
Combined		**315.8**	**217**	**41.2**	**0**	**12**	**2.7**	**2**	**2.1**	**1.0 to 4.0**
2	163	70.0	39	33.4	0	9	2.6	2.0	2.1	1.0 to 3.0
2	164	82.5	47	34.2	0	11	3.2	3.0	2.5	2.0 to 4.8
2	166	80.1	40	30.0	0	12	3.0	2.0	2.4	1.0 to 4.0
2	167	88.1	50	34.1	0	1	3.4	3.0	2.5	2.0 to 5.0
Combined		**320.7**	**176**	**32.9**	**0**	**12**	**3.1**	**3.0**	**2.4**	**1.0 to 4.0**
3	144	70.9	41	34.7	0	16	4.4	4.0	3.3	2.0 to 6.0
3	145	89.3	53	35.6	0	14	3.6	3.0	2.5	2.0 to 5.0
3	146	97.9	64	39.2	0	13	3.5	3.0	2.9	1.0 to 5.0
3	155	71.9	49	40.9	0	12	3.4	2.5	2.9	1.0 to 5.0
3	157	84.4	48	34.1	0	10	2.7	2.0	2.9	1.0 to 3.0
Combined		**414.4**	**255**	**36.9**	**0**	**16**	**3.5**	**3.0**	**2.9**	**1.0 to 5.0**
4		None								
All Subjects		**1050.9**	**648**	**37.0**	**0**	**16**	**3.1**	**2.3**	**0.4**	**1.0 to 5.0**

Table F-4.
Summary statistics for Roll excursions, slalom course, RWS.
(expressed in degrees)

Subject	Run	Time	# of Excursions	Exc/min	Min	Max	Mean	Median	S.D.	IQR
1	141	106.2	78	44.1	0	5	2.2	2.0	1.4	1.0 to 3.0
1	142	102.0	74	43.5	0	8	2.2	2.0	1.8	1.0 to 3.0
1	143	120.0	86	43.0	0	9	2.7	2.0	1.9	1.0 to 4.0
Combined		**328.2**	**238**	**43.5**	**0**	**9**	**2.4**	**2.0**	**1.7**	**1.0 to 3.0**
2	168	83.2	44	31.7	0	6	2.0	2.0	1.5	1.0 to 3.0
2	169	89.1	47	31.6	0	8	2.4	2.0	1.6	1.0 to 3.0
2	170	101.1	73	43.3	0	7	2.1	2.0	1.6	1.0 to 3.0
2	174	63.6	38	35.8	0	9	3.0	2.0	2.1	1.0 to 4.3
2	175	65.0	41	37.8	0	10	3.0	2.0	2.1	1.8 to 4.3
2	176	63.8	31	29.2	0	13	7.8	3.0	2.8	2.0 to 4.8
Combined		**465.8**	**274**	**35.3**	**0**	**13**	**2.6**	**2.0**	**2.0**	**1.0 to 3.0**
3	158	71.2	26	21.9	0	19	4.7	3.0	4.6	1.0 to 8.0
3	159	94.8	62	39.2	0	9	2.4	2.0	2.1	1.0 to 3.0
3	161	61.2	32	31.4	0	14	3.7	2.0	4.0	1.0 to 3.0
3	162	55.3	27	29.3	0	24	5.1	2.0	6.7	1.0 to 5.0
3	180	59.6	32	32.2	0	16	5.1	4.0	3.6	2.0 to 8.0
3	181	58.9	32	32.6	0	13	4.7	4.0	6.8	2.0 to 6.0
3	182	52.9	24	27.2	1	12	3.7	2.0	3.4	1.0 to 5.0
3	183	43.9	29	39.6	0	16	5.4	3.0	4.9	2.0 to 10.0
Combined		**497.8**	**264**	**31.8**	**0**	**24**	**4.4**	**3.0**	**4.3**	**1.0 to 6.0**
4	None									
All Subjects		**1291.8**	**776**	**36.0**	**0**	**24**	**3.4**	**2.0**	**1.5**	**1.0 to 5.0**

Appendix G.

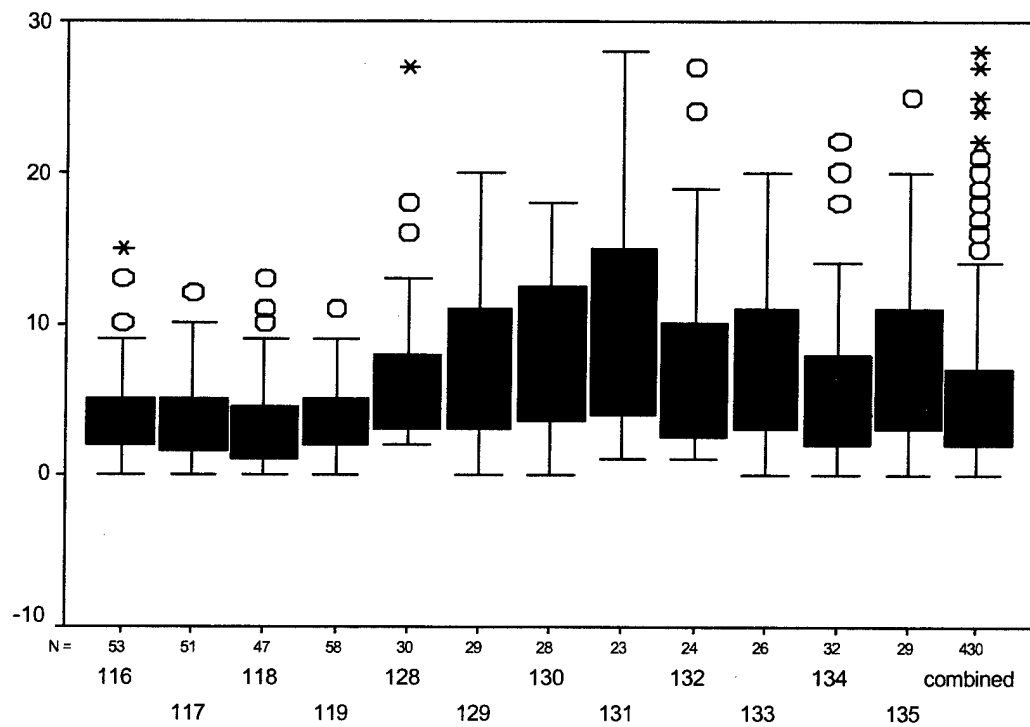## Roll excursion box plots.

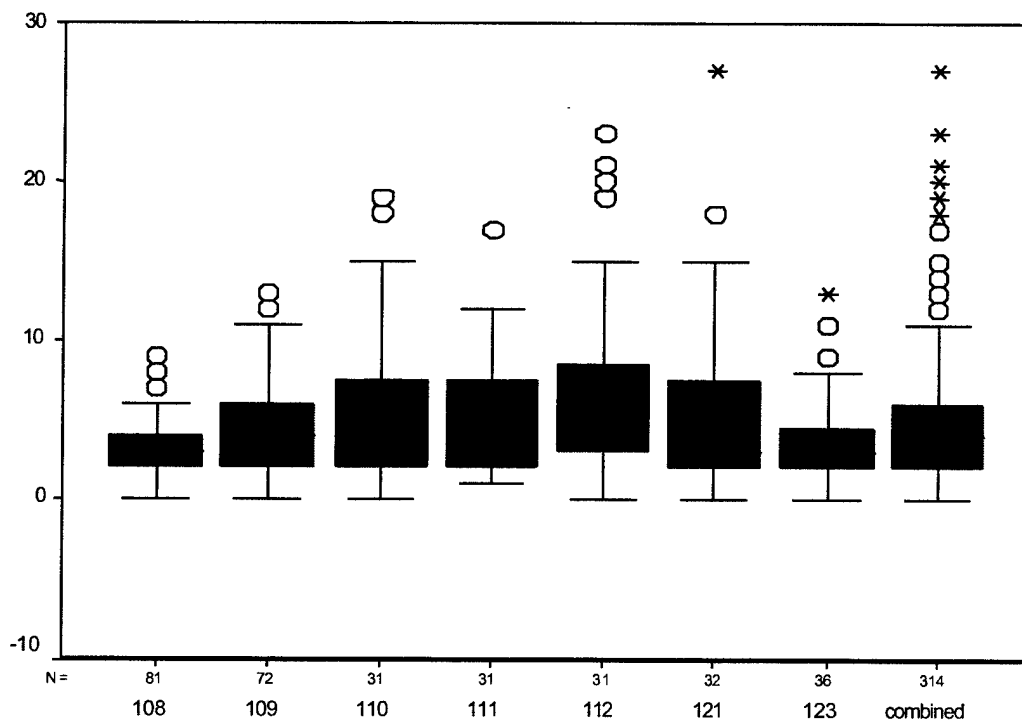Figure G-1. Subject #1 GVE excursion box plots.

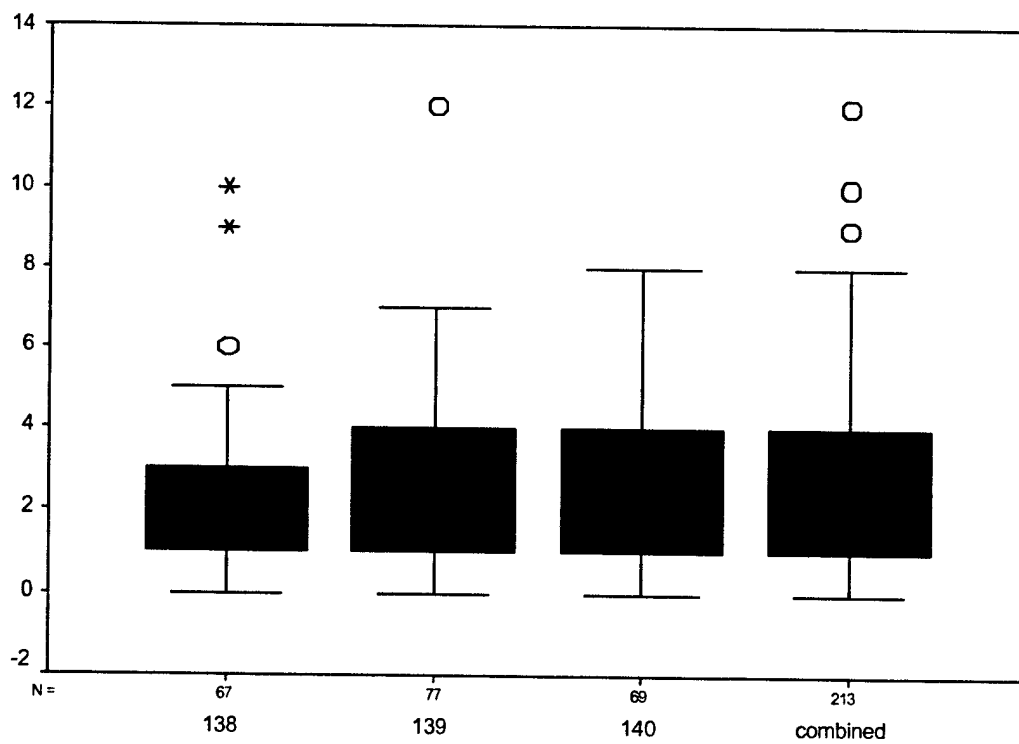Figure G-2. Subject #1 NVG excursion box plots.

Figure G-3. Subject #1 TIO excursion box plots.
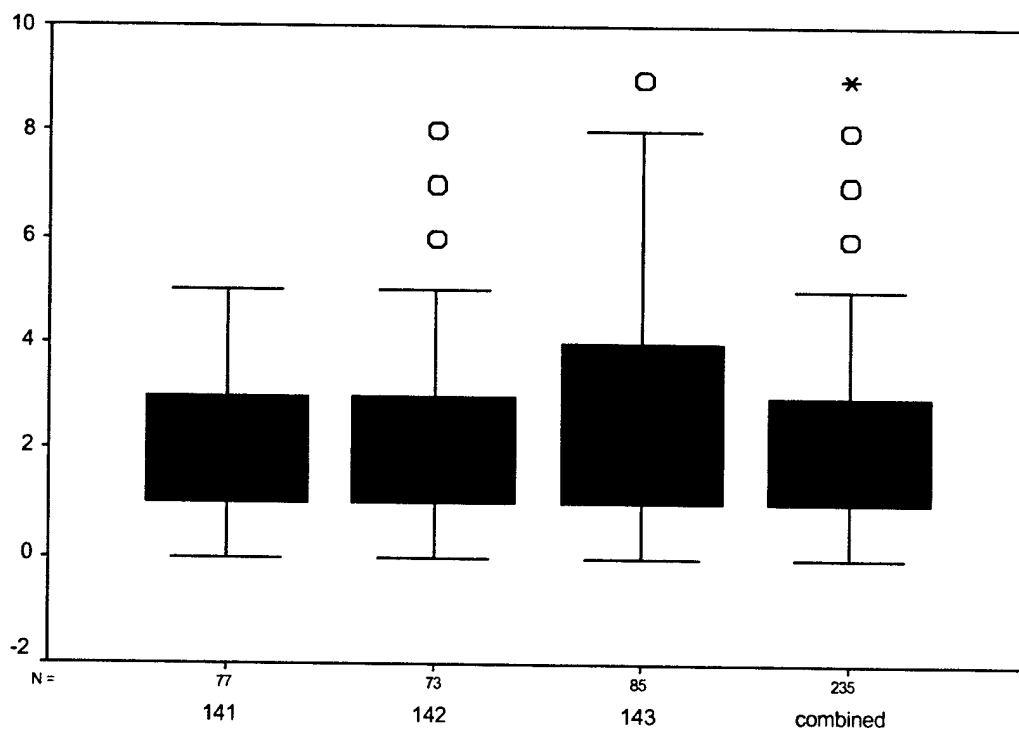

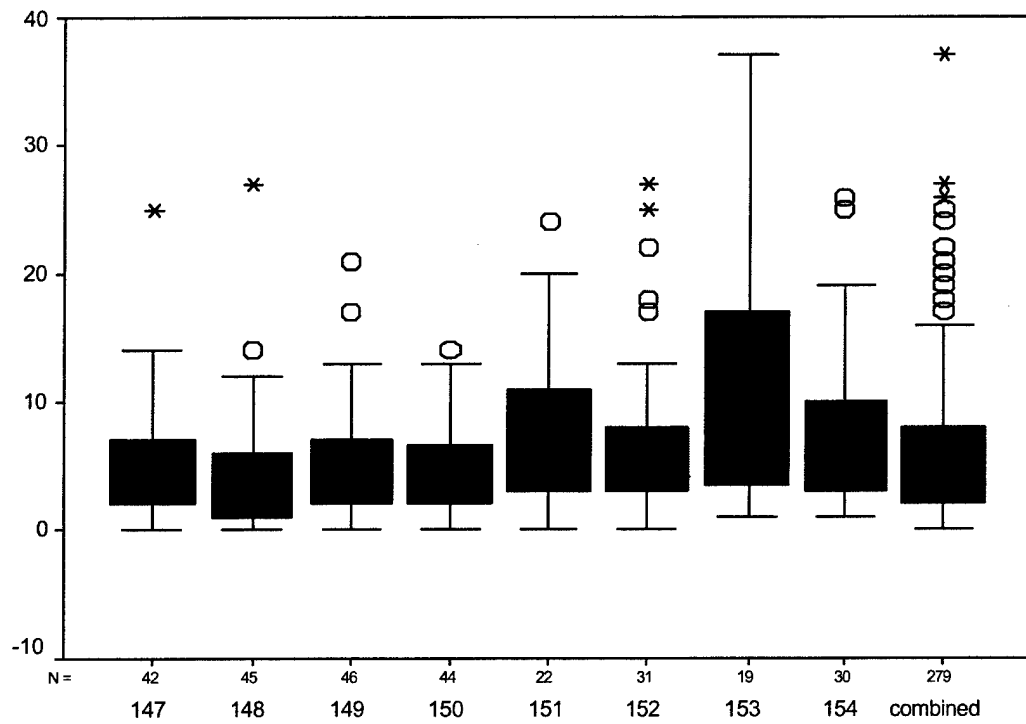Figure G-4. Subject #1 RWS excursion box plots.

Figure G-5. Subject #2 GVE excursion box plots.
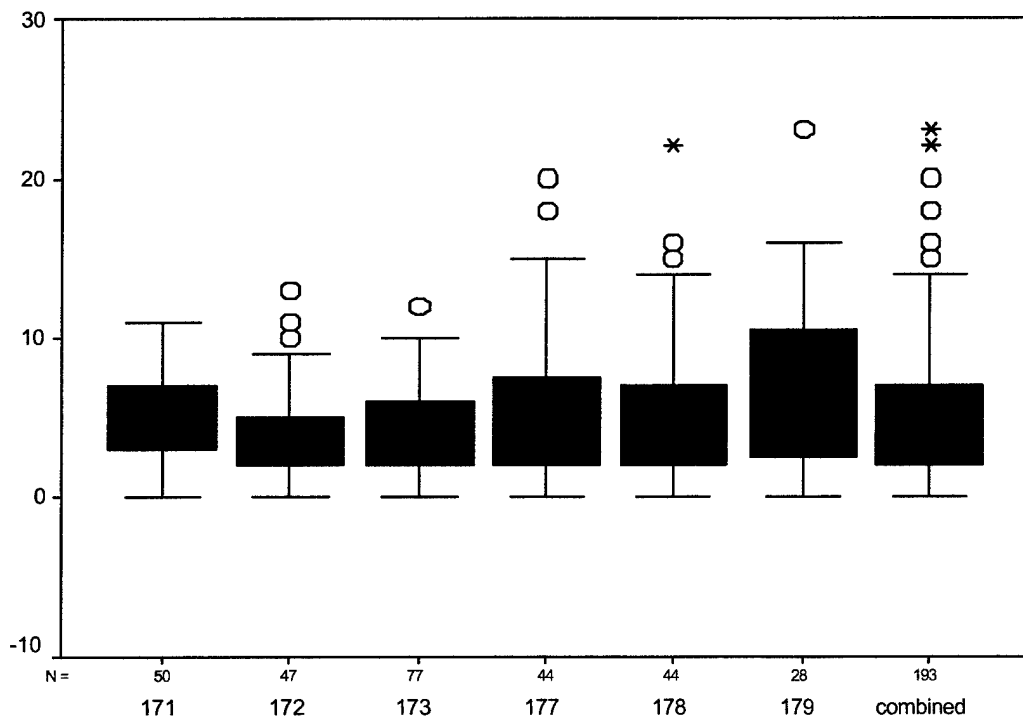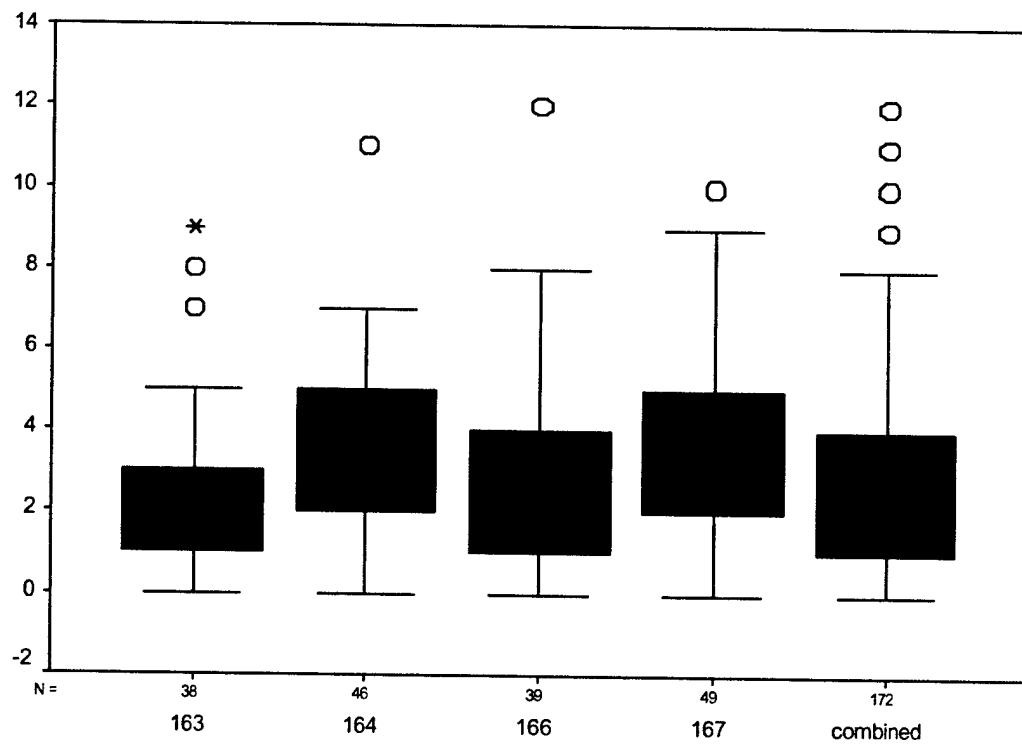

Figure G-6. Subject #2 NVG excursion box plots.

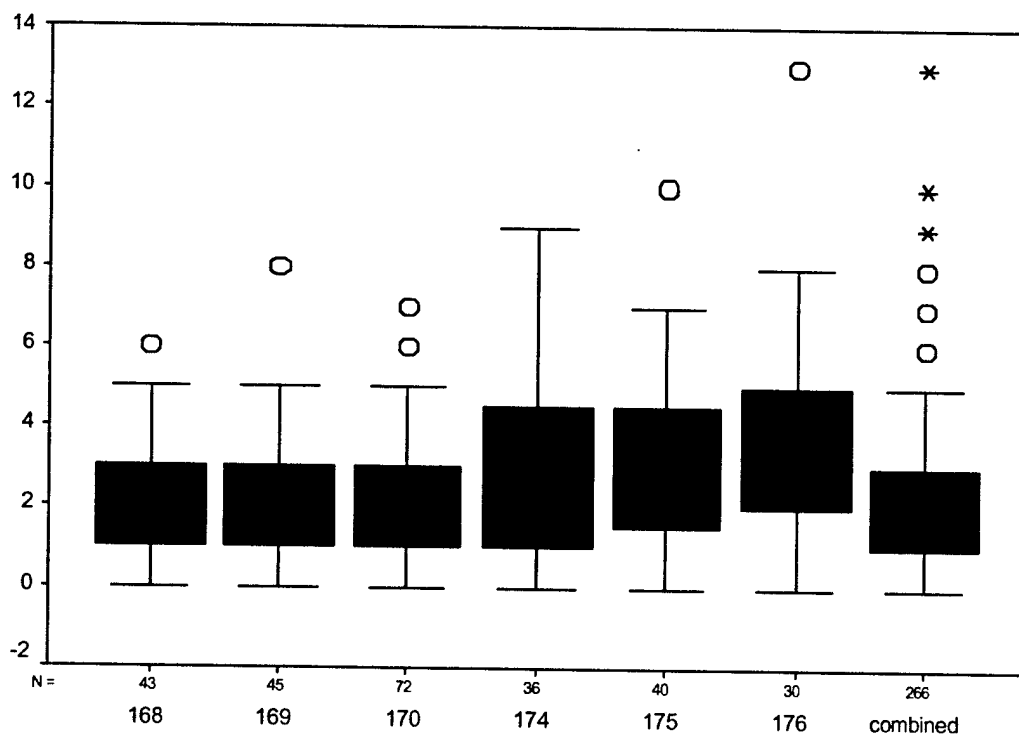Figure G-7. Subject #2 TIO excursion box plots.

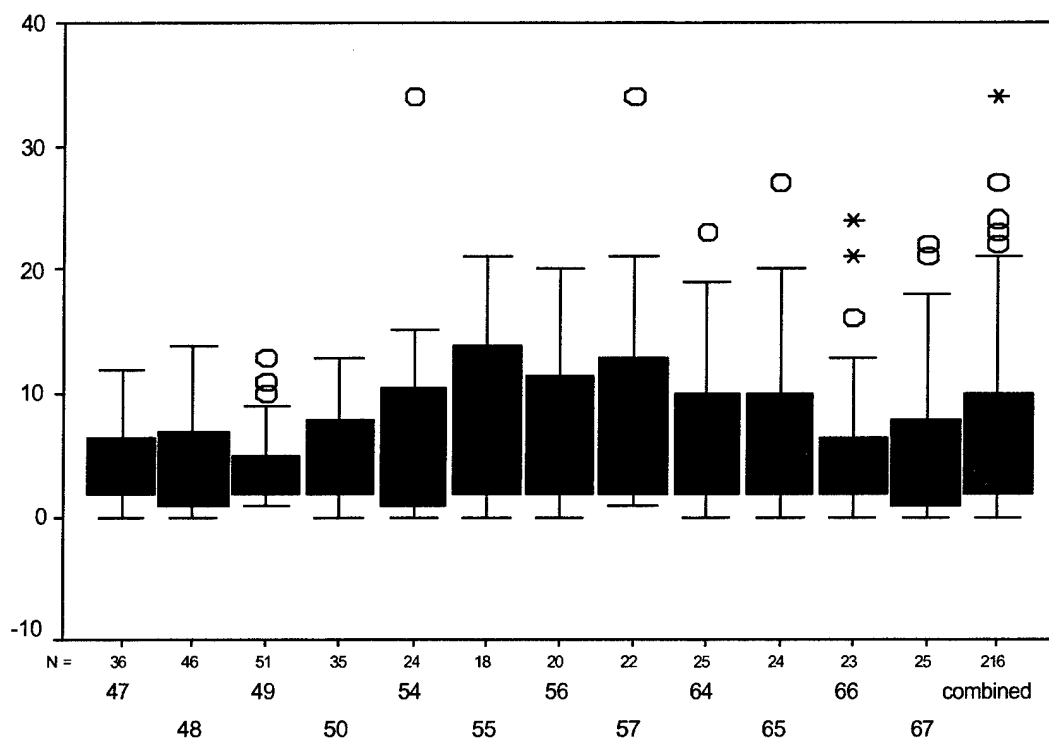Figure G-8. Subject #2 RWS excursion box plots.

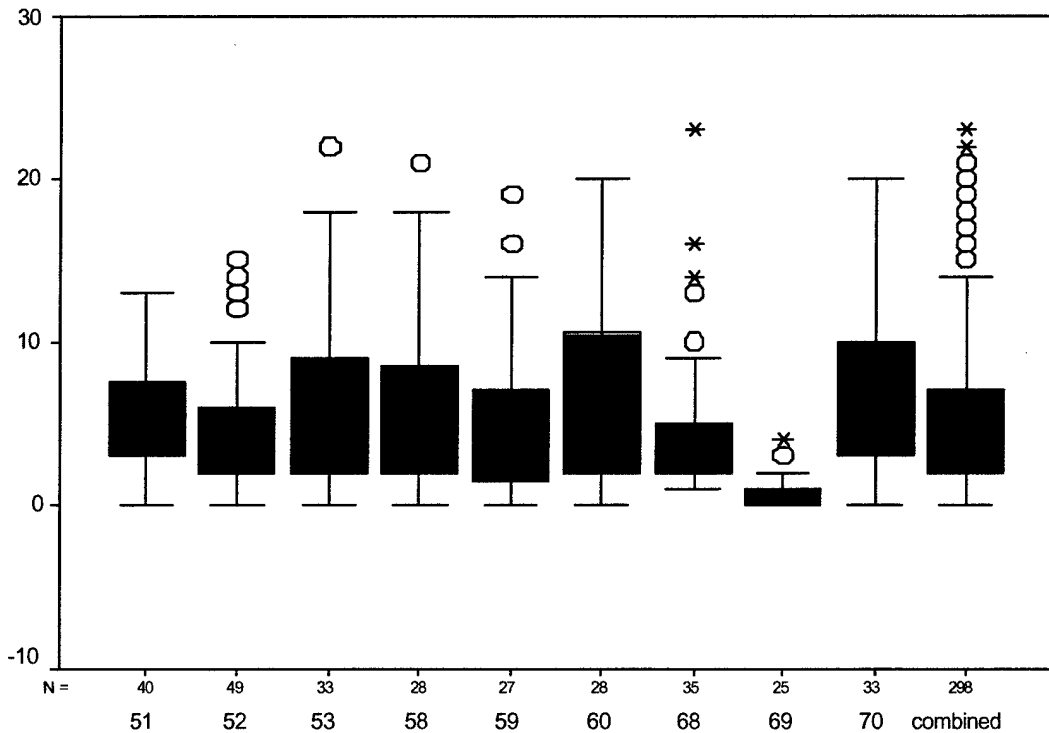Figure G-9. Subject #3 GVE excursion box plots.

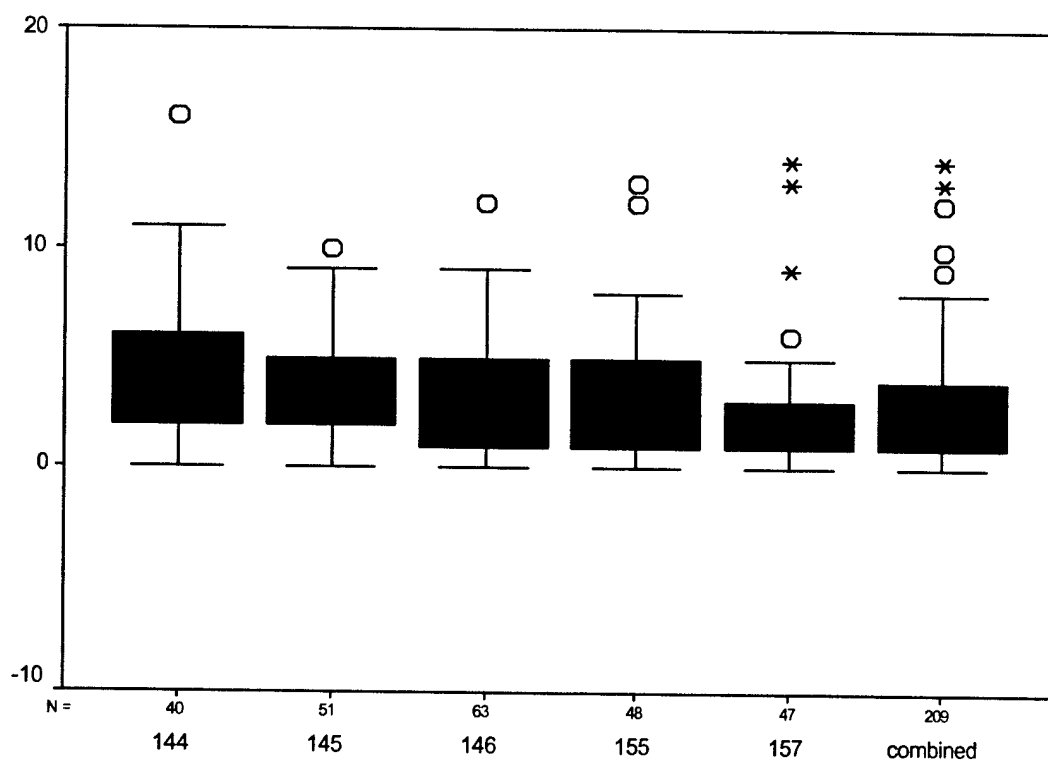Figure G-10. Subject #3 NVG excursion box plots.

Figure G-11. Subject #3 TIO excursion box plots.
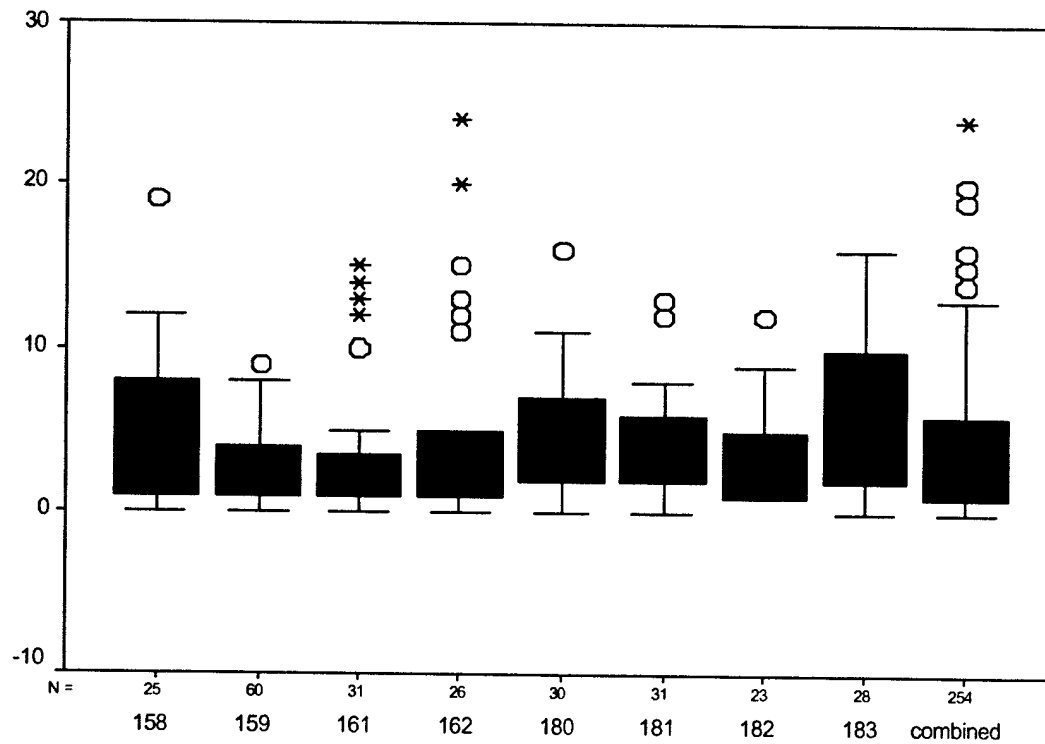

Figure G-12. Subject #3 RWS excursion box plots.
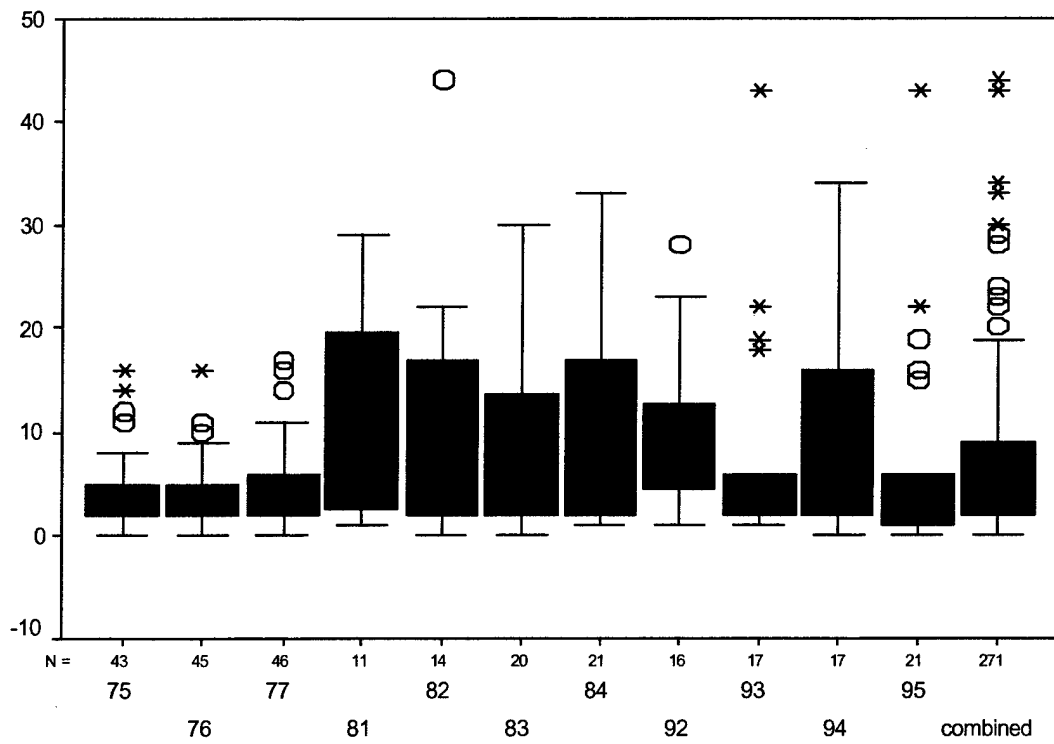
Figure G-13. Subject #4 GVE excursion box plots.
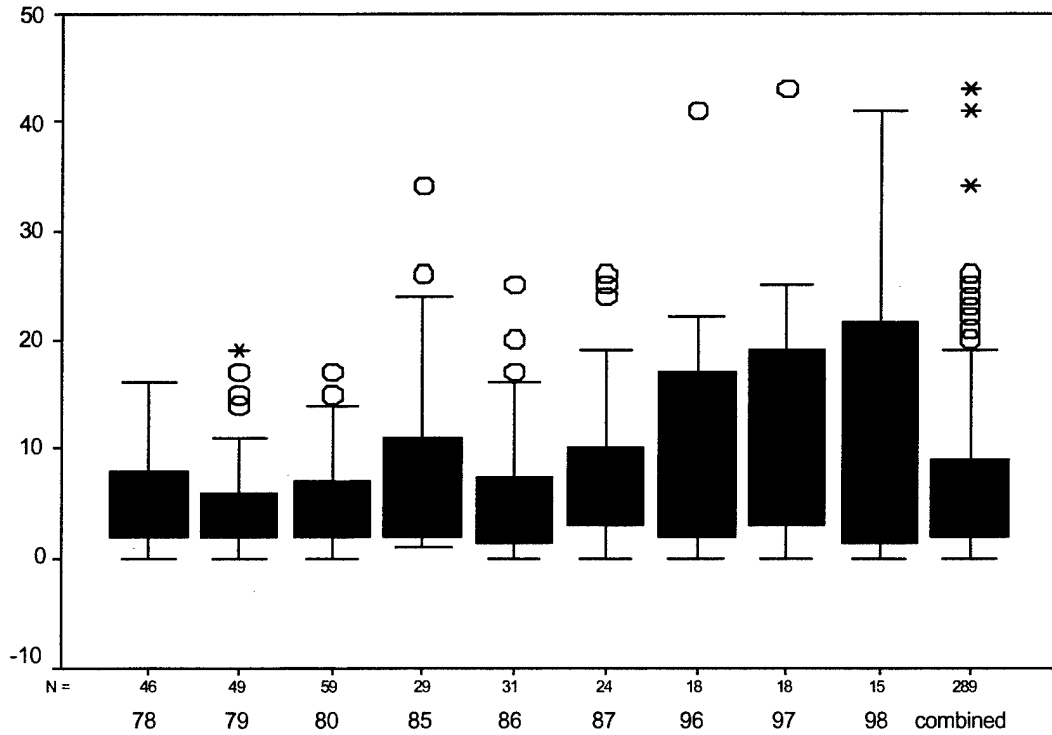
Figure G-14. Subject #4 NVG excursion box plots.

Appendix H

Roll velocity distributions.

Figure H-1. Subject #1 GVE head velocity distributions with cumulative frequency curves.

Figure H-2. Subject #1 NVG head velocity distributions with cumulative frequency curves.
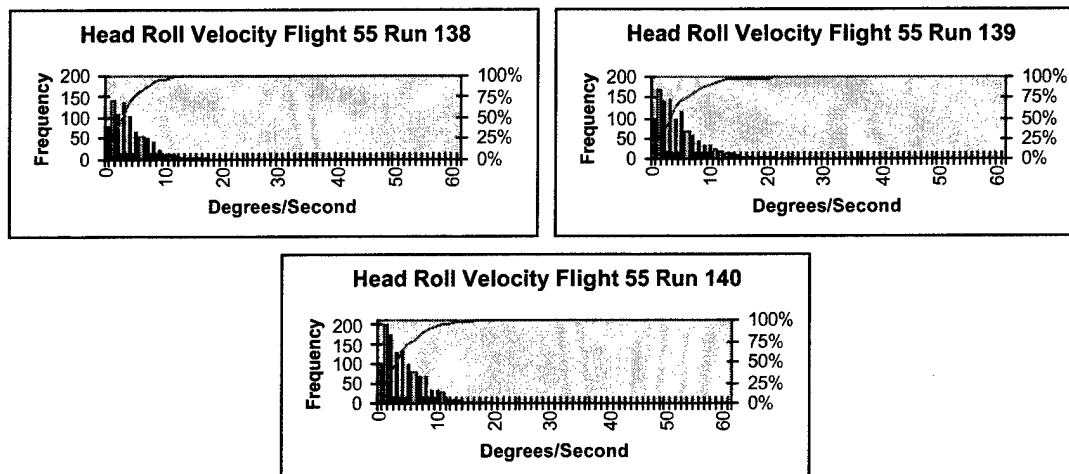
Figure H-3. Subject #1 TIO head velocity distributions with cumulative frequency curves.
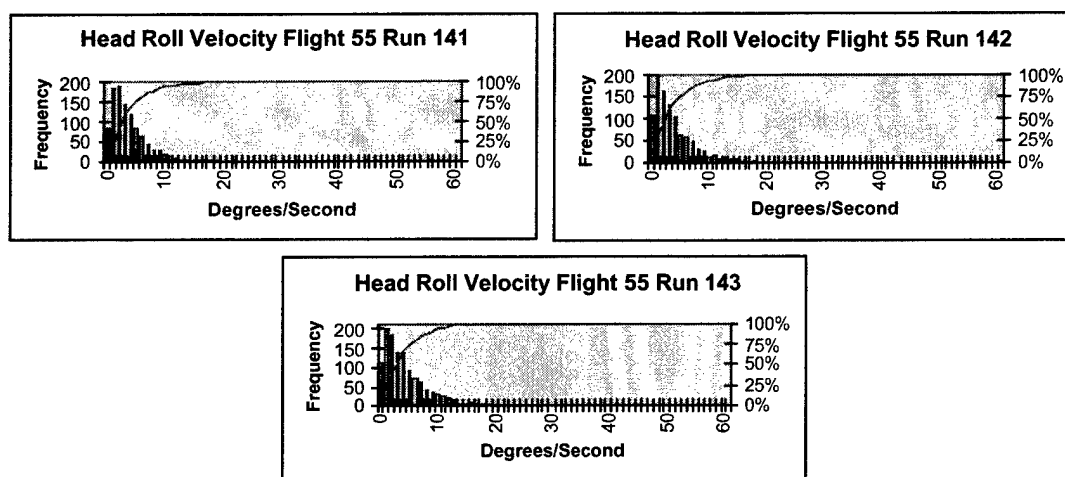
Figure H-4. Subject #1 RWS head velocity distributions with cumulative frequency curves.

Figure H-5. Subject #2 GVE head velocity distributions with cumulative frequency curves.

Head Roll Velocity Flight 68 Run 171

Head Roll Velocity Flight 68 Run 172

Head Roll Velocity Flight 68 Run 173

Head Roll Velocity Flight 71 Run 177

Head Roll Velocity Flight 71 Run 178

Head Roll Velocity Flight 71 Run 179

Figure H-6. Subject #2 NVG head velocity distributions with cumulative frequency curves.

Head Roll Velocity Flight 65 Run 163

Head Roll Velocity Flight 65 Run 164

Head Roll Velocity Flight 65 Run 166

Head Roll Velocity Flight 65 Run 167

Figure H-7. Subject #2 TIO head velocity distributions with cumulative frequency curves.

113
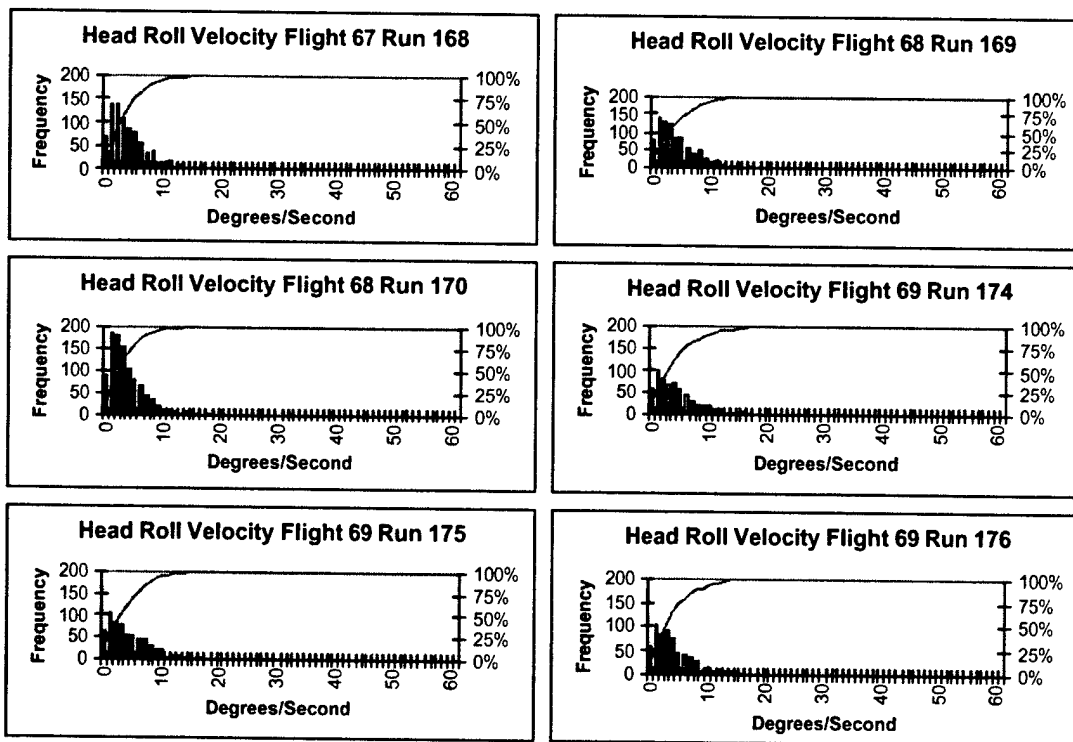
Figure H-8. Subject #2 RWS head velocity distributions with cumulative frequency curves.
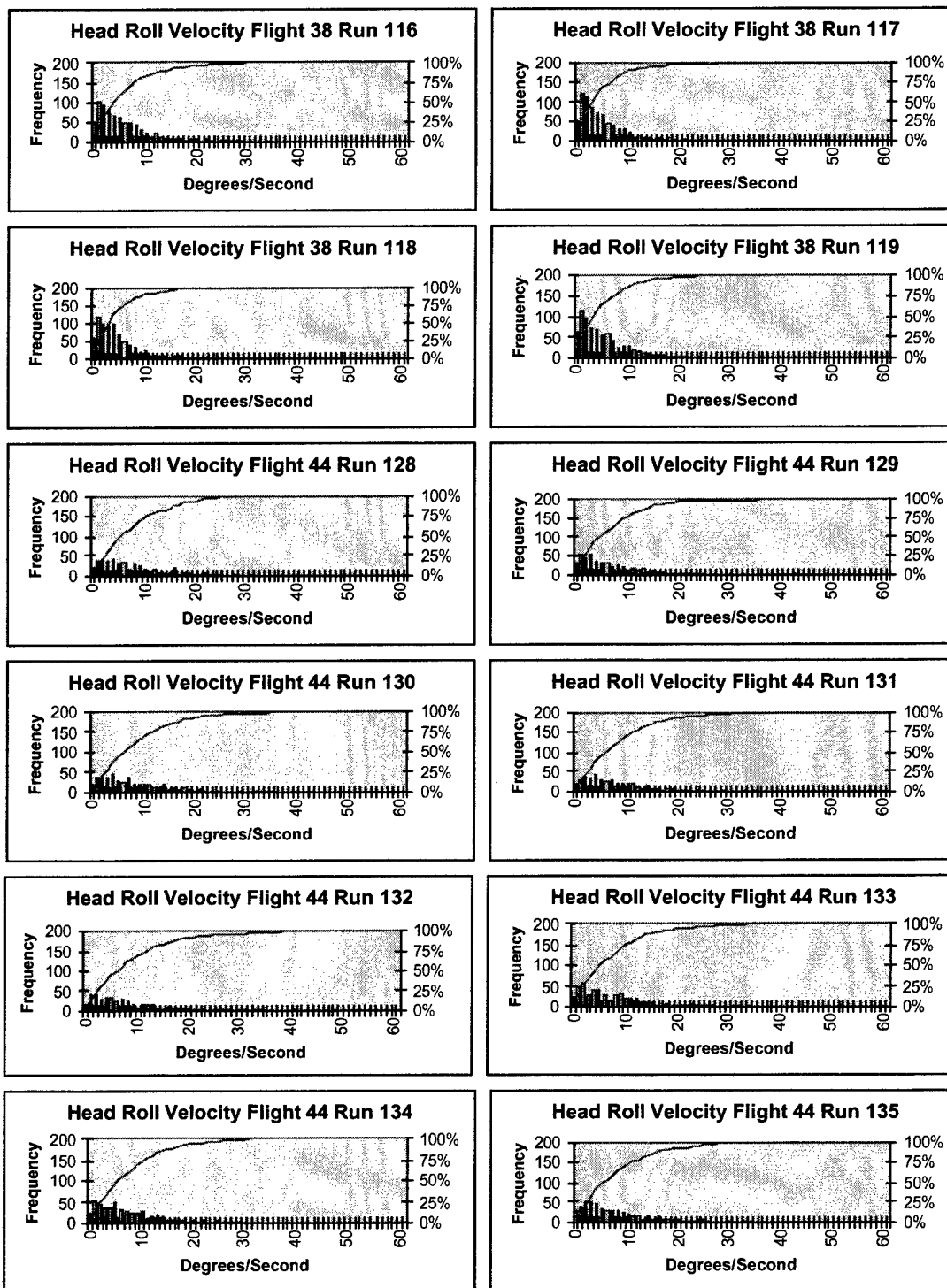
Figure H-9. Subject #3 GVE head velocity distributions with cumulative frequency curves.
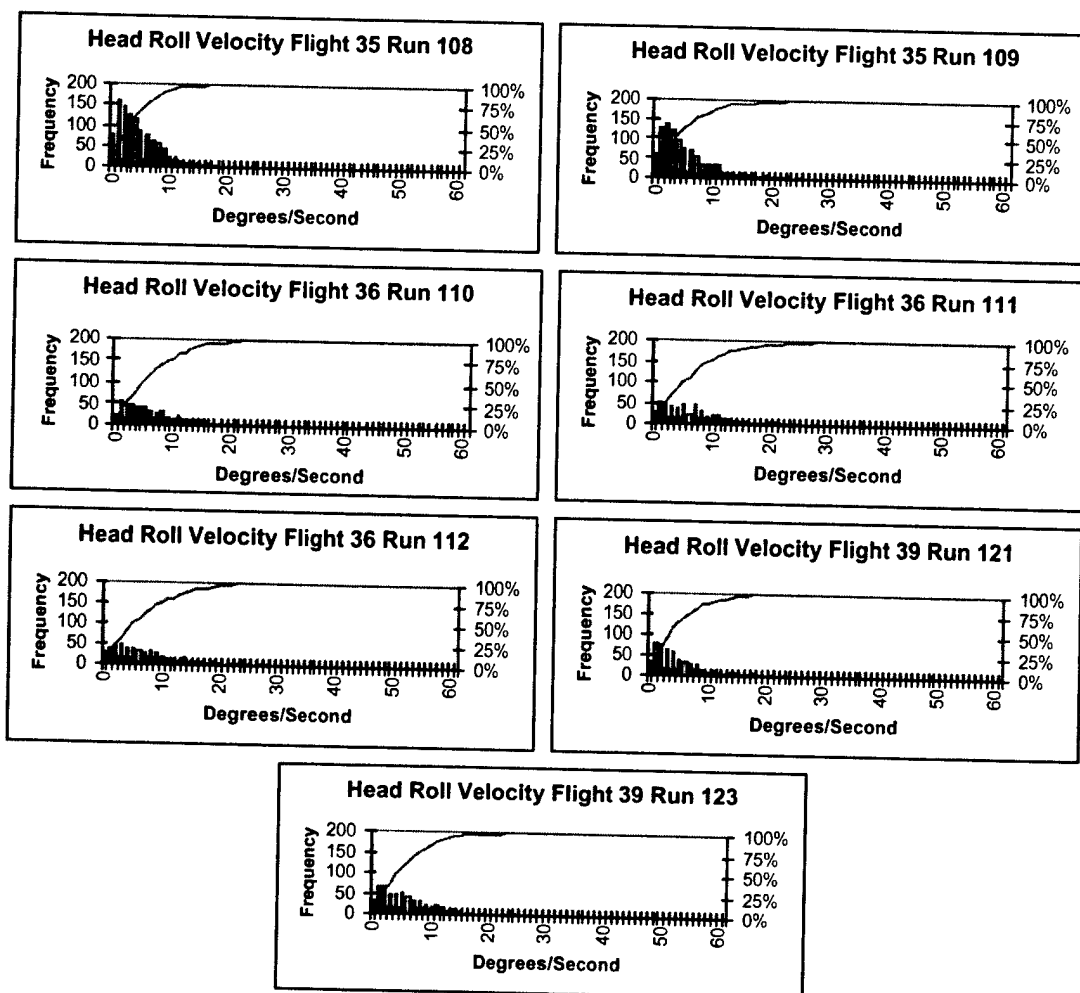
Figure H-10. Subject #3 NVG head velocity distributions with cumulative frequency curves.

Figure H-11. Subject #3 TIO head velocity distributions with cumulative frequency curves.

Figure H-12. Subject #3 RWS head velocity distributions with cumulative frequency curves.

Figure H-13. Subject #4 GVE head velocity distributions with cumulative frequency curves.

Figure H-14. Subject #4 NVG head velocity distributions with cumulative frequency curves.
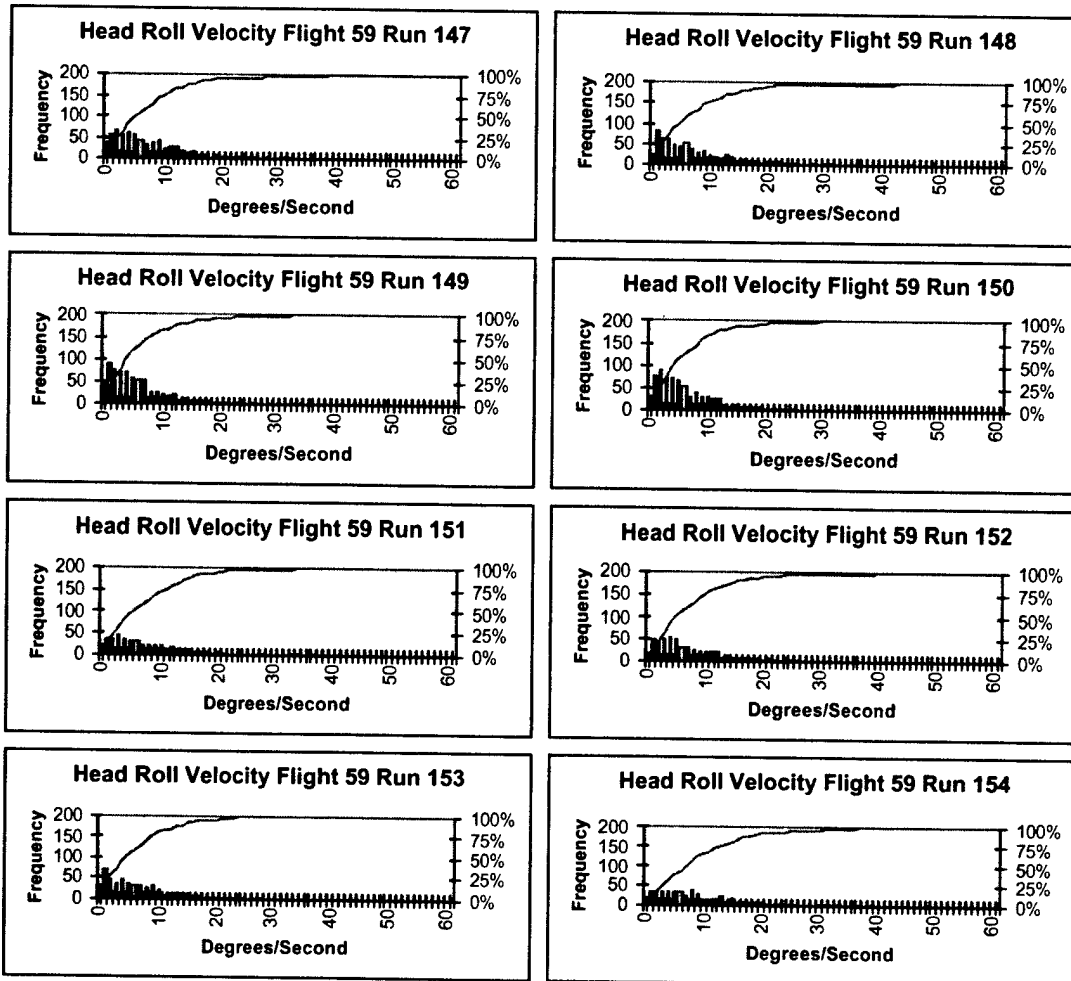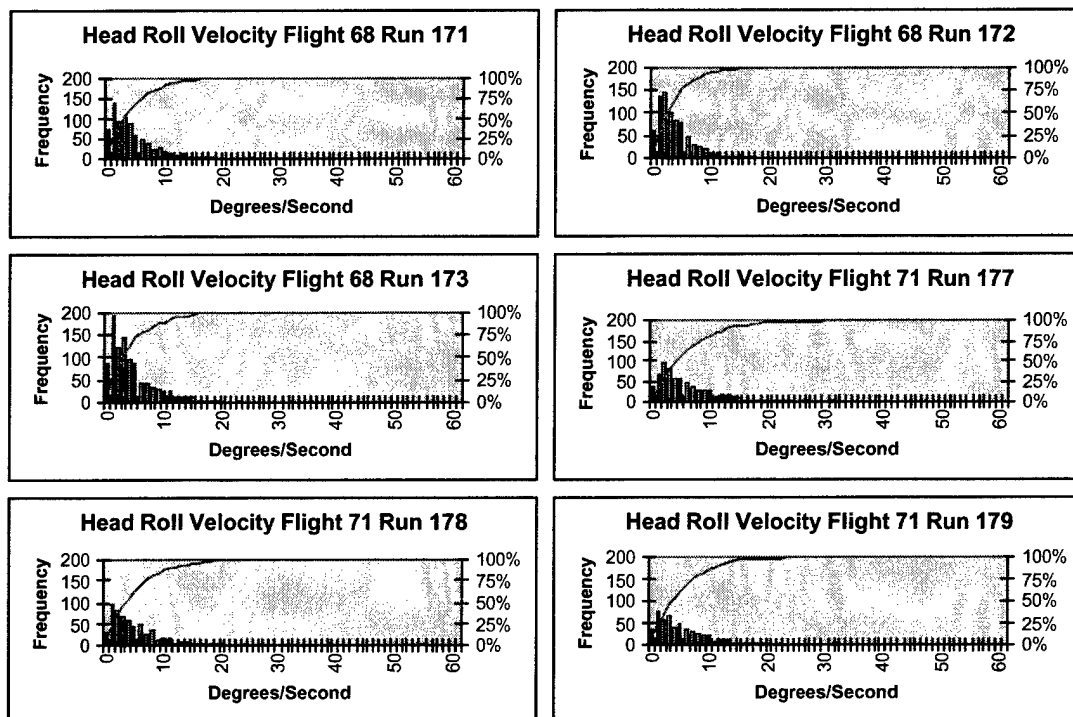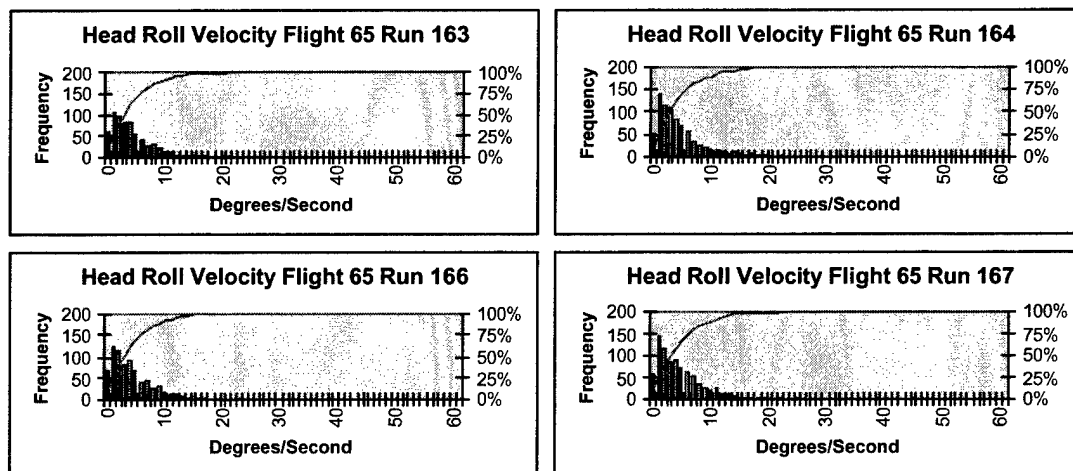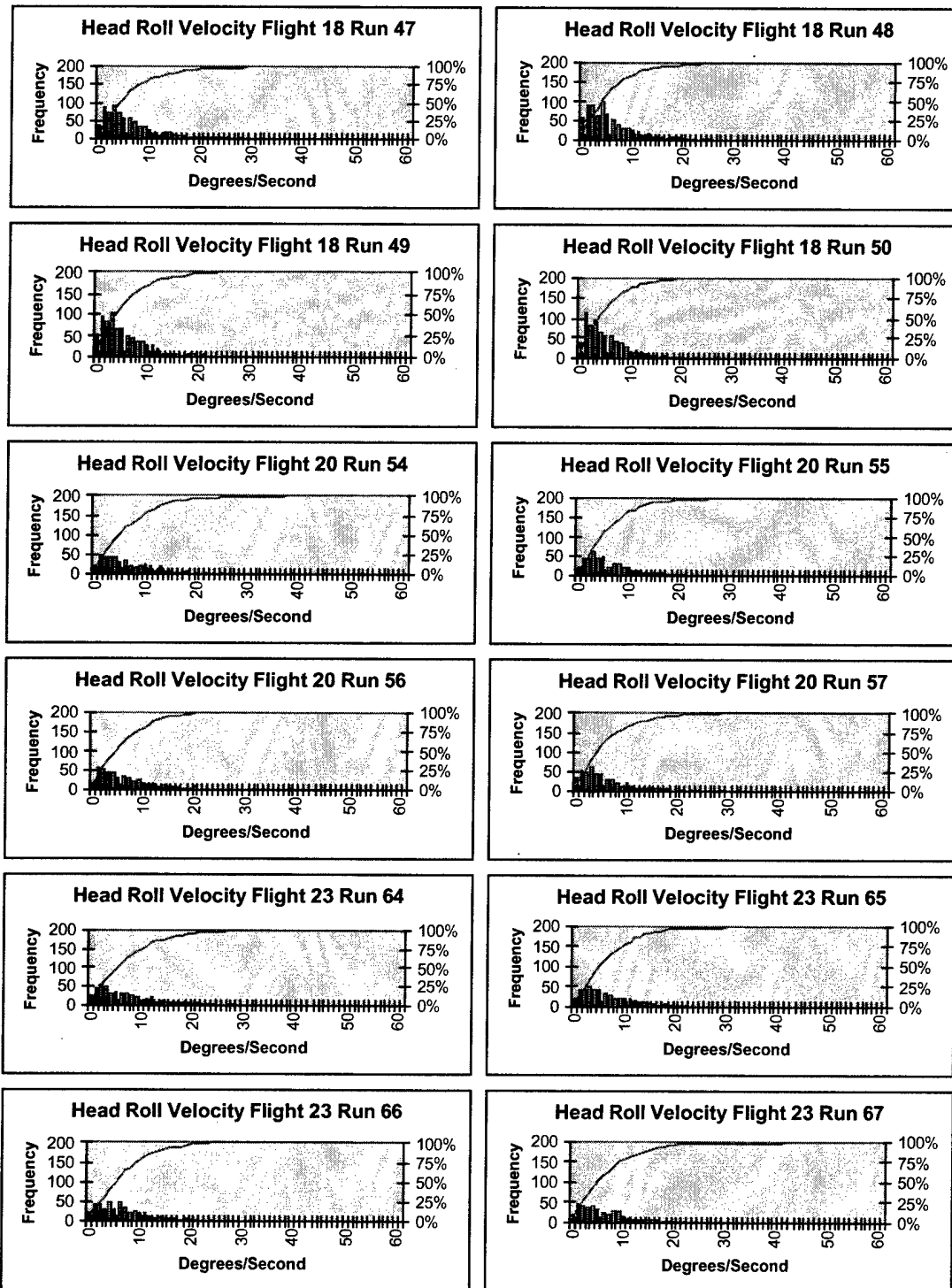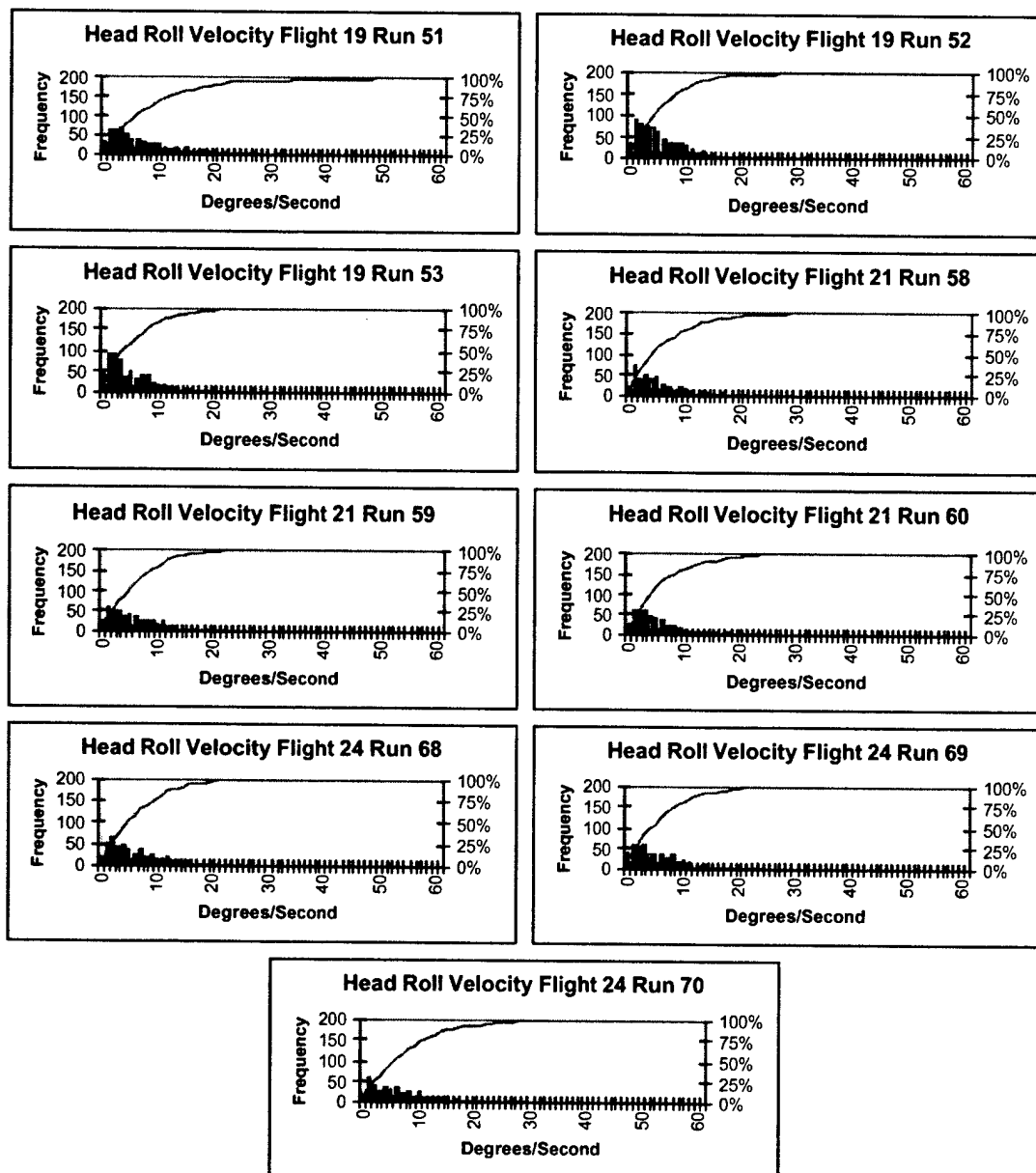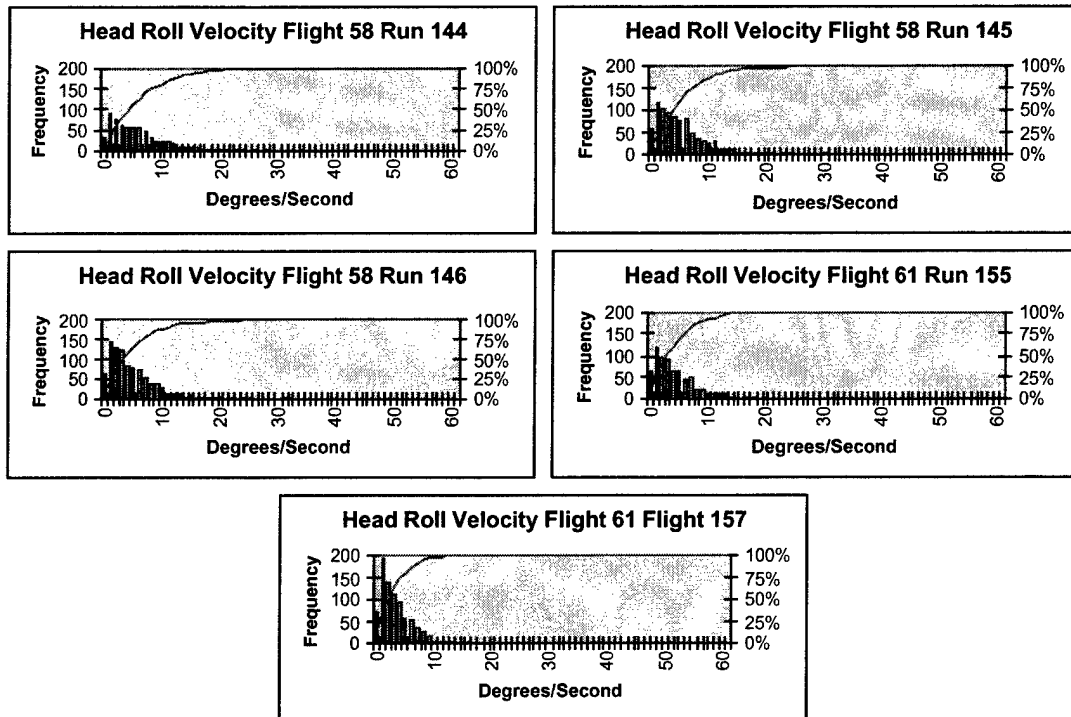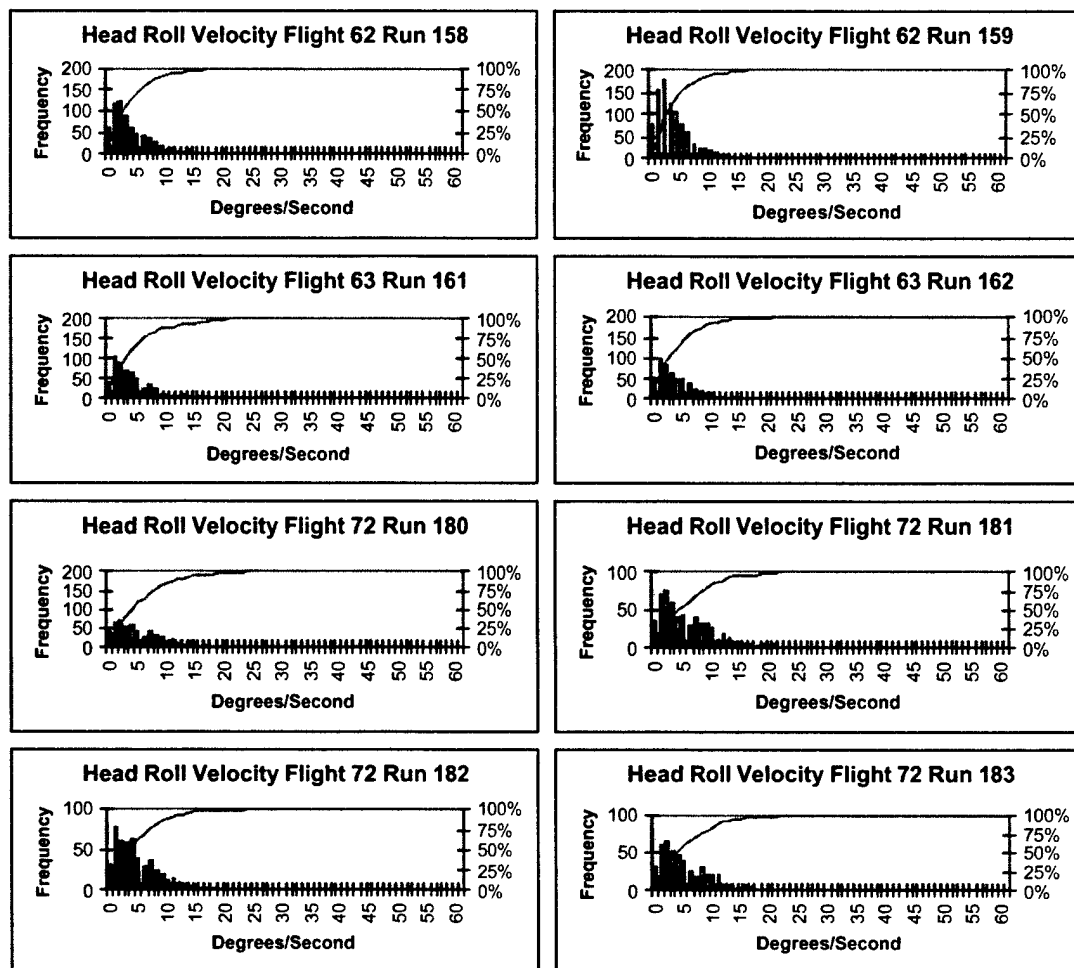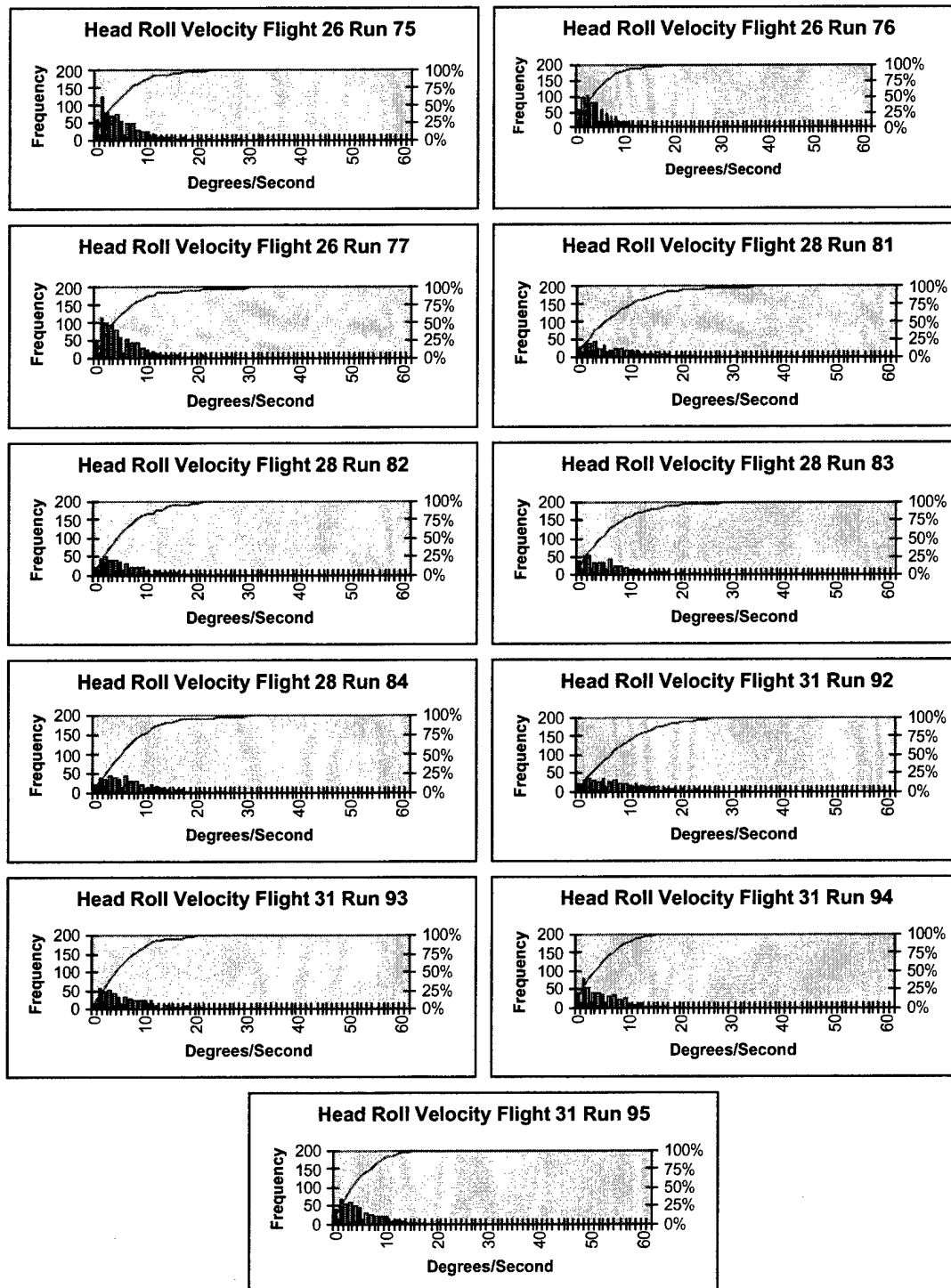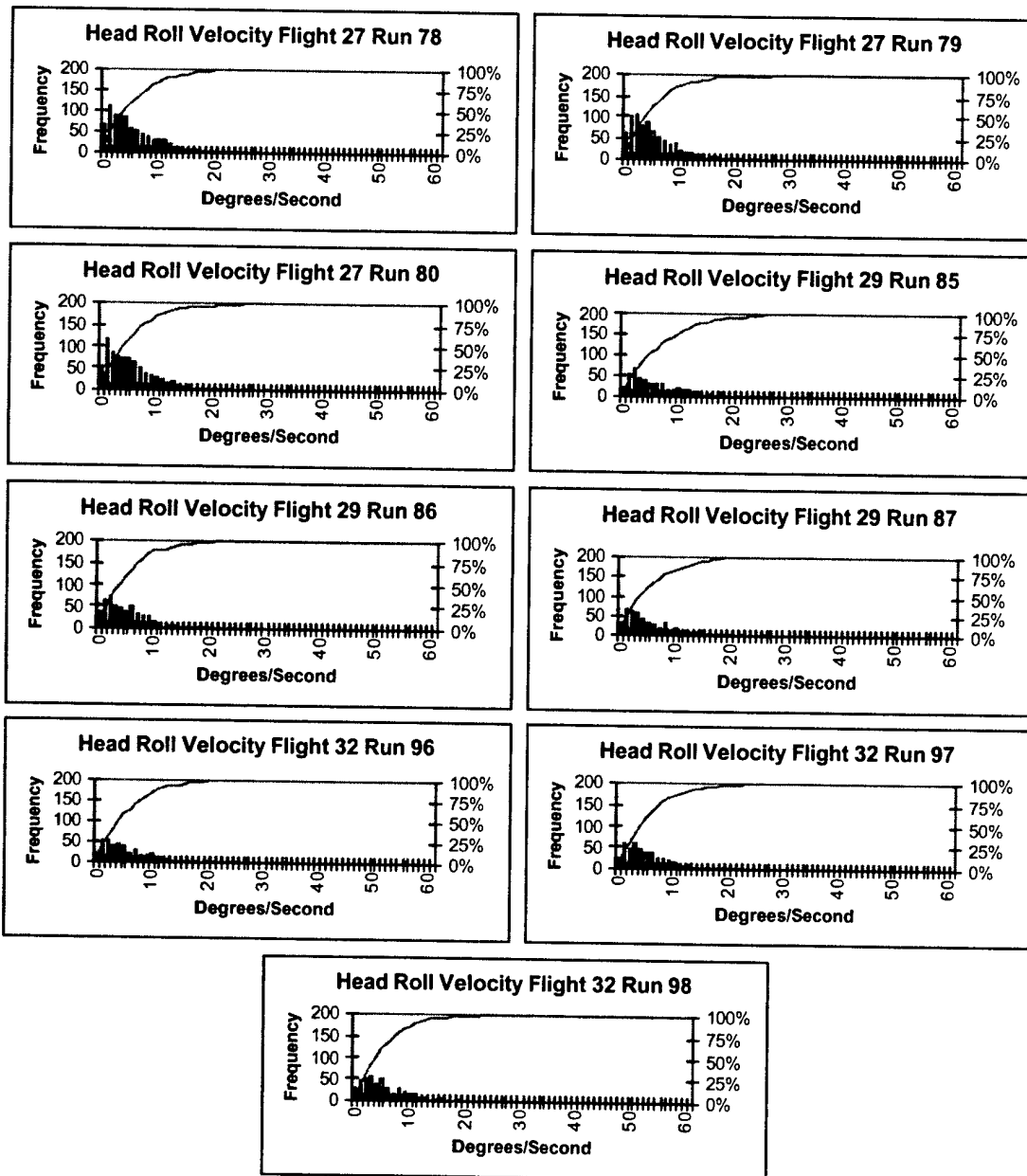
Appendix I.

Roll velocity summary tables for combined distributions.

Table I-1.
Summary statistics for roll velocity, slalom course, GVE.
(velocity values expressed in degrees/sec, time in seconds)

Subject	Run	Time	Min	Max	Mean	Median	S.D.	Skewness	Kurtosis
1	116	76.9	0	59	6.2	4	6.4	2.6	12.2
1	117	75.7	0	59	5.1	4	5.6	3.6	21.7
1	118	76.9	0	41	4.8	4	4.9	2.8	12.3
1	119	76.0	0	33	5.3	4	4.9	1.6	3.7
1	128	45.2	0	48	8.0	6	6.8	1.5	3.1
1	129	48.1	0	46	6.9	5	6.5	2.1	6.9
1	130	48.6	0	55	8.5	7	7.7	1.8	4.9
1	131	43.8	0	55	8.4	6	7.8	1.9	5.3
1	132	45.6	0	42	8.7	6	8.0	1.6	2.7
1	133	49.8	0	44	7.6	6	7.0	1.7	3.4
1	134	51.1	0	39	7.7	6	6.7	1.4	2.1
1	135	52.9	0	62	8.2	6	7.8	2.1	7.6
Combined		**690.6**	**0**	**62**	**6.8**	**5**	**6.7**	**2.1**	**7.1**
2	147	68.4	0	53	7.7	6	7.1	2.1	6.6
2	148	65.1	0	73	7.6	6	7.8	2.8	13.4
2	149	71.7	0	41	6.3	5	6.1	2.0	5.7
2	150	73.9	0	50	6.4	5	5.8	2.2	8.8
2	151	47.0	0	50	8.0	6	7.1	1.7	4.5
2	152	52.2	0	86	7.8	5	8.2	4.0	27.5
2	153	51.7	0	119	7.2	5	8.6	5.9	62.0
2	154	50.4	0	43	9.3	8	7.7	1.4	2.3
Combined		**480.4**	**0**	**119**	**7.4**	**5**	**7.3**	**3.1**	**22.4**
3	47	74.8	0	53	6.5	5	6.3	2.3	8.3
3	48	75.7	0	35	5.7	4	5.2	1.7	3.6
3	49	78.8	0	34	5.7	4	5.0	1.6	3.2
3	50	73.2	0	52	5.5	4	5.5	3.1	17.8
3	54	44.6	0	52	7.1	5	6.9	2.6	11.7
3	55	47.6	0	45	6.3	5	5.2	2.0	7.9
3	56	46.5	0	24	6.1	5	4.8	1.0	0.3
3	57	49.0	0	35	6.1	4.5	5.6	1.6	3.3
3	64	50.6	0	36	7.3	6	6.2	1.3	1.6
3	65	46.8	0	41	6.9	5	5.8	1.7	4.3
3	66	46.7	0	38	6.9	6	5.5	1.3	2.7
3	67	43.4	0	46	7.2	5	6.8	2.1	7.0
Combined		**677.7**	**0**	**53**	**6.3**	**5**	**5.8**	**2.0**	**7.3**
4	75	72.4	0	28	5.0	4	4.7	1.7	3.9
4	76	69.0	0	24	4.5	4	3.9	1.5	2.8
4	77	79.8	0	42	5.5	4	5.6	2.5	9.4
4	81	42.0	0	47	7.4	5	6.9	1.8	4.8
4	82	42.6	0	39	6.4	5	5.7	1.8	4.7
4	83	46.0	0	36	6.4	5	6.1	1.6	3.0
4	84	45.0	0	45	7.0	6	6.2	2.1	7.7
4	92	44.4	0	106	8.7	7	8.8	4.2	36.1
4	93	43.6	0	22	5.8	5	4.5	1.2	1.2
4	94	48.0	0	21	4.9	4	4.1	1.1	1.1
4	95	49.2	0	21	4.8	4	4.0	1.1	1.1
Combined		**582.0**	**0**	**106**	**5.9**	**4**	**5.7**	**2.9**	**23.5**
All Subjects		**2430.7**	**0**	**119**	**6.7**	**5**	**1.3**	**2.1**	**13.6**

122

Table I-2.
Summary statistics for roll velocity, slalom course, NVG.
(velocity values expressed in degrees/sec, time in seconds)

Subject	Run	Time	Min	Max	Mean	Median	S.D.	Skewness	Kurtosis
1	108	105.7	0	22	4.5	4	3.7	1.2	1.8
1	109	98.2	0	39	5.3	4	4.8	1.8	5.1
1	110	51.3	0	43	7.0	5	6.1	1.9	6.1
1	111	51.7	0	34	7.0	5	6.0	1.4	2.3
1	112	51.1	0	30	7.3	6	6.0	1.1	1.0
1	121	54.0	0	27	5.2	4	4.7	1.6	2.6
1	123	55.2	0	28	5.8	5	4.6	1.2	2.2
Combined		**467.2**	**0**	**43**	**5.8**	**4**	**5.1**	**2.2**	**4.3**
2	171	80.0	0	25	4.5	3	4.2	1.6	3.0
2	172	80.9	0	24	4.0	3	3.6	1.7	3.8
2	173	103.2	0	33	4.6	3	4.5	2.0	6.0
2	177	70.6	0	46	6.4	5	6.1	2.1	6.6
2	178	63.0	0	63	5.7	4	6.5	4.1	27.2
2	179	54.3	0	41	5.5	4	5.0	2.1	8.2
Combined		**452.0**	**0**	**63**	**5.0**	**4**	**5.0**	**2.8**	**16.4**
3	51	71.8	0	63	8.9	6	9.1	2.2	7.1
3	52	73.9	0	31	6.2	5	5.5	1.6	3.1
3	53	68.2	0	34	5.8	4	5.6	1.7	3.7
3	58	50.5	0	40	6.4	5	6.0	1.7	4.3
3	59	51.9	0	27	6.3	5	5.1	1.1	1.0
3	60	52.6	0	34	6.2	4	5.8	1.6	2.7
3	68	53.6	0	48	6.9	5	5.9	1.7	5.4
3	69	53.8	0	38	6.2	5	5.6	1.5	3.2
3	70	48.8	0	37	7.9	6	6.9	1.4	2.1
Combined		**525.1**	**0**	**63**	**6.8**	**5**	**6.4**	**2.1**	**7.4**
4	78	95.3	0	38	5.8	4	5.4	1.6	3.7
4	79	81.9	0	39	5.6	4	5.3	2.0	5.8
4	80	83.9	0	37	5.9	5	5.4	1.7	3.9
4	85	52.7	0	32	6.9	5	6.0	1.3	1.7
4	86	56.0	0	25	5.5	4	4.6	1.4	2.0
4	87	49.8	0	26	5.8	4	5.2	1.3	1.3
4	96	44.6	0	27	5.9	5	5.1	1.4	2.3
4	97	47.0	0	32	5.8	4	5.0	1.6	3.2
4	98	46.1	0	32	5.6	5	4.7	1.6	4.0
Combined		**557.3**	**0**	**39**	**5.9**	**4**	**5.2**	**1.6**	**3.4**
All Subjects		**2001.6**	**0**	**63**	**6.0**	**5**	**1.0**	**3.3**	**20.8**

123

Table I-3.
Summary statistics for roll velocity, slalom course, TIO.
(velocity values expressed in degrees/sec, time in seconds)

Subject	Run	Time	Min	Max	Mean	Median	S.D.	Skewness	Kurtosis
1	138	85.7	0	45	4.0	4.0	3.7	3.2	23.7
1	139	109.7	0	34	4.7	4.7	4.3	2.0	6.9
1	140	120.4	0	26	4.3	4.3	3.6	1.3	2.7
Combined		**315.8**	**0**	**45**	**4.3**	**4.3**	**3.9**	**2.1**	**9.6**
2	163	70.0	0	28	4.4	3	4.0	1.7	4.2
2	164	82.5	0	34	4.7	3	4.4	1.9	5.5
2	166	80.1	0	23	4.5	4	4.0	1.4	2.1
2	167	88.1	0	34	4.9	4	4.4	1.8	5.2
Combined		**320.7**	**0**	**34**	**4.6**	**4**	**4.2**	**1.7**	**4.6**
3	144	70.9	0	37	6.3	5	5.6	1.7	3.7
3	145	89.3	0	35	5.4	4	4.9	1.8	4.7
3	146	97.9	0	32	5.1	4	4.8	2.0	5.4
3	155	71.9	0	25	4.4	3	3.9	1.4	2.5
3	157	84.4	0	21	3.3	3	2.7	1.5	3.4
Combined		**414.4**	**0**	**37**	**4.9**	**4**	**4.6**	**2.0**	**5.7**
4		None							
All Subjects		**1059.9**	**0**	**45**	**4.6**	**3**	**0.7**	**1.6**	**3.7**

124

Table I-4.
Summary statistics for roll velocity, slalom course, RWS.
(velocity values expressed in degrees/sec, time in seconds)

| Subject	Run	Time	Min	Max	Mean	Median	S.D.	Skewness	Kurtosis
1	141	106.2	0	29	3.9	3	3.5	1.9	5.7
1	142	102.0	0	95	4.0	3	5.3	9.4	147.4
1	143	120.0	0	33	4.2	3	3.8	1.7	4.9
Combined		**328.2**	**0**	**95**	**4.0**	**3**	**4.2**	**6.5**	**112.0**
2	168	83.2	0	20	3.9	3	3.2	1.3	2.0
2	169	89.1	0	31	4.3	3	3.8	1.8	5.5
2	170	101.1	0	23	3.5	3	3.0	1.6	4.3
2	174	63.6	0	46	4.5	4	4.4	3.2	21.6
2	175	65.0	0	19	4.2	3	3.5	1.1	1.2
2	176	63.8	0	19	4.2	3	3.7	1.3	1.4
Combined		**465.8**	**0**	**46**	**4.1**	**3**	**3.6**	**2.0**	**9.6**
3	158	71.2	0	40	4.4	3	4.4	2.4	9.5
3	159	94.8	0	23	4.0	3	3.5	1.6	3.1
3	161	61.2	0	25	4.8	3	4.7	1.7	3.0
3	162	55.3	0	28	4.4	3	4.3	1.9	5.1
3	180	59.6	0	32	5.9	4	5.3	1.6	3.1
3	181	58.9	0	33	5.9	5	5.1	1.3	2.4
3	182	52.9	0	30	5.3	4	4.7	1.7	3.9
3	183	43.9	0	29	5.7	4	5.0	1.5	2.7
Combined		**497.8**	**0**	**40**	**4.9**	**4**	**4.6**	**1.8**	**4.3**
4	None								
All Subjects		**1291.8**	**0**	**95**	**4.5**	**3**	**0.7**	**3.7**	**16.3**

125

Appendix J.

Roll velocity box plots.
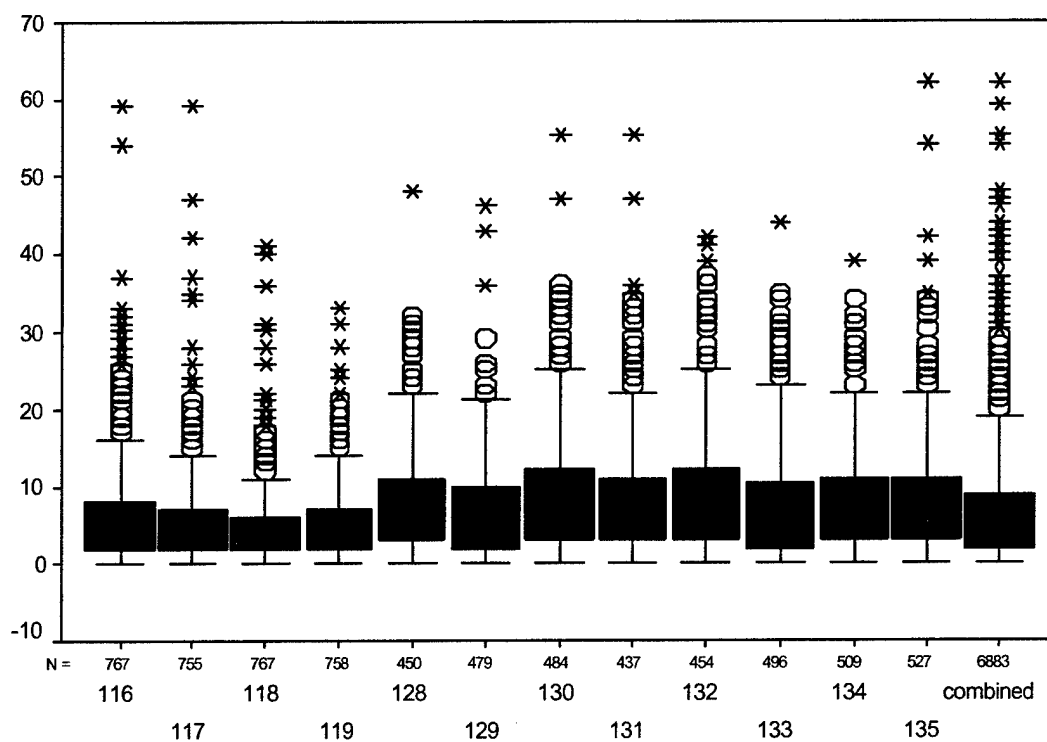
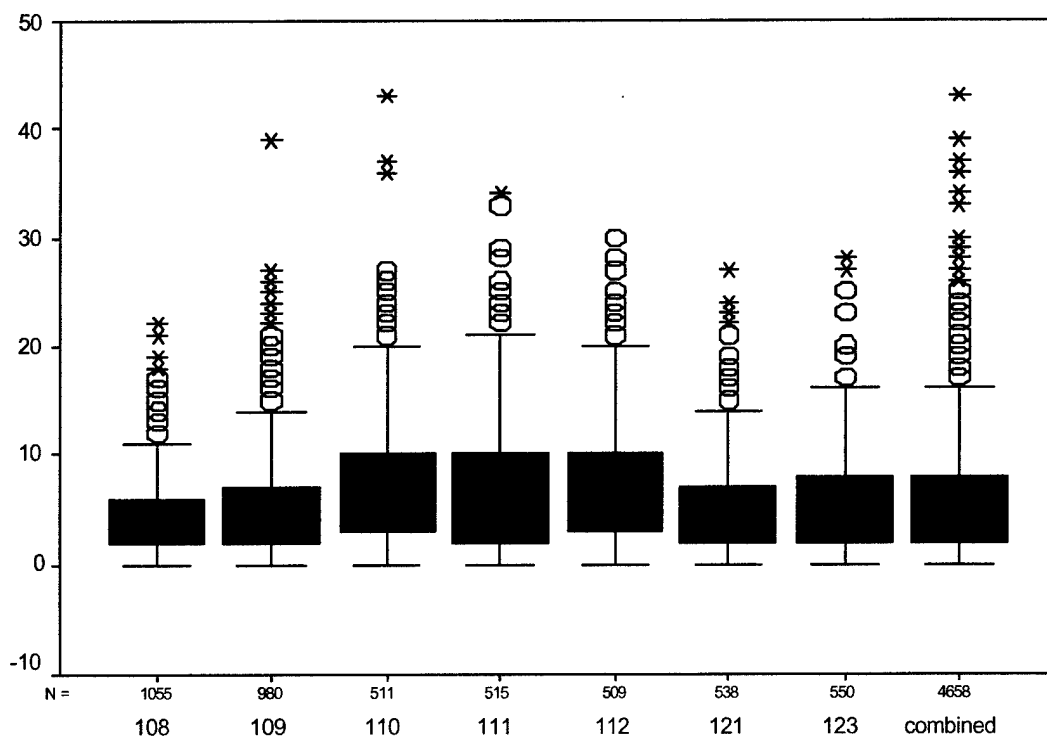Figure J-1. Subject #1 GVE head velocity box plots.

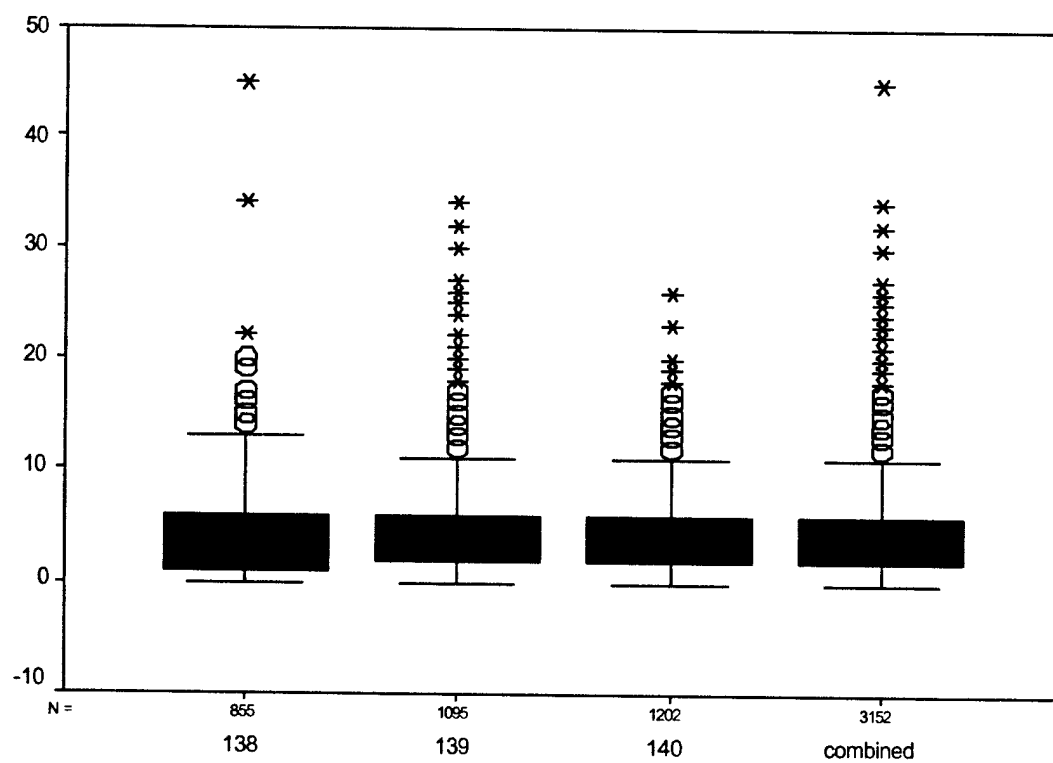Figure J-2. Subject #1 NVG head velocity box plots.

127

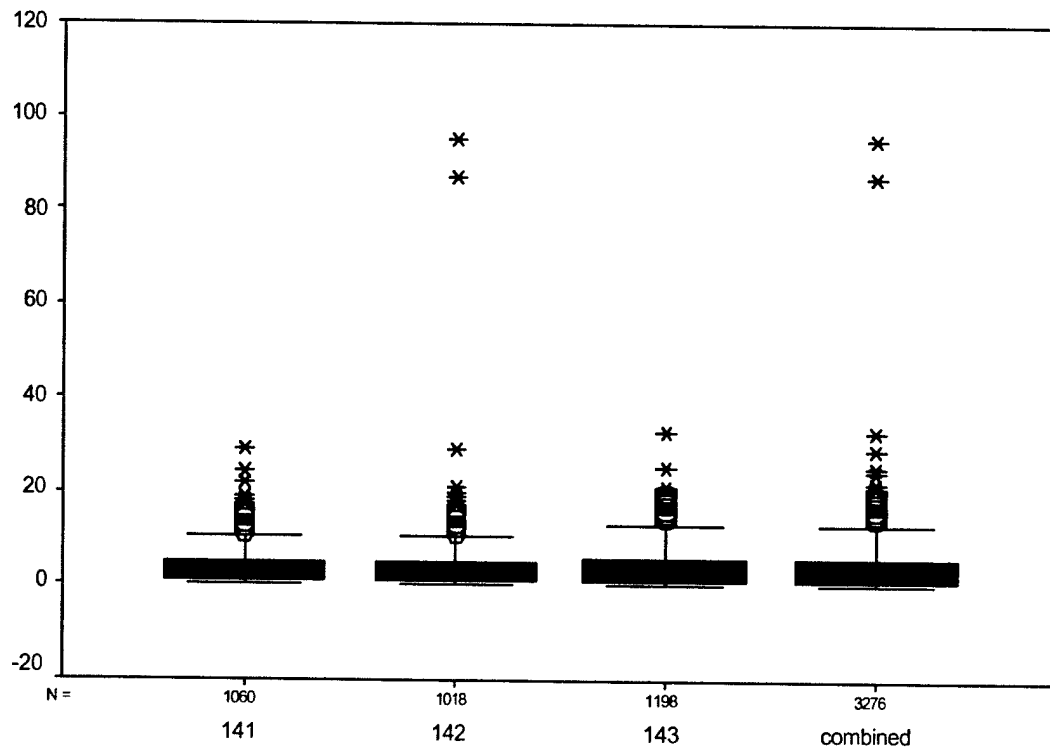Figure J-3. Subject #1 TIO head velocity box plots.

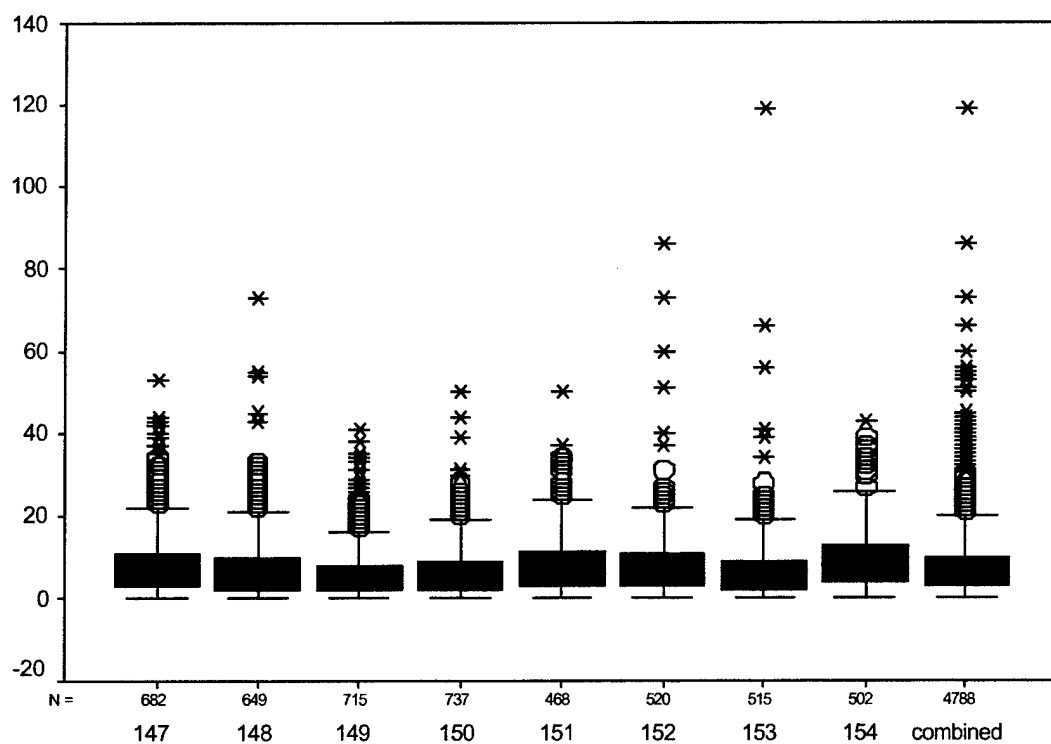Figure J-4. Subject #1 RWS head velocity box plots.
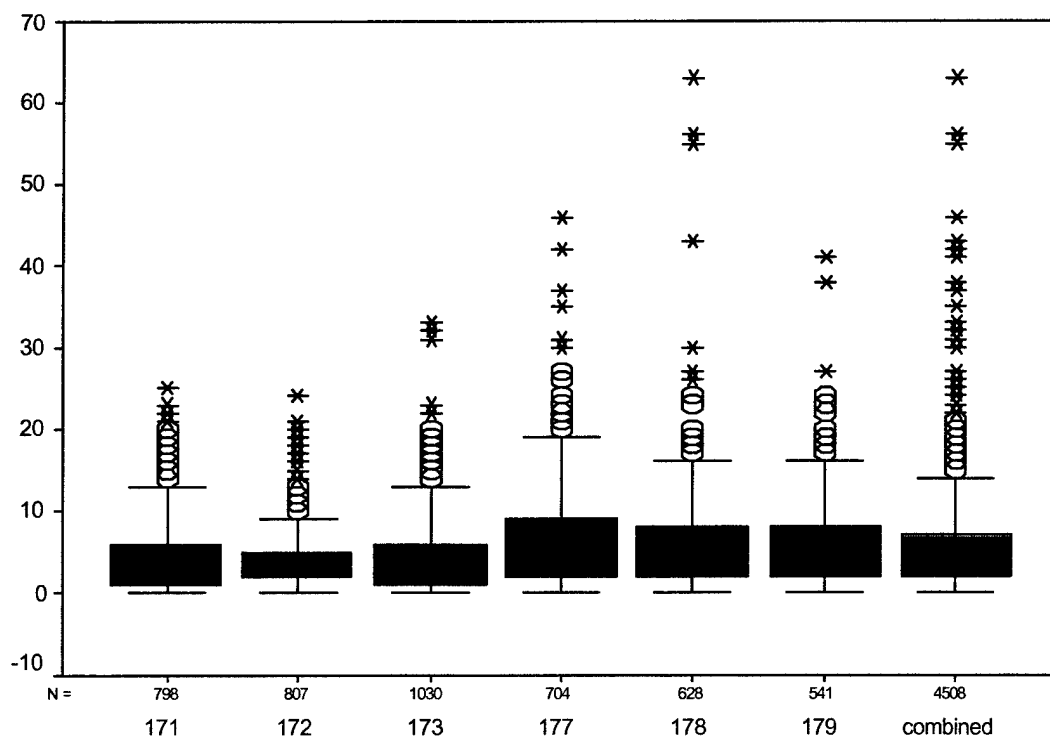
Figure J-5. Subject #2 GVE head velocity box plots.

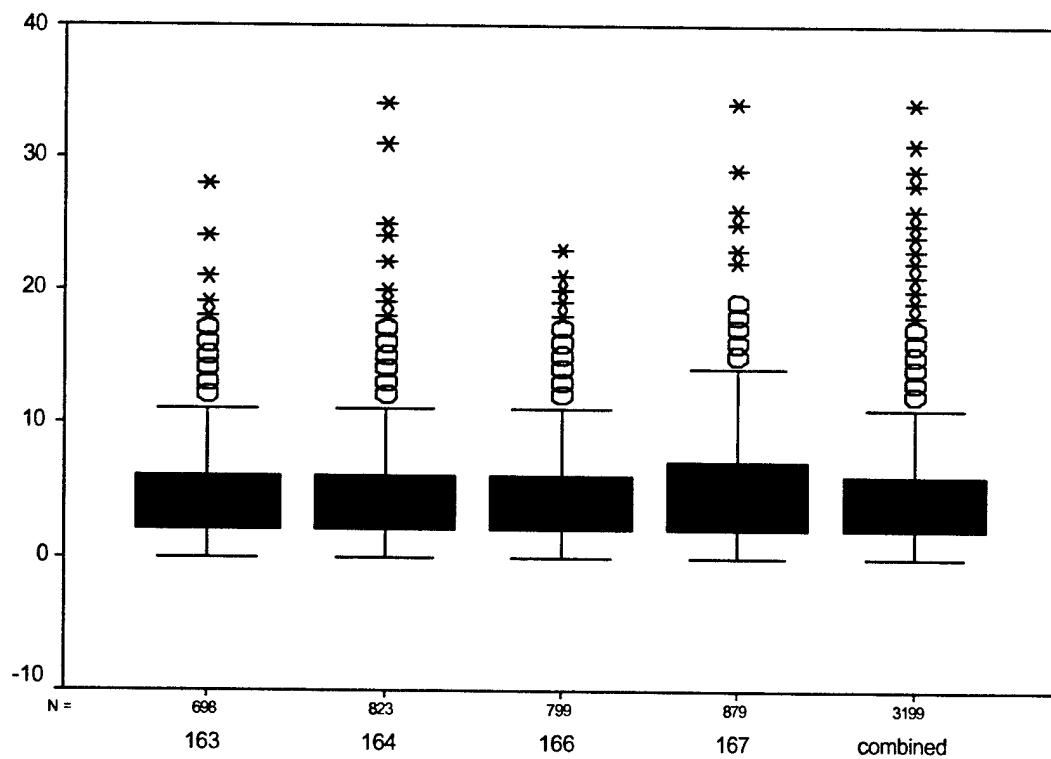Figure J-6. Subject #2 NVG head velocity box plots.

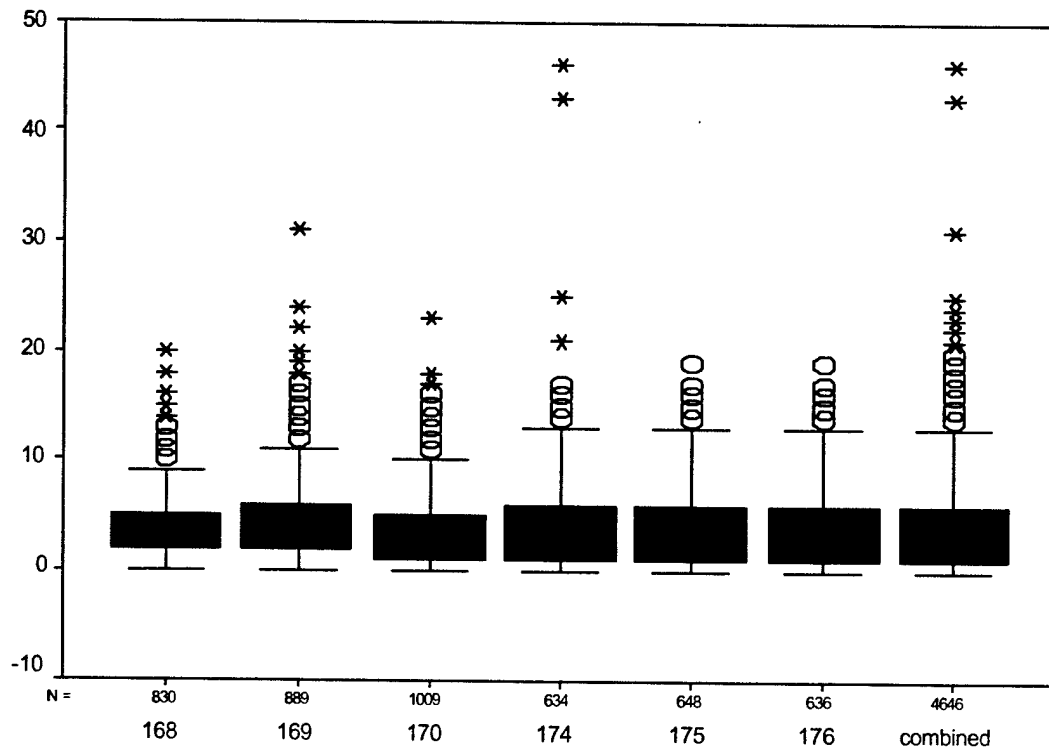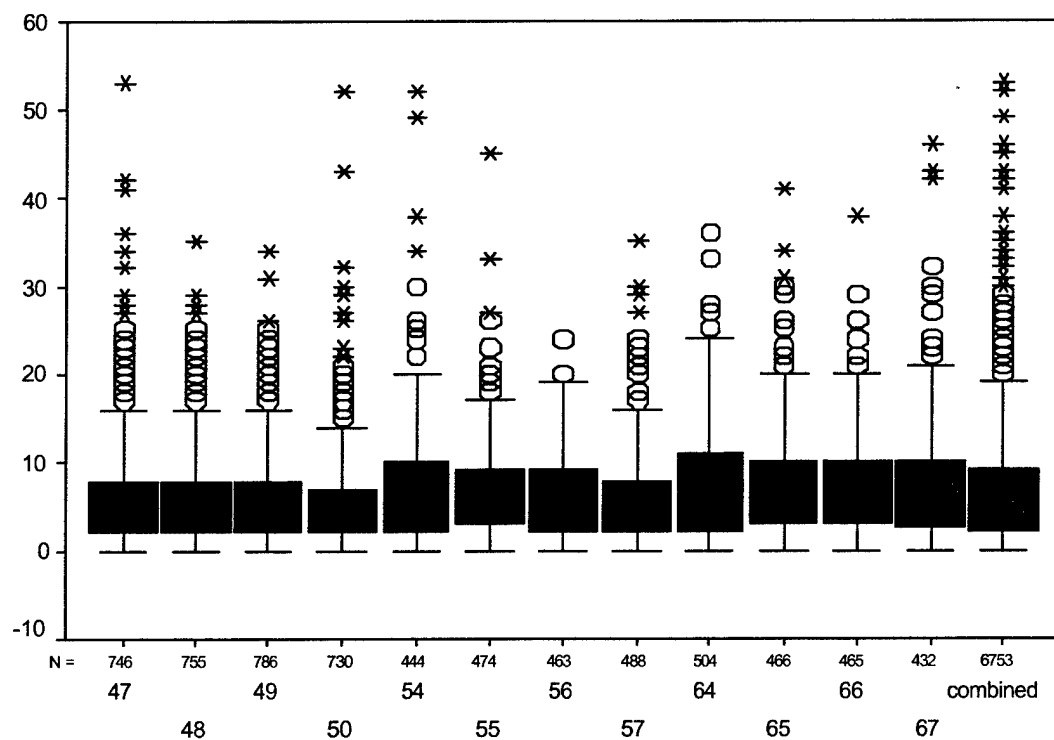Figure J-7. Subject #2 TIO head velocity box plots.

Figure J-8. Subject #2 RWS head velocity box plots.

130

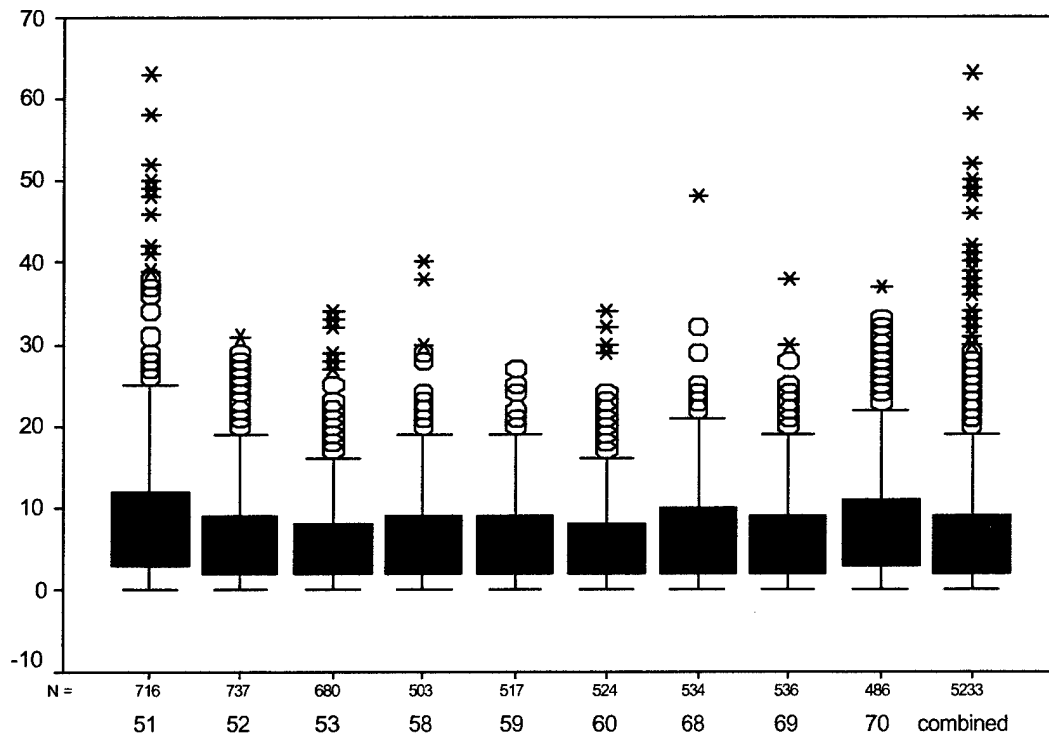Figure J-9. Subject #3 GVE head velocity box plots.

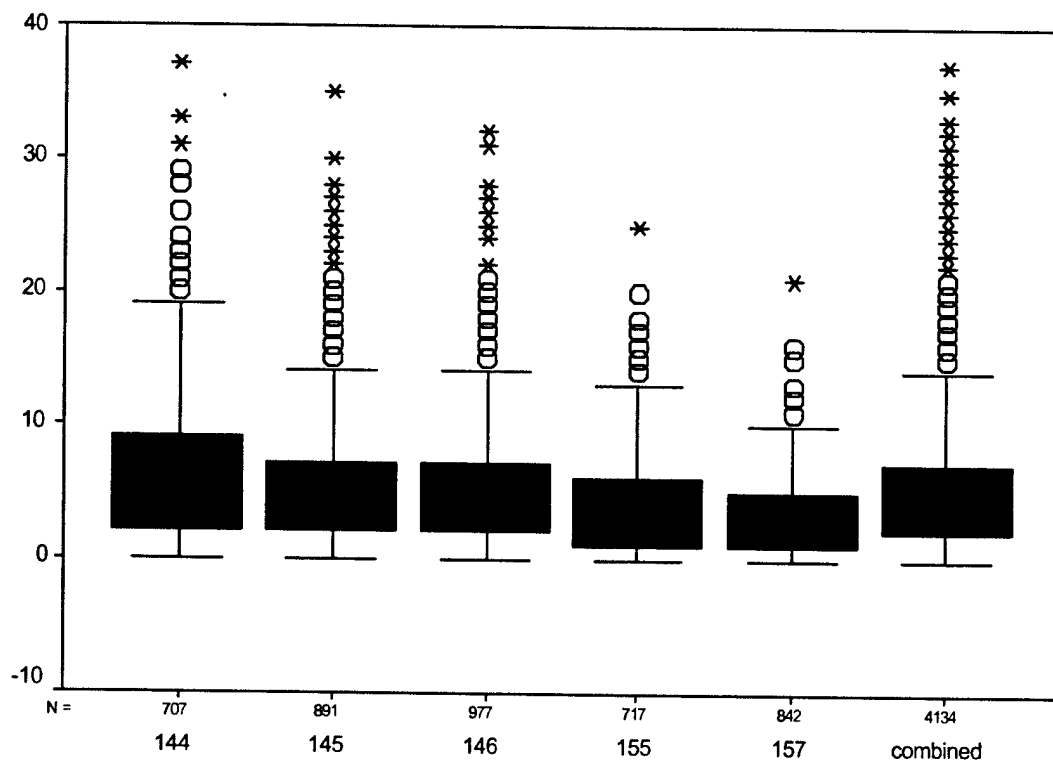Figure J-10. Subject #3 NVG head velocity box plots.
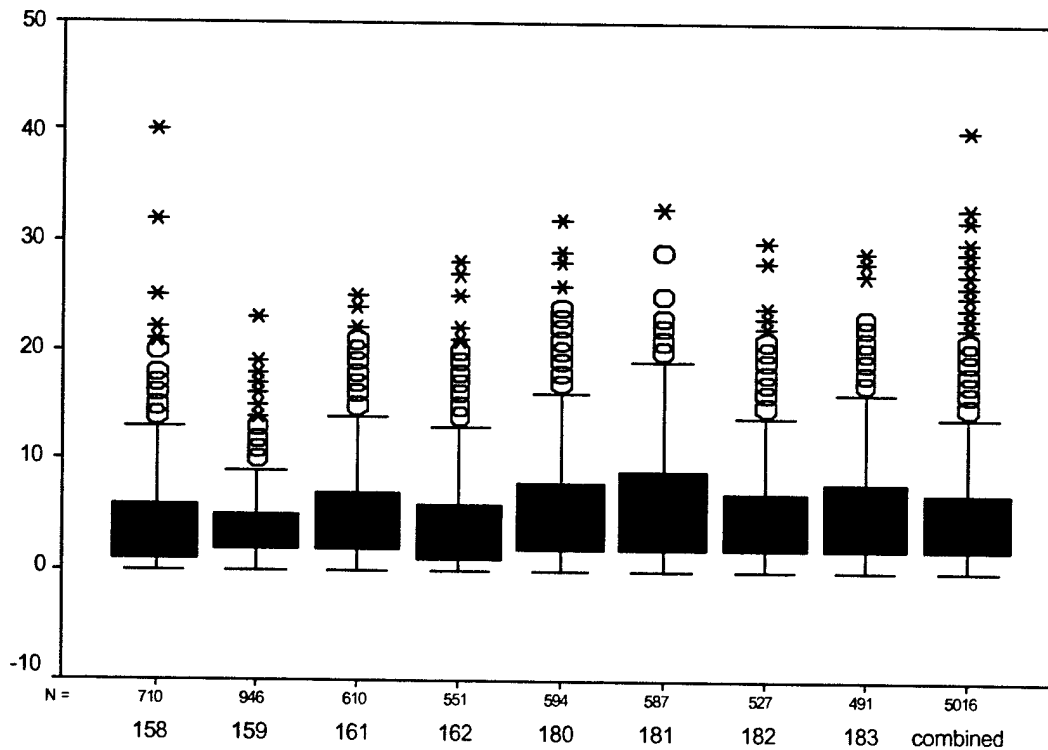
Figure J-11. Subject #3 TIO head velocity box plots.

Figure J-12. Subject #3 RWS head velocity box plots.

132

Figure J-13. Subject #4 GVE head velocity box plots.

Figure J-14. Subject #4 NVG head velocity box plots.

133